Molecular genetic studies on regulatory mechanisms for infection thread and root nodule formation in *Lotus japonicus*

Emiko Yoro

PhD Dissertation

2015

Department of Basic Biology
The Graduate University for Advanced Studies

TABLE OF CONTENTS

Chapter 1

GENERAL INTRODUCTION

1.1. Legume-rhizobial symbiosis

Since the 1830s, nitrogen has been known as one of the essential macronutrients for plant growth (Liebig, 1840). Nitrogen is a constituent of several critical biochemicals, such as amino acids, nucleotides, phytohormones (auxin and cytokinin), and chlorophylls. In fact, nitrogen deficiency induces chlorosis, which is characterized by insufficient chlorophyll and resulting pale yellow leaves. Most of the nitrogen on earth exists in the form of atmospheric dinitrogen, which is not biologically useable and needs to be fixed into biologically available forms (nitrate or ammonia). However, Liebig had expected that plant nitrogen comes directly from the atmosphere due to a special ability of legumes (Liebig, 1840). In 1888, his misunderstanding was corrected by Hellriegel and Wilfath. They recognized that root nodules are responsible for the conversion from atmospheric nitrogen to ammonia. At the same time, the responsible symbiotic bacteria was first purified from nodules of a number of different legume species by Beijerink in 1888, and a year later, Frank named these bacteria *Rhizobium leguminosarum* (Frank, 1889), which are commonly called rhizobia. In summary, legumes develop a specialized root organ called a root nodule where nitrogen fixing rhizobia reside, in order to adapt to nitrogen-limited soil.

After the discovery of rhizobia, symbiotic nitrogen fixation has been found not only in Fabales (including legumes) but also in some species in Cucurbitales, Fagales, and Rosales (Soltis et al., 1995; Kistner and Parniske, 2002; Sprent, 2007; Doyle, 2011). Among these, Fabales and one exception, *Parasponia* (belonging to Rosales), make

symbioses with rhizobia. On the other hand, the others species in Cucurbitales, Fagales, and Rosales harbor *Frankia* filamentous bacteria as their symbiotic partners. The morphology of the symbiotic organs is also a little different for these cases. Root nodules in legumes are mainly divided into two types, determinate nodules and indeterminate nodules. *Lotus japonicus* (*Lj*), soybean (*Glycine max*, *Gm*), and common bean (*Phaseolus* spp.) make determinate nodules, but *Medicago truncatula* (*Mt*), pea (*Pisum sativum*, *Ps*), and vetch (*Vicia* spp.) make indeterminate nodules that include the meristematic zone in the tip. Additionally, *Sesbania* and *Lupinus* respectively form stem nodules and collar nodules (Goormachtig et al., 2004; Sprent, 2007). In the case of a wide variety of host plants of *Frankia*, most nodules have a central vasculature, different from that of legumes. Further, these bacterial infection processes are more and more diversified (Swensen, 1996; Sprent, 2007; Madsen et al., 2010; Held et al., 2010; Doyle, 2011). Nevertheless, these nitrogen fixing symbioses are thought to have a single origin, because all genera of host plants fall into a single clade, the so-called nitrogen fixing clade (Soltis et al., 1995). When and how did the original nitrogen-fixing plant appear? This has remained a deep mystery. One possible scenario is that high CO_2 level triggered a limitation of nitrogen for plant growth and promoted evolution of symbiotic nitrogen fixation (Sprent, 2007).

We know the system for nitrogen fixing symbiosis was at least partially co-opted from another older symbiosis with arbuscular mycorrhizal fungi based on discovery of components of common symbiotic pathway (Kistner and Parniske, 2002; Markmann and Parniske, 2009). However, in contrast to arbuscular mycorrhizal symbiosis, which is widely found in land plants, the specificity between legumes and rhizobia is strictly restricted. This leads to the importance of tight mutual recognition. In addition, unlike

the maternal transfer of symbiotic bacteria as observed in insect-bacterial symbiosis (Russell and Moran, 2005; Serbus et al., 2008), legumes need to acquire their beneficial symbiotic partner in the soil in every generation. With respect to this aspect, the mutual recognition between host legumes and beneficial partner would be crucial for robustness of this mutualism. Strict recognition is accomplished by two molecular communication-steps. The first is between flavonoids specific to the host plant and rhizobial *nod* genes, which is required for the production of Nod factor, a lipochitooligosaccharide (Honma et al., 1990; Cooper, 2004; Peck et al., 2006). The second combination is Nod factor and the Nod factor receptor of the host plant. Nod factor induces multiple initial responses of host plants essential for further symbiotic signaling.

To understand the physiological aspects of initiating and regulating root nodule symbiosis, mutant screenings have been carried out, mainly using pea and soybean. In the post-genomic era, two diploid model legumes, *L. japonicus* and *M. truncatula*, have performed conspicuous roles in identification of their respective genes for mutations affecting symbiosis. In the remaining parts of this chapter, I mainly focus on my experimental material *L. japonicus*, and highlight major symbiotic events in host plants based on previous knowledge or isolated genes involved in rhizobial infection (**1.2.**), nodule organogenesis (**1.3.**), and negative regulation of nodulation (**1.4.**).

1.2. Rhizobial infection of epidermis through infection thread (IT)

Rhizobia penetrate the host plant root tissues from the tip of root hairs. When rhizobia become attached to a host root hair, root hair elongation and deformation are induced [Fig.1-1(1)], and rhizobia are entrapped in the tightly curled root hair, also referred to as a shepherd's crook [Fig. 1-1(2)]. Severe impairment of root hair deformation observed

in mutants for the Nod factor receptors suggest a requirement of Nod factor in these processes [Table 1-1(a)] (Ben Amor et al., 2003; Limpens et al., 2003; Madsen et al., 2003; Radutoiu et al., 2003). Among several growth stages of root hairs (Karas et al., 2005), it is thought that growth-terminating root hairs, which have a dense cytoplasmic region at the tip, are the most sensitive to Nod factor (Sieberer and Emons, 2000). Bigining about 90 minutes after Nod factor application, the tip starts to swell, and a new outgrowth develops from the site of swelling. These processes are accompanied by cytoplasmic streaming, reorientation of the ER, and movement of the nucleus and vacuole (Miller et al., 2000; Sieberer and Emons, 2000; Gage, 2004).

In the next step, rhizobia invade host root tissues through a plant-derived specialized intracellular tube-like structure, called an infection thread (IT) [Fig. 1-1(3)] (Vasse and Truchet, 1984; Gage, 2004; Jones et al., 2007; Fournier et al., 2008; Murray, 2011). At the initial step of IT organization, degradation of the root hair cell wall via the plant-side polygalacturonases and pectate lyase *Lj*NPL might be required for rhizobial entry (Munoz et al., 1998; Rodriguez-Llorente et al., 2004; Xie et al., 2012). Alternatively, this degradation could be achieved by rhizobial side cellulase (Laus et al., 2005; Robledo et al., 2008). The IT membrane originates from invagination of the plant cell membrane, or in other words, the lumen of the IT harboring the rhizobia is topologically outside of the root cell (Brewin, 2004; Gage, 2004). However, the components of the IT lumen seem to be different from normal cell wall components. Electron microscopic observation of ITs suggests that the IT membrane is resistant to plant cell wall degrading enzymes driselase (Higashi et al., 1986). Although the components of the IT membrane are largely unknown, a few IT membrane localized proteins have been discovered [Table 1-1(b)]. Considering the identification of

*Mt*FLOT2/4 (plant flotillin-like protein) and *Mt*SYMREM1 (symbiotic remorin 1), a lipid raft, which is a cholesterol-rich and detergent-resistant membrane microdomain, may play a key role in IT membrane organization (Haney and Long, 2010; Lefebvre et al., 2010). Moreover, live-cell imaging of IT reveals the dynamic morphology of IT: the speed of the growing IT is approximately 4-5 μm per hour, with frequent appearance of a rhizobial-free zone behind the tip of the growing IT, indicating that invagination of the IT membrane precedes rhizobial colonization [Fig. 1-1(3)] (Fournier et al., 2008; Perrine-Walker et al., 2014; Perrine-Walker et al., 2014).

Numerous genes functioning downstream of Nod factor receptors for further IT growth have been identified by mutant screening or reverse genetic approaches. These are listed in Table 1-1, according to the categories (a) impaired in root hair deformation, (b) IT membrane localized, (c) impaired in IT elongation, (d) no or low IT with no or low infected nodules, and (e) impaired in bacterial release. In particular, when special observations of ITs were performed in the original papers, they are categorized as impaired in IT elongation [Table 1-1(c)]. The individual molecular mechanisms involved in infection and their roles remain largely obscure; however, some genes or mutants provide an indication of how legumes develop and regulate ITs.

RAC/ROP-like small GTPases (*Mt*ROP9) and a major sperm protein (MSP) domain containing protein (*Lj*VAPYRIN) are generally required for vesicle trafficking (Murray, 2011; Murray et al., 2011; Kiirika et al., 2012). The pleiotropic defects of *crinkle* and *lot1* mutants indicate a common mechanism involved in growth of a series of tip growing cells (Tansengco et al., 2003; Tansengco et al., 2004; Ooki et al., 2005). These findings indicate mechanistic similarities between IT growth and other types of tip growth, that of root hairs, trichromes and pollen tubes (Hepler et al., 2001;

Campanoni and Blatt, 2007). Formation of a calcium gradient and production of reactive oxygen species (ROS) at the tip of root hairs also support these similarities (Hepler et al., 2001; Ramu et al., 2002; Esseling et al., 2003; Gage, 2004; Liu et al., 2009).

In addition, most of the plant genes involved in rhizobial infection are also involved in nodule organogenesis (see "Nodulation phenotype" column in Table 1-1), except for genes participating in actin rearrangement, such as *LjPIR*, *LjNAP/MtRIT*, and *LjAPRC*. This indicates the complexity of the two signaling pathways as further discussed below (**1.3.**, **2.1.**). Furthermore, several previous reports mentioned an increased number of early rhizobial infection events or ITs [Table 1-1 (f-h)]. Theses also observation remind me of another inter-relationship between these two pathways (**2.1.**, **2.3.1**).

1.3. Nodule organogenesis in root cortex

In parallel with rhizobial infection in epidermal cells (**1.2.**), organogenesis begins with re-initiation of cell division in the root cortex. Prior to cell division, the cortical cells are activated and seem to prepare for acceptance of rhizobial invasion [Fig. 1-1(4)]. In response to rhizobial inoculation or Nod factor application, the nuclei and cytoplasm of the cortex are re-localized to the center of the cells and are aligned in a way to guide the IT, a formation called a cytosolic bridge or pre-infection thread, as it occurs in preparation for the usual cell division (van Brussel et al., 1992; Timmers et al., 1999; Niwa et al., 2001). The activated cortical cells specifically express *HISTONE H4*, a marker for S-phase during the cell cycle, indicating reentry to the cell cycle occurs during nodule organogenesis (Yang et al., 1994; Foucher and Kondorosi, 2000).

Cytokinin signaling plays an important role in nodule organogenesis, given the low nodulation phenotype of a loss-of-function mutation or knockdown of the putative cytokinin receptors, LOTUS HISTIDINE KINASE 1 (LHK1) in *L. japonicus* and CYTOKININ RESPONSE 1 (CRE1) in *M. truncatula* (Gonzalez-Rizzo et al., 2006; Murray et al., 2007; Plet et al., 2011). Recently, three redundantly functioning cytokinin receptors were found (Held et al., 2014). More importantly, the *spontaneous nodule formation* (*snf*) *2* mutant, which has a gain-of-function mutation in LHK1 yields a nodule-like structure even in the absence of rhizobia, known as a spontaneous nodule (Tirichine et al., 2007). Likewise, ectopic cortical cell division is also induced by exogenous cytokinin application (Bauer et al., 1996; Heckmann et al., 2011). These provide a direct evidence for the involvement of cytokinin in cell division in root cortex. Further, two potential direct targets of cytokinin signaling, type-A *RESPONSE REGULATOR (RR) 4* and *NODULATION SIGNALING PATHWAY 2 (NSP2),* may play pivotal roles in activating nodule organogenesis (Ariel et al., 2012).

Downstream of cytokinin signaling, auxin polar transport is inhibited via altering expression of auxin carrier proteins, PIN-FORMEDs (PINs) (Plet et al., 2011). This leads to accumulation of auxin at the site where cell division will start in the cortex, confirmed by the observation of nodule-like structures induced by auxin transport inhibitors (Hirsch et al., 1989; Rightmyer and Long, 2011; Suzaki et al., 2012). Next, identification of genes encoding components of topoisomerase VI, *VAGRANT INFECTION THREAD 1* (*VAG1*) and *SUNERGOS 1*, suggests a key role for endoreduplication in the activation of cortical cells (Suzaki et al., 2014; Yoon et al., 2014). Moreover, the misguided IT phenotype of the *vag1* mutant indicates the importance of endoreduplication for appropriate IT growth. Lastly, newly divided cells

accept rhizobia by endocytosis, forming a special organelle-like structure termed a symbiosome, where symbiotic nitrogen fixation takes place [Fig. 1-1(5)]. Several mutations involved in this bacterial release have been identified, mainly in *M. truncatula*, which makes indeterminate type nodules rather than the determinate type of *L. japonicus* [Table 1-1(e)]. In later nodule developmental processes, specifically in indeterminate nodules (**1.1.**), the symbiosome becomes enlarged in parallel with bacterial differentiation, which results in nodule differentiation. Therefore, mutations of genes required for rhizobial release affect the final size or morphology of indeterminate nodules.

1.4. Negative regulation of nodulation

Forming nodules requires the consumption of energy for organogenesis and allocation of photoassimilate to the rhizobia (Tjepkema and Winship, 1980; Udvardi et al., 1988; Udvardi and Poole, 2013). Thus, legumes have developed mechanisms for maintaining a balance between forming nodules and satisfying their own nitrogen requirements. Observations that the elimination of earlier nodules promotes further nodulation suggest that early-forming nodules contribute to the inhibition of subsequent nodulation, which is termed autoregulation of nodulation (AON) (Nutman, 1952; Kosslak and Bohlool, 1984; Caetano-Anollés and Gresshoff, 1990; Caetano-Anollés and Gresshoff, 1991). The idea of systemic long-distance control of nodulation originally arose from experiments using split-root and grafting techniques (Kosslak and Bohlool, 1984; Delves et al., 1986). The detailed molecular mechanisms involved in AON have been gradually elucidated from the screening of several hypernodulation mutants in model legumes (reviewed in Oka-Kira and Kawaguchi, 2006; Ferguson et al., 2010; Reid et al.,

2011b; Mortier et al., 2012b).

Grafting experiments showed that some hypernodulation mutant phenotypes were determined by their shoot genotype (Delves et al., 1986; Krusell et al., 2002; Nishimura et al., 2002a; Penmetsa et al., 2003; Oka-Kira et al., 2005), indicating that the corresponding genes mediate the systemic control of nodulation on shoots, not on roots. These shoot factors are *HYPERNODULATION AND ABERRANT ROOT FORMATION1 (LjHAR1)* (Krusell et al., 2002; Nishimura et al., 2002a), *NODULE AUTOREGULATION RECEPTOR KINASE (GmNARK)* (Searle et al., 2003), *SUPER NUMERIC NODULES (MtSUNN)* (Schnabel et al., 2005), *SYMBIOSIS 29* (*PsSYM29)* (Krusell et al., 2002), and *KLAVIER (LjKLV)* (Oka-Kira et al., 2005; Miyazawa et al., 2010). *Lj*HAR1/*Mt*SUNN/*Gm*NARK/*Ps*SYM29 are orthologous to CLAVATA1 (CLV1) which is a leucine-rich repeat receptor-like kinase (LRR-RLK) in *Arabidopsis thaliana* (Arabidopsis or *At*). *AtCLAVATA3* encodes a putative signaling molecule that belongs to the CLAVATA3/EMBRYO SURROUNDING REGION-related (CLE) peptide family and acts as a ligand of CLV1 (Fletcher et al., 1999; Ogawa et al., 2008). These findings stimulated investigation of potential ligands for *Lj*HAR1/*Mt*SUNN/*Gm*NARK/*Ps*SYM29. Consequently, CLE-root signal 1/2 (*Lj*CLE-RS1/2) (Okamoto et al., 2009), RHIZOBIA-INDUCED CLE (*Gm*RIC1/2) (Lim et al., 2011; Reid et al., 2011a), and *Mt*CLE12/13 (Mortier et al., 2010) were identified as candidates for such ligands. Furthermore, a recent report demonstrated that at least *Lj*CLE-RS2 is post-translationally arabinosylated and directly binds to *Lj*HAR1 (Okamoto et al., 2013a). Another gene functioning in long-distance control encodes an F-box/Kelch-repeat protein, named *TOO MUCH LOVE (LjTML),* which is a root factor but not a shoot factor (Magori et al., 2009; Takahara et al., 2013).

A current plausible model for the HAR1-mediated long-distance control of nodulation in *L. japonicus* is the following (Fig. 1-2). Nodule symbiotic signaling, especially downstream of cytokinin signaling, induces the expression of the *CLE-RS1/2* genes directly mediated by NODULE INCEPTION (NIN) transcription factor (Soyano et al., 2014) [Fig. 1-2(1); **Chapters 2, 3**]. The *Lj*CLE-RS1/2 peptides are modified with tri-arabinoside in the Golgi complex, mediated by a putative post-translational modification enzyme, PLENTY, which is orthologous to Arabidopsis hydroxyproline O-arabinosyltransferases (HPATs) (Ogawa-Ohnishi et al., 2013) [Fig. 1-2(2), **Chapter 4**]. Then, these CLE-RS1/2 peptides are secreted into xylem as a root-derived signal, also known as "Q" (Okamoto et al., 2013a). The peptides are transmitted from roots to shoots and directly bind HAR1 or a putative HAR1-KLV receptor complex expressed in the phloem of leaf tissue at shoots (Nontachalyapoom et al., 2007; Miyazawa et al., 2010; Okamoto et al., 2013a) [Fig. 1-2(3)]. Other candidates for the peptide receptors have been are reported based on Arabidopsis studies [Fig. 1-2(3), **Chapter 4**]. Next, downstream of peptide binding, *ISOPENTENYLTRANSFERASE 3* (*IPT3*) expression and subsequent production of cytokinin are induced (Sasaki et al., 2014) [Fig. 1-2(4)]. Cytokinin, a strong candidate for the shoot-derived inhibitor (SDI), is transported to roots via the phloem and directly or indirectly activates TML, which is putatively involved in proteasome-mediated degradation of the unknown positive regulator of nodulation (Magori et al., 2009; Takahara et al., 2013) [Fig. 1-2(5)]. Other candidates for SDI have been explored in other legumes (Kinkema and Gresshoff, 2008; Lin et al., 2010; Reid et al., 2012).

Other negative regulators of nodulation have also been identified: the transcription factor *Mt*EFD (for an ethylene response factor required for nodule

differentiation) (Vernie et al., 2008), the regulator of photomorphogenesis *Lj*ASTRAY (Nishimura et al., 2002b), the ethylene receptor *Lj*ETR (Lohar et al., 2009), and ethylene signaling components *Mt*SICKLE and *Lj*ETHYLENE INSENSITIVE1/2 (*Lj*EIN2) (Penmetsa and Cook, 1997; Penmetsa et al., 2003; Miyata et al., 2013). Among them, *Mtsickle* and *Mtefd* also show hyperinfection [Table 1-1(h)], and additive nodulation of a *sickle sunn* double mutant in *M. truncatula* clearly showed that ethylene-mediated control and *Lj*HAR1/*Mt*SUNN-mediated long-distance control are genetically independent (Penmetsa et al., 2003).

In this dissertation, I analyzed two *L. japonicus* mutants, *daphne* and *plenty*, in order to understand the molecular mechanisms of host plant that maintain the balance of the symbiosis with rhizobia, especially the regulatory mechanisms involved in control of IT numbers and nodule numbers. First, in **Chapter 2**, I explored the interactive nodulation signaling pathways between infection and organogenesis and identify a negative feedback loop for IT formation based on the analysis of a novel mutant, *daphne*, which shows hyperinfection and non-nodulation. Then, in **Chapter 3**, I identified a common mechanism for controlling both ITs and nodules using the *daphne* mutant, a powerful tool for studying control of IT development. In **Chapter 4**, I analyzed the hypernodulation mutant *plenty*, whose responsible gene is a new key player involved in controlling nodulation. I focused on recent studies of PLENTY homologs in three other plant species, pea, *M. truncatula*, and Arabidopsis. Lastly, in **Chapter 5**, I further discussed the inter-relationship between infection and organogenesis, the commonality of negative feedback regulation of both infection and nodule formation, and perspectives on the future based on my studies.

Table 1-1. Plant genes or mutants involved in rhizobial infection

Genes / mutants	Gene Products	Nodulation phenotypes (Nod^-/ low Nod / Nod^+ / Nod^{++})	References
(a) Impaired in root hair deformation			
LjNFR1 / MtLYK3 / MtHCL	Nod factor receptor	Nod^-	Limpens et al., 2003; Radutoiu et al., 2003; Smit et al., 2007
LjNFR5 / MtNFP / PsSYM10	Nod factor receptor	Nod^-	Ben Amor et al., 2003; Madsen et al., 2003; Radutoiu et al., 2003; Ovtsyna et al., 2005; Rival et al., 2012
(b) ITmembrane localized			
LjFLOT4	Plant flotillin-like protein	see *LjFLOT2/4-RNAi*	Haney and Long, 2010; Haney et al., 2011
AtPIP2;1	Aquapolin	-	Fournier et al., 2008
MtDMI2	Receptor-like kinase	Nod^-	Limpens et al., 2005
MtSYMREM1	Plant-specific remorin protein	low Nod	Lefebvre et al., 2010
(c) Impaired in IT elongation			
LjNIN / MtNIN / PsSYM35	RWP-RK TF	Nod^-	Schauser et al., 1999; Borisov et al., 2003; Marsh et al., 2007; Soyano et al., 2013
MtERN / MtBIT1 / Mtpdl	ERF TF	Nod^-	Middleton et al., 2007
LjNPL (*Ljnpl-2 / Ljitd1*)	Pectate lyase	Nod^+ (white nodule)	Xie et al., 2012

Table 1-1. Plant genes or mutants involved in rhizobial infection

LjPIR1	SCAR/WAVE components	Nod^+ (white nodule)	Yokota et al., 2009
LjNAP1/ MtRIT	SCAR/WAVE components	Nod^+ (white nodule)	Yokota et al., 2009; Miyahara et al., 2010
LjARPC1	ARP2/3 components	Nod^+ (white nodule)	Hossain et al., 2012
LjCERBERUS / MtLIN	E3 ubiquitin ligase	low Nod	Kuppusamy et al., 2004; Yano et al., 2009
LjCYCLOPS / MtIPD3	Coiled coil domain, TF	low Nod	Messinese et al., 2007; Yano et al., 2008; Horvath et al., 2011; Ovchinnikova et al., 2011
MtRPG	Long coiled coil protein	low Nod	Arrighi et al., 2008
MtVPY	MSP domain, Ankyrin repeat	low Nod	Murray et al., 2011
MtLATD / MtNIP	NRT1 transporter	low Nod	Bright et al., 2005; Yendrek et al., 2010
MtNF-YA1 (*MtHAP2-1*), *MtNF-YA2*	CCAAT-binding TF	low Nod	Laloum et al., 2014; Laporte et al., 2014
PvNF-YC-RNAi	CCAAT-binding TF	low Nod	Eugenia Zanetti et al., 2010
PvSIN1-RNAi	GRAS TF	low Nod	Battaglia et al., 2014
Mthcl-4 / Mtlyk3-4 (weak allele)	Nod factor receptor	low Nod	Smit et al., 2007
Ljsymrk-14 (specific allele of *symrk*)	Receptor-like kinase	low Nod	Kosuta et al., 2011
Ljalb1 / Ljsym74	N.D.	low Nod	Imaizumi-Anraku et al., 2000; Kawaguchi et al., 2002; Yano et al., 2006

(d) No or low IT with no or low infected nodules

Table 1-1. Plant genes or mutants involved in rhizobial infection

LjCCaMK / MtDMI3 / PsSYM9 / PsSYM30	Calmodulin-dependant protein kinase	Nod$^-$	Catoira et al., 2000; Levy et al., 2004; Mitra et al., 2004; Miwa et al., 2006
LjSYMRK / MtDMI2 / PsSYM19	Receptor-like kinase	Nod$^-$	Catoira et al., 2000; Stracke et al., 2002; Bersoult et al., 2005; Limpens et al., 2005; Ovtsyna et al., 2005
LjNSP1 / MtNSP1, *LjNSP2 / MtNSP2 / PsSYM7*	GRAS TF	Nod$^-$	Tsyganov et al., 2002; Kalo et al., 2005; Smit et al., 2005; Heckmann et al., 2006; Murakami et al., 2006
LjCASTOR, *LjPOLLUX / MtDMI1 / PsSYM8*	Ion channels	Nod$^-$ / low Nod	Ane et al., 2004; Imaizumi-Anraku et al., 2005; Edwards et al., 2007; Peiter et al., 2007; Riely et al., 2007
LjNUP85	Nucleoporin	Nod$^-$ / low Nod	Saito et al., 2007; Madsen et al., 2010
LjNUP133	Nucleoporin	Nod$^-$ / low Nod	Kanamori et al., 2006; Madsen et al., 2010
MtCRE1, *MtCRE1-2*, and *MtCRE3*	Cytokinin receptors	low Nod	Gonzalez-Rizzo et al., 2006; Plet et al., 2011
LjnsRING-RNAi	RING-H2 finger domain	low Nod	Shimomura et al., 2006
MtROP9-RNAi	Rac1 small G protein	low Nod	Kiirika et al., 2012
MtSINA	E3 ubiquitin ligase	low Nod	Den Herder et al., 2008
LjNENA	Related to nucleoporins	low Nod	Groth et al., 2010)
Ljbrush	N.D.	low Nod	Maekawa-Yoshikawa et al., 2009
Ljlot1	N.D.	low Nod	Ooki et al., 2005
Ljcrk / Ljsym79	N.D.	low Nod	Kawaguchi et al., 2002; Tansengco et al., 2003; Tansengco et al., 2004; Yano et al., 2006
Ljitd3, *Ljitd4*	N.D.	low Nod	Lombardo et al., 2006
Mtapi	N.D.	low Nod	Teillet et al., 2008

Table 1-1. Plant genes or mutants involved in rhizobial infection

proSYMRK::LjSYMRK-ΔMLD in *symrk-3*	Receptor-like kinase	low Nod	Antolin-Llovera et al., 2014
(e) Impaired in bacterial release			
MtLATD / MtNIP	NRT1 transporter	low Nod	Veereshlingam et al., 2004; Bright et al., 2005; Yendrek et al., 2010
MtIPD3	Coiled coil domain, TF	low Nod	Horvath et al., 2011; Ovchinnikova et al., 2011
MtDMI2 / SrSYMRK	Receptor-like kinase	Nod^-	Capoen et al., 2005; Limpens et al., 2005
MtNF-YA1 (*MtHAP2-1*), *MtNF-YA2*	CCAAT-binding TF	low Nod	Combier et al., 2006
MtEFD	AP2/ERF TF	Nod^{++}	Vernie et al., 2008
MtSYMREM1-RNAi	Plant-specific remorin protein	low Nod	Lefebvre et al., 2010
MtNFP-RNAi	Nod factor receptor	low Nod	Moling et al., 2014
(f) Increased early infection events with low or no nodulation			
Mthcl-1 / Mthcl-2 / Mthcl-3 (strong alleles)	Nod factor receptor	Nod^-	Smit et al., 2007
LjSYMRK / MtDMI2	Receptor-like kinase	Nod^-	Catoira et al., 2000; Stracke et al., 2002; Miwa et al., 2006
Ljnin /Mtnin	RWP-RK TF	Nod^-	Schauser et al., 1999; Marsh et al., 2007
Ljpir1	SCAR/WAVE components	Nod^+ (white nodule)	Yokota et al., 2009
Ljnap1	SCAR/WAVE components	Nod^+ (white nodule)	Yokota et al., 2009

Table 1-1. Plant genes or mutants involved in rhizobial infection

Mtkce (*Mtlin-4*, specific allele of *Mtlin*)	E3 ubiquitin ligase	low Nod	Guan et al., 2013
Mtnf-ya1-1	CCAAT-binding TF	low Nod	Laporte et al., 2014
(g) Hyperinfection mutants with low or no nodulation			
Ljdaphne (specific allele of *Ljnin*)	RWP-RK TF	Nod^-	Yoro et al., 2014
Ljvag1	Subunit of topoisomerase VI	Nod^- / low Nod	Suzaki et al., 2014
Ljsuner1	Subunit of topoisomerase VI	low Nod	Yoon et al., 2014
Ljlhk1 (*Ljhit1*)	Cytokinin receptor	low Nod	Murray et al., 2007; Held et al., 2014
MtSYMREM1-RNAi	Plant-specific remorin protein	low Nod	Lefebvre et al., 2010
Mtlatd / Mtnip	NRT1 transporter	low Nod	Veereshlingam et al., 2004
Ljccamk-14 (specific allele of *Ljccamk*)	Calmodulin-dependent protein kinase	Nod^+ (white nodule)	Liao et al., 2012
(h) Hyperinfection mutants with hypernodulation			
Mtsickle	Ethylene signaling protein	Nod^{++}	Penmetsa and Cook, 1997; Penmetsa et al., 2003
Mtefd	AP2/ERF TF	Nod^{++}	Vernie et al., 2008
MtPUB1-RNAi in *Mtlyk3-4*	E3 ubiquitin ligase	Nod^{++}	Mbengue et al., 2010

Abbreviations (gene / mutant names): Nod factor receptor 1 (NFR1); LysM receptor kinase 3 (LYK3); Hair curling (HCL); Nod factor receptor 5 (NFR5); Nod factor perception (NFP); Symbiosis (SYM); Flotillin (FLOT); Plasma membrane intrinsic protein (PIP); Does not infection 1/2/3 (DMI1/2/3); Symbiotic remorin 1 (SYMREM1); Nodule inception (NIN); ERF required for nodulation (ERN); Branching infection threads 1 (BIT1); poodle (pdl); Nodulation pectate lyase; infection-thread deficient (itd); 121F-specific p53 inducible RNA (PIR1); Nck-associated protein 1 (NAP1);

Table 1-1. Plant genes or mutants involved in rhizobial infection

Actin-related protein component 1 (ARPC1); Required for infection thread (RIT); Lumpy infections (LIN); Interacting protein of DMI3 (IPD3); Rhizobium-directed polar growth (RPG); Vapyrin (YPY); Lateral root organ-defective (LATD), Numerous infections and polyphenolics (NIP); Nuclear Factor Y (NF-Y); Heme-Activated protein 2-1 (HAP2-1); Scarecrow-like13 Involved in Nodulation (SIN1); Symbiosis receptor-like kinase (SYMRK); aberrant localization of bacteria inside nodule 1 (alb1); Ca^{2+}/calmodulin-dependent protein kinase (CCaMK); Nodulation signaling pathway 1/2 (NSP1/2); Cytokinin Response (CRE); Lotus histidine kinase (LHK); Nodule-specific RING-H2 finger protein (nsRING); ρ-related GTPases of plants (ROP); Seven in absentia (SINA); low nodulation and trichome distortion (lot1); crinkle (crk); altered nodule primordium invasion (api); Ethylene response factor required for nodule differentiation (EFD); knocks but can't enter (kce); vagrant infection thread 1 (vag1); sunergos 1 (suner1); Plant U-box E3 ubiquitin ligase 1 (PUB1)

Abbreviations (etc.): *Lotus japonicus (Lj)*; *Medicatgo truncatula (Mt)*; *Pisum sativum (Ps)*; *Phaseolus vulgaris (Pv)*; *Sesbania rostrata (Sr)*; Infection thread (IT); Not determined (N.D.); Transcription factor (TF); Ethylene Responsive Factor (ERF); Suppressor of cAMP receptor / Wiskott-Aldrich syndrome protein (SCAR/WAVE); Actin-related protein (ARP); Major sperm protein (MSP); Nitrate transporter (NRT); GAI, RGA, and SCR members (GRAS); Really interesting new gene (RING); Non-nodulation (Nod^-); Decreased nodulation (low Nod); Normal number of nodules (Nod^+); Increased nodulation or hypernodulation (Nod^{++})

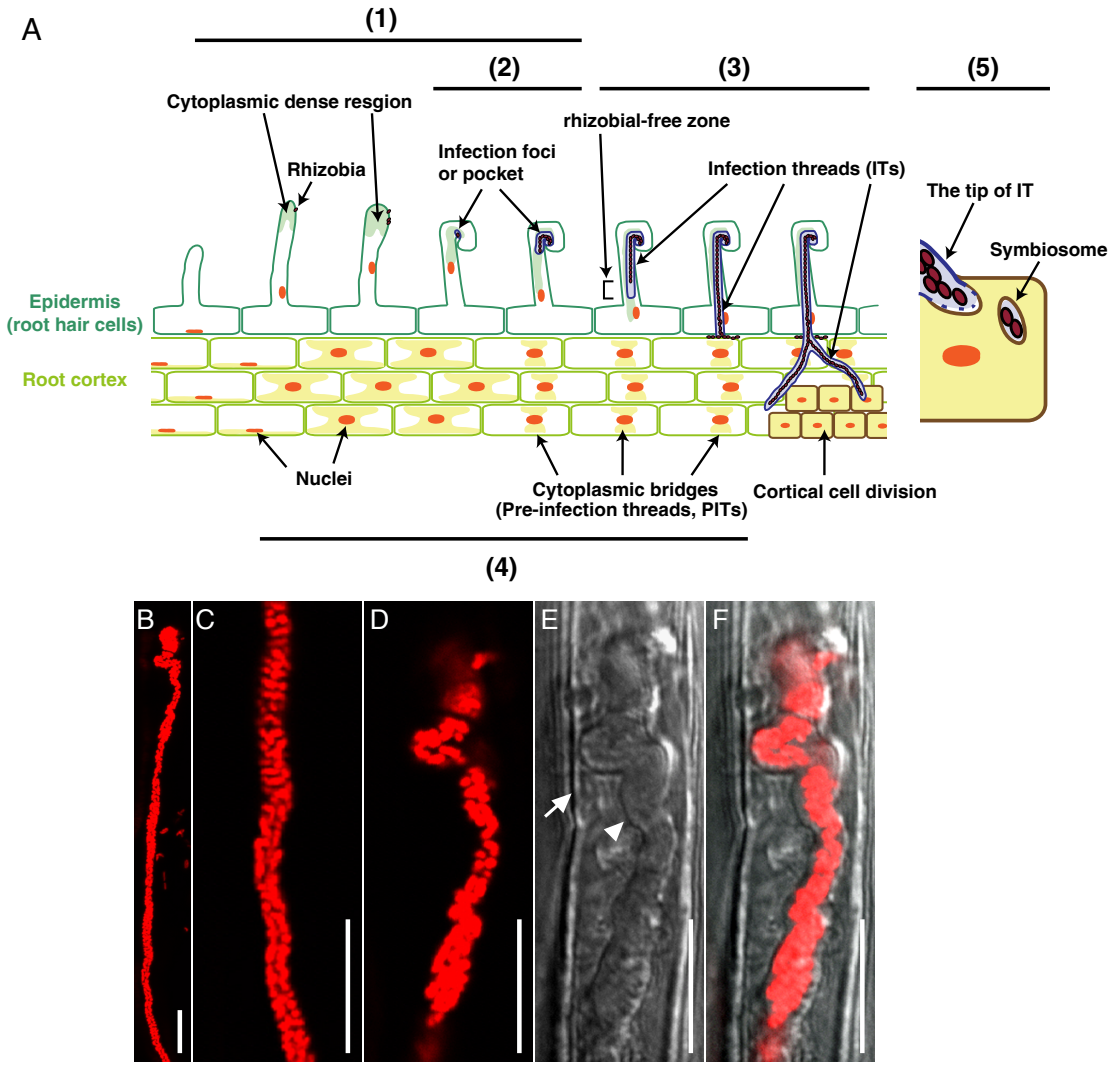

Figure 1-1. The major events of nodulation in epidermis and root cortex.

A, Outline of nodulation: (1) Rhizobial attachment to root hair and accumulated Nod factor induce initial responses involving root hair deformation and curling. (2) At the tightly curled root hair, cell wall degradation occurs and invagination of the IT membrane in the root hair cell is induced. (3) IT elongation occurs, which is accompanied by cytoplasmic streaming and nuclear movement. (4) During rhizobial infection [(1)-(3)], in the root cortical cells, a cytoplasmic bridges or preinfection thread (PITs) are formed to guide elongating ITs. In the activated cortex, re-initiation of cell division occurs, termed cortical cell division (CCD). (5) When an IT reaches the newly divided cortical cell, the IT membrane collapses and rhizobia are released into the cortical cell to form a specialized nitrogen-fixing organelle, the symbiosome. A confocal microscopic image of IT (B), magnified images of B (C,D), a bright-field image of D (E), a merged image of D and E (F) are shown. Red round-like structure represents rhizobia. Arrow and arrowhead indicate root hair membrane and IT membrane, respectively. Scale bars = 10 μm.

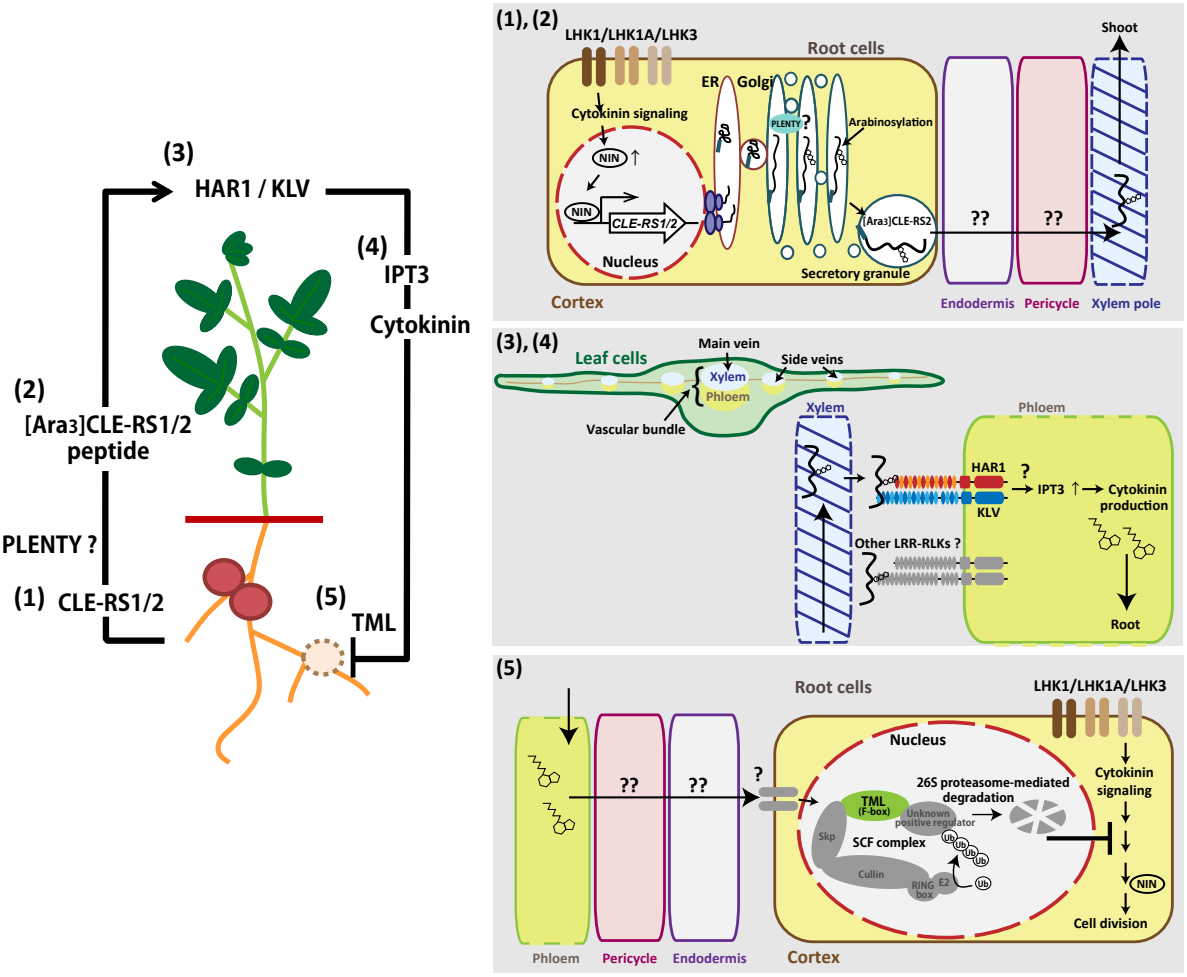

Figure 1-2. Current model of the long-distance control of nodulation.

(1) Nodulation signaling pathway, particularly downstream of cytokinin receptors, which ultimately activate *NIN* expression. The NIN transcription factor activates *CLE-RS1/2* expression through direct binding to their promoter. (2) It is likely that the CLE-RS1/2 peptides are post-translationally modified with triarabinoside, a reaction mediated by an enzyme similar to *At*HPATs in the Golgi apparatus. A strong candidate of the enzyme thought to be PLENTY. These modified CLE-RS peptides are transported to the xylem by an unidentified mechanism. (3) These peptides are transmitted from roots to shoots and directly bind to HAR1 or a putative HAR1-KLV receptor complex in the phloem of leaf cells. The other receptors might function in a parallel pathway based on the molecular similarity to the shoot apical meristem maintenance in Arabidopsis. (4) Downstream of the CLE-RS/HAR1 signaling pathway, activated IPT3 produces cytokinin, which is transported to roots through phloem tissue. (5) Shoot-derived cytokinin is directly or indirectly involved in proteasome-mediated degradation of an unidentified positive regulator of nodule organogenesis. TML may act as a component of the SCF complex. The site of AON action seems to be downstream of cytokinin signaling.

Chapter 2

A new interactive signaling pathway between rhizobial infection and organogenesis mediated by NODULE INCEPTION (NIN)

2.1. Introduction

As I mentioned above (**1.3.**, **1.4.**), it is essential for a successful symbiotic association that the two phenomena which are rhizobial infection and cell division proceed mostly at the same time in different root tissues, epidermis and root cortex (Crespi and Frugier, 2008; Madsen et al., 2010; Oldroyd, 2013). The two signaling pathways are tightly coupled, which has made it difficult to understand the two processes separately. Recently, however, the situation has been partially resolved by several reports. Firstly, Madsen et al. performed large-scale phenotyping of infection-defective mutations in the presence of two gain-of-function type mutations, *snf1* and *snf2* (Madsen et al., 2010). *snf1*and *snf2* has a mutation in *CCaMK* and *LHK1*, respectively. The introduced *snf1* mutation rescues defects of IT formation in *symrk*, *nup85*, *nup133*, *castor*, and *pollux*; but not those of *pir1*, *nap1*, *cyclops*, *cerberus*, *nsp1* and *nsp2*. Thus, CCaMK has the ability to induce rhizobial infection in the epidermis. The responsible genes of all unrescued mutants seem to work downstream of CCaMK (Madsen et al., 2010). Moreover, by characterization of those phenotypes, symbiotic genes in *L. japonicus* have been categorized into four groups: (1) genes for only infection, such as *NAP1*, *PIR1*, and *CERBERUS*; (2) genes for organogenesis and indirectly for infection, such as *SYMRK*, *NUP85*, and *POLLUX*; (3) genes for both infection and organogenesis, such as *NIN*, *NSP1*, and *NSP2*; (4) genes for cross-talk between infection and organogenesis,

such as *CCaMK* and *CYCLOPS*. All these are already introduced as factors required for rhizobial infection [**Chapter 1**, Table 1-1(c,d)].

Secondly, another approach in *M. truncatula* focuses on tissue-dependent requirements for *Mt*NFP/*Lj*NFR5 and *Mt*DMI3/*Lj*CCaMK using an epidermis- or cortex-specific promoter (Rival et al., 2012), and has led to the conclusion; (1) epidermal NFP is sufficient to induce cell division in the cortex, (2) epidermal DMI3 but not NFP is sufficient for rhizobial infection in the root hair and for activating cell division, and (3) epidermal and cortical expression of DMI3 is required for both processes. This part of the conclusion is also supported by another study in *L. japonicus* using a similar tissue-specific promoter system (Hayashi et al., 2014).

Thirdly, a study of *Ljsymrk* mutant alleles proposed different contributions of *Lj*SYMRK to each pathway depending on different protein domains (Kosuta et al., 2011). SYMRK may play an important role as a 'hub' for coordinating the two signaling pathways. Unlike typical non-nodulation *symrk* mutants, a unique allele *symrk-14* forms uninfected white nodule bumps with many arrested ITs (Kosuta et al., 2011). SYMRK consists of a cytosolic kinase domain and an ectodomain encompassing a malectin-like domain (MLD), GDPC motif, and three LRRs. Recent work revealed that the MLD domain is released by a cleavage reaction (Antolin-Llovera et al., 2014); *symrk-14* has a mutation within the GDPC motif, causing a defect in MLD release. Furthermore, a truncated SYMRK that lacks the MLD domain (SYMRK-ΔMLD) is able to interact with NFR5, but is rapidly degraded. Thus, SYMRK-ΔMLD is required for rhizobial infection, and control of SYMRK protein turnover may be essential for balancing the signal transduction pathways of infection and cell division.

Altogether, these studies have shown that the SYMRK-CCaMK-CYCLOPS signaling cascade has two roles: rhizobial infection in the epidermis and nodule organogenesis in root cortex. However, the tissue-specific role or cellular interactions between the epidermal event and the cortical event of transcription factors functioning in the downstream of SYMRK-CCaMK-CYCLOPS signaling, such as NIN, NSP1, and NSP2 remain still unclear.

Among mutants of these transcriptional factors, *nin* mutant is defective in both IT initiation and nodule formation. It is believed that *NIN*, a transcription factor containing a RWP-RK domain, functions in both the infection and organogenesis pathways (Schauser et al., 1999; Borisov et al., 2003; Marsh et al., 2007). The expression pattern of the *GUS* reporter gene driven by the *NIN* promoter *(ProNIN)* indicates that epidermal expression a short time after inoculation is correlated with rhizobial infection, whereas expression in the root cortex at a later stage contributes to cell division (Heckmann et al., 2011; Kosuta et al., 2011; Popp and Ott, 2011). *NIN* transcription is highly induced only after rhizobial inoculation, and constitutive expression of *NIN* can lead to the ectopic division of cortical cells in the absence of rhizobia. These results indicate that NIN plays a central role in nodule organogenesis (Schauser et al., 1999; Tirichine et al., 2007; Suzaki et al., 2012; Soyano et al., 2013). As cytokinin plays an important role in cortical cell division (**1.3.**), *NIN* expression is also highly induced by cytokinin. Interestingly, cytokinin activates the cortical expression of *NIN* but does not induce the epidermal expression, suggesting that cytokinin activates only the organogenesis pathway and not the infection pathway mediated by NIN (Heckmann et al., 2011).

In this chapter, I identified a novel *nin* mutant allele, named *daphne*, which showed the interesting phenotypes of non-nodulation and hyperinfection in *L. japonicus*. The mutant showed an altered expression pattern of *NIN*. In view of the relationship between the spatio-temporal expression pattern of *NIN* and the symbiotic phenotype of *daphne*, I proposed a new cellular communication model controlled by NIN involving in cross-talk between infection and organogenesis, for regulating rhizobial infection processes.

2.2. Results

2.2.1. Isolation of the *daphne* mutant, which showed non-nodulation and dramatically increased infection of rhizobia

To date several host genes necessary for nodule development have been identified (Madsen et al., 2010; Oldroyd, 2013). However, most of non-nodulation mutants have defect in both the rhizobial infection and organogenesis pathways, so that the molecular relationship between these two pathways and the mechanisms for controlling each pathway has remained obscure. To find new components involved in the infection or organogenesis pathways, in our laboratory a large screening for non-nodulation mutant had done from the ion-beam-mutagenized *L. japonicus* Miyakojima MG-20 seeds (3400 M1 lines) and evaluated their ability of rhizobial infection. I focused on a mutant, named *daphne*, displaying the novel phenotype of non-nodulation and hyperinfection. The *daphne* mutant was completely defective in nodule formation (Fig. 2-1A-C,J), being different from *hyper infected 1 (hit1)*, which was previously isolated as a hyperinfection mutant able to form a few nodules (Fig. 2-2) (Murray et al., 2007). In the *daphne* mutant, no nodules were observed even 28 days after inoculation (DAI) (Fig.

2-1A-C,J). *daphne* showed a typical non-nodulation phenotype, with pale-yellow leaves and growth delay under low-nitrogen conditions (Fig. 2-1A). However, in *daphne*, the number of ITs per root was dramatically increased, to 15-fold greater than that on the MG-20 wild type (Fig. 2-1D-G,I,K). In the wild type, ITs tend to be formed in small restricted regions called susceptible zone (Vasse et al., 1993; Penmetsa and Cook, 1997; Krusell et al., 2002; Gage, 2004). On the other hand, ITs were observed on almost all regions of *daphne* roots. This extended rhizobial susceptibility has been previously observed in the *nin* mutant as increased root hair deformation (Schauser et al., 1999) [**Chpater 1**, Table 1-1 (f)]. Additionally, IT elongation in *daphne* was visible in root hair but aborted and burst in the epidermal cell layer, and no cortical infection thread was observed (Fig. 2-3).

To identify the step of the organogenesis pathway that is blocked in *daphne*, I utilized the ability of spontaneous formation in *snf2* (Tirichine et al., 2007) (**1.3.**). I made *daphne snf2* double mutant and evaluated its ability of spontaneous nodule formation. The non-spontaneous nodule formation phenotype of the *daphne snf2* double mutant indicates that the non-nodulation phenotype of *daphne* is caused by defects downstream of cytokinin signaling (Fig. 2-1H,K).

2.2.2. Identification of *daphne* mutation by map-based cloning

I roughly identified two loci on chromosome II and III linked to the non-nodulation phenotype of *daphne* using a small F_2 mapping population by map-based cloning with a a series of genetic markers (http://www.kazusa.or.jp/lotus/markerdb_index.html/, Sandal et al., 2006) (Fig. 2-4). This result was apparently inconsistent with the observation that the F_2 population segregated in approximate 3:1 ratio, indicating that *daphne* is a

recessive mutant (Table 2-1). I further explored the locus using a large F_2 population with markers on linkage group III, and the translocation fusion point was identified by reverse transcription (RT)-PCR and genomic PCR (Table 2-2; Fig. 2-5; Fig. 2-6A,B). I finally detected the fused sequences originated from chromosome II and III in *daphne* genome by inverse PCR (Fig. 2-5C). This finding suggested that the ion beam irradiation had induced a reciprocal chromosomal translocation. The translocation points lie in the second intron of the *Translocase of the inner membrane (TIM)* gene (chr3.CM0423.360.r2.d) on chromosome III and in an intergenic region (IGR) on chromosome II. The IGR sequence on IGR lies approximately 7 kb upstream of *NIN*, which is known to be an essential gene for nodule development (Schauser et al., 1999). No mutation in *NIN* coding region was detected in the *daphne* genome.

2.2.3. *daphne* is a novel *nin* mutant allele, different from the *nin* null mutant

As described above, I determined two candidate loci responsible for the non-nodulation phenotype in *daphne*: *TIM* on chromosome III, and *NIN* on chromosome II. Although I introduced the coding sequence of *TIM* gene under the control of the ubiquitin promoter (*ProLjUBQ*) (Maekawa et al., 2008) by hairy-root transformation, the non-nodulation phenotype was not complemented (Fig. 2-6C-F). I next hypothesized that a translocation near the *NIN* locus causes the *daphne* phenotype, a notion supported by previous characterization of a *nin* mutant which displays non-nodulation and no IT formation (Schauser et al., 1999). By crossing *daphne* (accession Miyakojima MG-20) and *nin-2* (accession Gifu B-129), I tested whether *daphne* is a *nin* mutant allele. All *daphne* × *nin-2* F_1 plants originating from three independent seed pods exhibited the non-nodulation (Fig. 2-7A). The success of crossing experiments using pollen of *nin-2*

was judged by the accumulation of anthocyanin on stems, the dominant characteristic phenotype of Gifu B-129 (*nin-2*) (Fig. 2-7B). In terms of IT phenotype, normal infection phenotype of *daphne* × wild type F_1 plants and F_2 segregation ratio indicates that hyper-formation of ITs is also recessive (Table 2-1); nevertheless, *daphne* × *nin-2* F_1 plants showed hyperinfection (Fig. 2-7C,D). These results suggested that *daphne* and *nin-2* are allelic. Moreover, the excessive root hair deformation phenotype in *daphne* was similar to the phenotype of the *nin* mutant, but the *nin* could not form any IT as already reported (Fig. 2-7E-J). For the subsequent analysis described below, I used *nin-9* (Suzaki et al., 2012) as a canonical *nin* mutant because it has same genetic background as *daphne* (Miyakojima MG-20).

2.2.4. *daphne* has completely lost the *NIN* expression induced by cytokinin application

NIN is a putative key transcription factor that plays a role in the infection and nodule organogenesis pathways. The expression level of *NIN* is strongly elevated in an inoculation-dependent manner (Schauser et al., 1999). Because the allelism test showed that *daphne* was a *nin* mutant allele, I next investigated the *NIN* expression pattern in *daphne*. Expression in whole roots was slightly induced by inoculation with *Mesorhizobium loti*. The transcript levels of *NIN* at earlier stages were almost identical in the wild type and *daphne*, whereas at 7 DAI the level of *NIN* expression in *daphne* is almost 1/3rd of that in the wild type (Fig. 2-8A). The induction level of *NF-YA*, known as a downstream target of NIN (Soyano et al., 2013), also indicates that *daphne* partially retains the function of NIN, compared to almost no induction of *NF-YA* in a typical *nin* mutant, *nin-9* (Fig. 2-8B).

Next, I evaluated the cytokinin-induced expression level of *NIN*, finding it to be completely absent in *daphne* (Fig. 2-8C). This loss is in good agreement with the finding that the *snf2* mutation spontaneously activating cytokinin signal does not rescue the non-nodulation phenotype of *daphne* (Fig. 2-1H,K), because cytokinin is believed to induce only the organogenesis and not the infection pathway (Heckmann et al., 2011). The cytokinin-induced expression of *LjRR6* (den Camp et al., 2011) was detected even in *daphne*, suggesting that *daphne* retains the cytokinin responsiveness of genes other than *NIN* (Fig. 2-8D).

2.2.5. *daphne* shows broad epidermal expression patterns of *NIN*

How is the lower expression of *NIN* in the *daphne* mutant implicated in the increased number of IT? To identify the underlying mechanism of increased infection events, I investigated the spatial expression pattern of *NIN*. I cloned approximately 4 kb of *ProNIN* and approximately 2 kb of the *NIN* terminator (*TerNIN*) for promoter-*GUS* analysis. For 10 out of 14 *nin-9* plants, their IT formation was rescued by introducing the *ProNIN::NIN::TerNIN* construct. This indicated the *NIN* promoter was sufficient for the function of NIN at least as involved in rhizobial infection (Table 2-3; Fig. 2-7K,L). In the wild type, blue staining was restricted into several small epidermal regions of the root (Fig. 2-9A,C,E), as previously reported (Radutoiu et al., 2003; Kosuta et al., 2011). The inner cells of nodule primordia in the wild type were also stained, as observed previously (Fig. 2-9I) (Heckmann et al., 2011). In contrast, I observed a broad range, almost the whole root area, of *NIN* promoter activity in the *daphne* root (Fig. 2-9B,D,F). The broader activity of *ProNIN::GUS::TerNIN* in *daphne* coincided with the region where excessive root hair curling and IT formation occur (Fig. 2-9G,H).

2.2.6. Overexpression of *NIN* strongly represses the hyperinfection in *daphne*

The above result showed that *daphne* exerts broad *ProNIN*–activity in the epidermis, indicating a broader susceptible zone for rhizobial infection than in the wild type. Based on the results, I hypothesized that NIN itself negatively regulates rhizobial infection. To address the negative function, I accordingly overexpressed *NIN* under *ProLjUBQ* in *daphne* roots and observed the IT formation phenotype with *M. loti* expressing *DsRED*. Surprisingly, the hyperinfection phenotype of *daphne* was strongly suppressed in *NIN*-overexpressing transgenic roots, whereas *GUS*-overexpressing roots and non-transformed (GFP-negative) roots retained the excessive IT formation phenotype (Fig. 2-10A-C,E-G,I-K; Table 2-3). The hyperinfection phenotype of non-transformed roots indicates that the negative feedback regulation of IT formation is not long-distance signaling mediated by the shoot, in contrast to the regulation of number of nodules (Okamoto et al., 2009). I also observed no normal nodules, but some lateral roots with enlarged tips and bumps in *ProLjUBQ::NIN* transgenic roots in *daphne* (Fig. 2-11, Table 2-3) (Suzaki et al., 2012; Soyano et al., 2013).

Next, I confirmed the positive function of NIN in rhizobial infection in *daphne* mutant background. I expressed a chimeric protein of NIN and the SRDX domain, a transcriptional repressor domain in the Arabidopsis SUPERMAN repressor (Oshima et al., 2011). *ProLjUBQ::NIN::SRDX* dominantly repressed the target gene expression of *NIN* in MG-20 wild type, causing a reduction in the number of nodules (Fig. 2-12, Table 2-3). In *daphne*, the ITs almost disappeared only in *ProLjUBQ::NIN::SRDX* expressing transgenic roots (Fig. 2-10D,H,L; Table 2-3), phenocopying the previously observed phenotype of a typical *nin* mutant (Schauser et al., 1999; Marsh et al., 2007). This

suggests that *daphne* maintains the positive function of NIN in rhizobial infection, unlike a typical *nin* mutant.

These results indicate that NIN plays not only positive but also negative roles in IT formation, and *daphne* maintains the positive role, but loses the negative role. In contrast to *daphne*, MG-20 wild type plants formed a few number of ITs (less than 20 per root) (Fig. 2-1K), which may account for the observation that *ProLjUBQ::NIN* had apparently no strong suppressive effects on IT numbers in wild type (Table 2-3).

2.2.7. Cortical but not epidermal expression of *NIN* was specifically lost in *daphne*

Both positive and negative roles of NIN in rhizobial infection had now been demonstrated. To further investigate the underlying mechanism, I hypothesized that the positive and negative actions of NIN are generated by epidermis and cortex, respectively, given that the lack of cytokinin-induced NIN in *daphne* results in an increase in the number of ITs and a typical *nin* mutant does not form ITs. I speculated that a less negative role of NIN in IT formation (cytokinin-induced NIN) resulted in excessive IT formation.

To address the tissue-specific activity of NIN, I attempted to express *NIN* using a cortex- and endodermis-specific enhancer isolated from Arabidopsis J0571 (Miyashima et al., 2011). The J0571 enhancer element was identified from the Arabidopsis GAL4-GFP enhancer-trap lines. First, I tested the fluorescent marker (*mCherry* with *nuclear localization signal*, *NLS*) expressed by *J0571* in hairy roots of *L. japonicus*. Although no marker expression was detected in the epidermis, signal was detected in inner layers of the root, including cortex and endodermis (Fig. 2-13), suggesting that the cortex- and endodermis-specific expression of *J0571* is conserved in *L. japonicus*. Both

the non-nodulation phenotype and excessive IT formation in *daphne* were partially rescued by *J0571>>NIN* (Fig. 2-14, Table 2-3), confirming that the *daphne* phenotype was caused by the loss of *NIN* expression specifically in the cortex.

2.3. Discussion

2.3.1. Working model of positive and negative roles of NIN in nodulation

NIN was first identified as a gene responsible for the non-nodulation phenotype in legumes (Schauser et al., 1999). Since then, it has been believed that NIN, a putative transcription factor, plays a positive role in nodule organogenesis and IT formation. Meanwhile, the possibility has been discussed that NIN also has a negative role in the rhizobial infection processes, based on the excessive root hair response or the expanded *EARLY NODULIN 11* expression pattern in *nin* mutants and the lower expression of *NIN* in another hyperinfection mutant, *hit1-1* (Schauser et al., 1999; Marsh et al., 2007; Murray et al., 2007). In this chapter, I identified the *daphne* mutant, a novel *nin* mutant allele displaying excessive IT formation as well as non-nodulation. The spatio-temporal expression patterns of the *NIN* gene in *daphne* provided new evidence of negative feedback regulation of the infection process mediated by NIN. In *daphne*, the level of *NIN* transcription from whole roots was less than that in wild type. In contrast, the epidermal expression of *NIN* was broader than that in the wild type, indicating that the susceptible zone for rhizobial infection was enlarged in *daphne*. This increased susceptibility for infection could account for the excessive IT formation in *daphne*. Furthermore, although overexpression of *NIN* suppressed excessive infection, inner cell layer-specific expression of *NIN* rescued nodule formation in *daphne*. Based on these observations, I propose a negative feedback regulation of rhizobial infection mediated

by NIN (Fig. 2-15).

In this model, NIN plays two important roles, one in infection and the other in organogenesis. NIN functioning in infection is located in the epidermis in an earlier stage (in the susceptible zone) for proceeding with IT formation, whereas NIN functioning in organogenesis act in a later stage. NIN functioning in organogenesis has not only a positive role in promoting cell division in the cortex but also a negative role in inhibiting rhizobial infection. In *daphne*, owing to the loss of expression of such NIN functioning in organogenesis, the root area for rhizobial infection becomes broader. Several reports have already suggested that genes downstream of cytokinin signaling or *NIN* itself are involved in preserving the balance of the nodule symbiosis (Murray et al., 2007; Saur et al., 2011; Mortier et al., 2012a). My study has experimentally confirmed one of those mechanisms, a negative role of NIN in rhizobial infection. Excessive root hair curling of a typical *nin* mutant also may be explained by the working model of NIN.

Altogether, this model suggests that NIN may switch between positive and negative influence on rhizobial infection in different tissues or in nodule developmental stages. NIN could be controlling the balance between infection and organogenesis. In the next chapter (**Chapter 3**), I will analyze the downstream of the NIN-mediated IT control, comparing to the known long-distance control of nodulation.

2.3.2. Unidentified responsible element to induce *NIN* gene expression

Although NIN is a key transcriptional factor in nodule development, the functional *NIN* promoter region necessary for nodule organogenesis has not yet been elucidated. Only IT formation, and not nodule formation was rescued in *nin-9* by the introduction of

ProNIN(~4 kb)::NIN::TerNIN (Fig. 2-7K,L; Table 2-3). In this study, I identified a novel mutant allele of *nin*, *daphne* whose genome was changed approximately 7 kb upstream of NIN by chromosomal translocation (Fig. 2-5). These results raise at least two possibilities. One is that a *cis*-regulatory element necessary for the organogenesis pathway, including the cytokinin response element, has been lost from the upstream region of *NIN* in the *daphne* genome. In other words, a 7 kb segment of the *NIN* promoter region is sufficient for the function of NIN in the infection pathway. The other possibility is that epigenetic alteration leads to a different *NIN* expression pattern in *daphne*. Furthermore, *ProUBQ::NIN* induced aberrant roots including bumps in wild type, *daphne*, and *nin-9* (Fig. 2-11), but I failed to rescue IT formation in *nin-9* by the introduction of *ProUBQ::NIN* (Fig. 2-7M,N; Table 2-3). This implies that the induction mechanism of *NIN* transcript is more complex than so far anticipated; spatial and temporal expression of *NIN* may need to be strictly controlled in order to achieve its function in both infection and organogenesis pathways. The elucidation of the mechanism remains an important challenge.

In this chapter, a novel *nin* mutant allele, *daphne* was identified. I demonstrated that NIN, known to date as a positive factor for IT formation and nodule organogenesis, has a negative role in rhizobial infection processes. The multiple functions of the transcription factor NIN will afford an opportunity to investigate potential cross-talk between infection in the epidermis and cell division in the cortex during the course of establishment of the nodule symbiosis.

2.4. Materials and Methods

Plant materials and growth conditions

The *daphne* mutant was isolated by screening of M2 progeny derived from *L. japonicus* Miyakojima MG-20 wild type seeds mutagenized by irradiation with a carbon ion beam (C^{5+}). The details of the ion beam irradiation have been previously reported (Oka-Kira et al., 2005; Magori et al., 2009; Yoshida et al., 2010). Seeds were sown in sterilized vermiculite soaked in autoclaved vermiculite supplied with Broughton and Dilworth (B&D) solution (Broughton and Dilworth, 1971) containing 0.5 mM KNO_3 with or without *M. loti* MAFF 303099, respectively, under 16-h light/8-h dark cycles. Cytokinin treatment was applied by incubation of seedlings in vermiculite supplied with B&D solution containing 10^{-7} M benzylaminopurine (BAP) for 16 h. ITs were observed or counted after inoculation of rhizobia *M. loti* constitutively expressing *LacZ* (Yoshida et al., 2010) or *DsRED*. *nin-2* was kindly provided by Dr. Stougaard (Aarhus University, Denmark) (Schauser et al., 1999) and was used for the allelism test. *nin-9* (Suzaki et al., 2012) was used for gene expression analysis and complementation testing.

Microscopic observation

Bright-field and fluorescence images were viewed with an SZX12/16 stereomicroscope, BX50 microscope (Olympus). Images were acquired with a DP Controller (Olympus). Confocal images were viewed with an A1 confocal laser-scanning microscope (Nikon) and NIS Elements (Nikon).

The quantification of ITs

At 5 days after germination (DAG), plants were inoculated with *M. loti* constitutively expressing *LacZ.* At 7 DAI, roots were stained for beta-galactosidase activity. ITs on all parts of the root were counted under the microscope (BX50, Olympus).

Map-based cloning and inverse PCR in *daphne*

The *daphne* locus was mapped using F_2 progeny of *daphne* and Gifu B-129. Two loci located on LG II and LG III were identified using 52 F_2 plants. Fine mapping was performed in by 2048 F_2 plants. The newly developed genetic markers in this study are shown in Table 2-2. The deleted region located on CM0423 (chromosome III) was identified. *daphne* genomic DNA was extracted with a DNeasy Plant Mini Kit (Qiagen) and digested with EcoO109I, ApoI, and EcoRI. The digested DNA fragments were self-ligated with T4 DNA ligase (TaKaRa, Japan). Then, using inverse PCR analysis with two sets of primers designed on sequences in CM0423, the fused sequences originated from CM0423 (chromosome III) and CM0102 (chromosome II) was detected (Fig. 2-5). The primers used in inverse PCR analysis are shown in Table 2-4.

Gene expression analysis

Total RNA was isolated from each plant tissue using the RNeasy Plant Mini Kit (Qiagen). First-strand cDNA was prepared using a QuantiTect Reverse Transcription Kit (Qiagen). Real-time RT-PCR was performed using an ABI Prism 7000 (Applied Biosystems) with a THUNDERBIRD SYBR qPCR Mix (Toyobo, Japan) or with a QuanTitect SYBR Green RT-PCR Kit (Qiagen) according to the manufacturer's protocol. The expression of *UBIQUITIN* or *EF-1a* (GNf095a12) was used as the reference (Takeda et al. 2009; Groth et al.,2010). The primers used in expression analysis are shown in Table 2-4. The relative expression amount was calculated by the ΔΔ Ct method. Data are the mean ± S.D. of three biological replicates or three technical replicates.

Plant transformation

The recombinant plasmids were introduced into *Agrobacterium rhizogenes* strain AR1193 and were transformed into roots of *L. japonicus* by a hairy-root transformation method previously described (Okamoto et al., 2013b; http://www.bio-protocol.org/e795).

Cloning of *NIN* promoter constructs and promoter–GUS assay

A 1.7 kb gateway-cassette (GW) fragment was excised from DR5::GFP-NLS construct (Suzaki et al., 2012), and inserted into the *Bam*HI site of pCAMBIA1300-GFP, named pCAMBIA1300-GW-GFP. Next, the *GFP* in the vector was removed using *Xho*I, and PCR-amplified *GFP-LjLTI6b* (Suzaki et al., 2012) was inserted into the *Xho*I site to create a new binary vector pCAMBIA1300-GW-GFP-LjLTI6b. Then, using two sets of primers for amplification of approximately 4 kb of *ProNIN* and approximately 2 kb of *TerNIN*, two fragments were cloned into pCAMBIA1300-GW-GFP-LjLTI6b. In the final step, *GUS* in pDONR221 (Invitrogen) which was provided by Detlef Weigel, and the *NIN* cDNA in pENTR/D-TOPO (Suzaki et al., 2012) were inserted between the *ProNIN* and *TerNIN* by an LR recombination reaction (Invitrogen). A T-DNA construct expressing *ProNIN::GUS::TerNIN* was transformed into MG-20 and *daphne*. GFP fluorescence was checked as a marker for transformation. Transformed roots were inoculated with *M. loti* MAFF303099. At 7 DAI, a GUS staining procedure was performed as previously described (Jefferson et al., 1987).

Analysis of the IT phenotype with overexpressing NIN or chimeric repressor of

NIN

NIN cDNA without a stop codon in pENTR/D-TOPO was generated from *NIN* cDNA in pENTR/D-TOPO (Suzaki et al., 2012) by site-directed mutagenesis with primers (Table 2-4). A *GW::SRDX* fragment was amplified from the pDEST-BCKH plasmid (Oshima et al., 2011), and inserted between the KpnI and AscI sites of pUB-GFP (Maekawa et al., 2008), named pUB-GW-SRDX-GFP. *NIN* cDNA in pENTR/D-TOPO (Suzaki et al., 2012) and *NIN* cDNA without a stop codon were inserted into the GW site of pUB-GW-GFP (Maekawa et al., 2008) and pUB-GW-SRDX-GFP, respectively, with the LR recombination reaction (Invitrogen). As a control, *GUS* in pDONR221 (Invitrogen) was inserted into the GW site of pUB-GW-GFP by the LR recombination reaction (Invitrogen). *daphne* plants were treated with *M. loti* MAFF303099 constitutively expressing *DsRED*. At 14 DAI, ITs were observed.

Analysis of tissue specificity using a cortex- and endodermis-specific expression system

GAL4-VP16 and NOS terminator sequence with flanking genomic region were amplified by PCR from an enhancer trap line Arabisopsis J0571 (http://www.plantsci.cam.ac.uk/haseloff; http://www.arabidopsis.org/abrc/haseloff.jsp; Miyashima et al., 2011) and cloned into the HindIII site of pGWB501:5xUAS (Goh et al., 2012) using an In-fusion HD cloning kit (TaKaRa, Japan), named pGWB501:5xUAS-J0571. Next, *GW::SRDX::TerNOS* fragment was excised from pUB-GW-SRDX-GFP by KpnI and ScaI double digestion, and inserted into pCAMBIA1300-GFP, named pCAMBIA1300-GW-SRDX-GFP. A J0571-GAL4-VP16-TerNOS-5xUAS-35Sminimal promoter was amplified by PCR

from the template plasmid pGWB501:5xUAS-J0571 and inserted into the KpnI site of pCAMBIA1300-GW-GFP or pCAMBIA1300-GW-SRDX-GFP, named pCAMBIA1300-J0571-GW-GFP and pCAMBIA1300-J0571-GW-SRDX-GFP, respectively. In the final step, *NIN* and *mCherry-NLS* coding sequence (Suzaki et al., 2012), or *NIN* and *mKO2* coding sequence without a stop codon was inserted into the GW site of pCAMBIA1300-J0571-GW-GFP or pCAMBIA1300-J0571-GW-SRDX-GFP by the LR recombination reaction (Invitrogen). As a control, *mKO2* without a stop codon was amplified from the plasmid including *mKO2* [Medical and Biological Laboratories (Sakaue-Sawano et al., 2008)] by PCR, and cloned into pENTR/D-TOPO vector using a TOPO cloning kit (Invitrogen).Primers used for these constructs are listed in Table 2-4. At 21 DAI, nodules and ITs were observed in transformed hairy roots.

Table 2-1. The segregation ratio of mapping population and backcrossing population

Parental lines (female × male)	experiment	Total F_2 progeny analyzed	Nod+[a] IT(Low)[c]	Nod-[b] IT(++)[d]	X^2 value
daphne × Gifu B-129	1	383	299	84	0.84
	2	342	271	71	1.51
	3	232	193	39	4.22
daphne × Miyakojima MG-20	1	435	323	112	0.03

[a] $X^2_{0.05} = 3.84$ (df = 1)

[b] plants with wild type-like nodulated root.

[c] plants showing typical *daphne* phenotype, non-nodulation.

[d] plants with wild type-like infection thread number.

[e] plants showing typical *daphne* phenotype, highly increased infection thread number.

Table 2-2. The newly developed genetic markers list used for fine mapping in this chapter

marker	clone / contig	sequence before polymorphisms	polymorphisms		sequence after polymorphisms	primers for detecting polymorphism		restriction enzyme	length of fragment (bp)
			MG-20	B-129		direction	sequence		
EY001	BM2282	TCAGTAATGTTCTGCACAAG	T	C	ACTACATGGTACTTTATGAT	F	TCAGTAATGTTCTGC**G**C**T**AGTAC	NheI	MG-20, 171
						R	CACTACAATGGCACGCTAGG		B-129, 150+21
EY002	CM0423	ATCAGTTTAAGCATGACAA	-	TATAGCATAACAA (insertion)	ATGCTATTAAGTGTGAGTTG	F	TTGAAAGATCCAATTATTTTATGGAA	no	MG-20, 163
						R	CGATGGCATGATATTTTGATTT		B-129, 163+13
EY003	TM1993	TTTGCAAATTTGTCAAAGTA	A	T	GAAGCTGGATAAAATTGTGC	F	GATTTTGCAAATTTGTCAAAG**CT**	HindIII	MG-20, 149
						R	TTCGTCGACCGTATTTGACA		B-129 130+19

Table 2-3. The phenotypic effect of the expression of the NIN or NIN chimeric repressor in MG-20 wild type, *daphne*, and *nin*.

J0571>>NIN rescued non-nodulation phenotype. *ProLjUBQ::NIN* and *J0571>>NIN* inhibits hyperinfection in *daphne*. *ProLjUBQ::NIN::SRDX* showed the repression of both nodulation in MG-20 and infection in *daphne*. *ProNIN::NIN::TerNIN* rescued no infection phenotype of *nin*, yielding *NIN* promoter used in this study is sufficient for *NIN* expression for infection pathway. These important results are highlighted in **boldface**.

		Nodule			abLR[b]	Infection thread			
plant genotype	trans gene	+	Low[a]	-		++ [c]	Low[d]	-	total plants
MG-20	*ProLjUBQ::GUS*	20	0	0	0	0	20	0	20
	ProLjUBQ::NIN	19	0	0	10	0	19	0	19
	ProLjUBQ::NIN::SRDX	**5**	**7**	**6**	5	0	18	0	18
	J0571>>mCherry-NLS	20	0	0	0	0	20	0	20
	J0571>>NIN	20	0	0	3	0	20	0	20
daphne	*ProLjUBQ::GUS*	0	0	18	0	18	0	0	18
	ProLjUBQ::NIN	0	0	20	4	**0**	**18**	**2**	20
	ProLjUBQ::NIN::SRDX	0	0	19	2	**3**	**14**	**2**	19
	J0571>>mCherry-NLS	0	0	25	0	25	0	0	25
	J0571>>NIN	**6**	**0**	**17**	6	13	10	0	23
nin-9	*ProLjUBQ::GUS*	0	0	15	0	0	0	15	15
	ProLjUBQ::NIN	0	0	6	5	0	0	6	6
	ProNIN::NIN::TerNIN	0	0	14	0	0	**10**	**4**	14
	J0571>>NIN	0	0	22	2	0	0	22	22

[a] Roots with small size and number of nodules (Fig. 2-12). [b] Roots with aberrant lateral root such as enlarged tips and bumps (Fig. 2-11). [c] Roots with typical *daphne* phenotype, highly increased infection thread number. [d] Roots with wild type-like infection phenotype, normal infection thread number.

Table 2-4. Primers used in this chapter

Use	Primer Name	Sequence	References
Inverse PCR	TIM22_head_R1	TTGTTTTCAACAAGGTACTAATGCG	
	TIM22_head_R2	CAGCCTATGACAACCCTAGT	
	TIM22_head_F1	TGGCTGTATTGTAAACACTTCCG	
	TIM22_head_F2	TTCAATAAG GTATCGAGAGCAGTC	
	TIM22_tail_R1	ATGCACTTCACCAACAAGCAATT	
	TIM22_tail_R2	GTCTATCAATCACCAAAAGTAAGCA	
	TIM22_tail_F1	GCTTTTTAGGAGGTCATCTTGGA	
	TIM22_tail_F2	TCCGATACTCCGTGATCTTTG	
Real-time RT-PCR	NIN_F	TGGATCAGCTAGCATGGAAT	Groth et al., 2010
	NIN_R	TCTGCTTCTGCTGTTGTCAC	Groth et al., 2010
	NF-YA_F	GAAGCTGCTTCAACCTTAAAGTC	Soyano et al., 2013
	NF-YA_R	CGAGATGTAGAACTGAACTTGTCA	Soyano et al., 2013
	RR6_F	GATGAGCAGAAGAAACACGAGCC	Ishida et al., 2009
	RR6_R	AGGTTCACTTCTGCATCCTGTTG	Ishida et al., 2009
Construction	NINpromoter_F	AAAAGAGCTCACCCAAACTGGAATTAAGCC	
	NINpromoter_R	AAAAGAGCTCGCTAGCTGATCCAATTAAGT	
	NINterminator_F	AAAAACTAGTCATAA -CACCAATTCTCTGCT	
	NINterminator_R	AAAAGTCGACCTGACATCTCACGTCGAGC	
	pGWB501-J0571_F	GGCCAGTGCCAAGCTTAGTGAAAGCTGAGAAAGCAGAAAGAAGGAC	
	pGWB501-NOSter_R	GCAGGCATGCAAGCTTCCGATCTAGTAACATAGATGACACCGCGC	
	J0571-35Smini_F	TTTTGGTACCAGTGAAAGCTGAGAAAGCAGAAA	
	J0571-35Smini_R	TTTTGGTACCCAGGTCGTCCTCTCCAAATG	
	mKO2_F	CACCATGGTGAGTGTGATTAAACCAGAGA	
	mKO2_delta-stop_R	GGAATGAGCTACTGCATCTTCTACC	
	NINCDS_F	CAATAGCAGCCCATCTAAGGGTGGGCGCGCC	
	NINCDS_delta-stop_R	GGCGCGCCCACCCTTAGATGGGCTGCTATTG	
	GW-SRDX_F	GGGGTACCGGATCCACAATTACCAACAACA	
	GW-SRDX_R	GGCGCGCCCGACTTAAGCGAAACCCAAA	
the expression of *TIM* gene	TIM_CM0423.360_F	ATGGGTTCTGAGAATCAAGGA	
	TIM_CM0423.360_R	TCAAGATTCTTCTTCCTTAG	
	CM0423.60.r2_F (control)	ATGGTTTTAACAGGTAAAGTTGTC	
	CM0423.60.r2_R (control)	CTAAGCCTTTAGAAGATGAGCA	

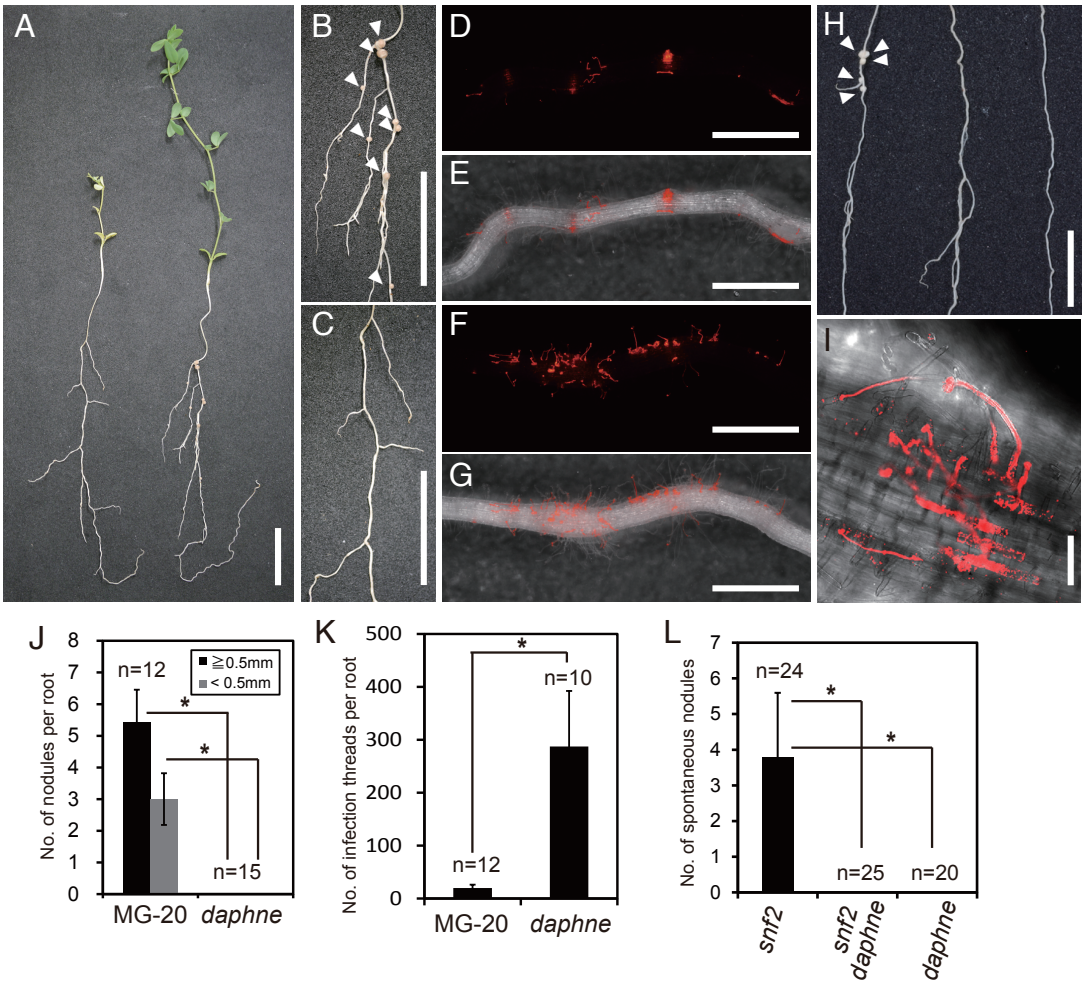

Figure 2-1. Isolation of a novel non-nodulation mutant, *daphne*.

A, Shoot and root phenotype of the *daphne* mutant (left) and the Miyakojima MG-20 wild type (right) at 28 DAI. B, Nodulation phenotype of MG-20. Arrowheads indicate nodules. C, The non-nodulation phenotype of *daphne*. D-G, IT phenotypes of the MG-20 root (D,E) and of the *daphne* root (F,G,I) following inoculation with *M. loti* MAFF303099 constitutively expressedsing *DsRED*. Red fluorescence images of roots (D,F). Linear red signals indicate ITs. Red fluorescence images and transmitted light images are merged (E,G,I). H, Spontaneous nodule formation in *snf2* (left), the *daphne snf2* double mutant (middle), and the *daphne* mutant (right). Arrowheads indicate spontaneous nodules. I, Confocal microscopic image of *daphne* root. z-stack series are in Fig. 2-3. J, Nodules were counted at 28 DAI with *M. loti* MAFF303099. K, The number of ITs per root was counted at 7 DAI with *M. loti* MAFF303099 constitutively expressing *LacZ*. L, Six weeks after germination, spontaneous nodules were counted without rhizobial infection under a no-nitrogen condition. Scale bars = 2 cm in A-C,H; 1 mm in D-G. Error bars indicate S.D. **P* < 0.05, Student's *t*-test.

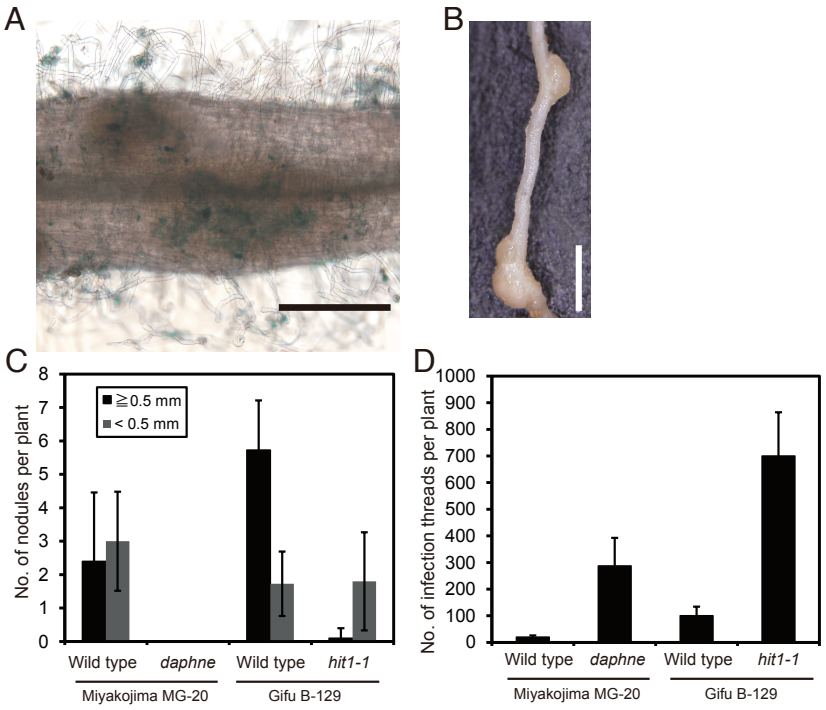

Figure 2-2. The phenotype of nodule formation in *hit1-1* mutant.

A, *hit1-1* mutant root with *M. loti* MAFF303099 constitutively expressing *lacZ*. B,C, Low nodulation phenotype of *hit1* at 7 DAI. D, Hyper-infection phenotype of *hit1-1* with Gifu B-129 (the parent ecotype of *hit1-1*). Nodules and ITs were counted at 7 DAI. Scale bars = 100 μm in A; 200 μm in B.

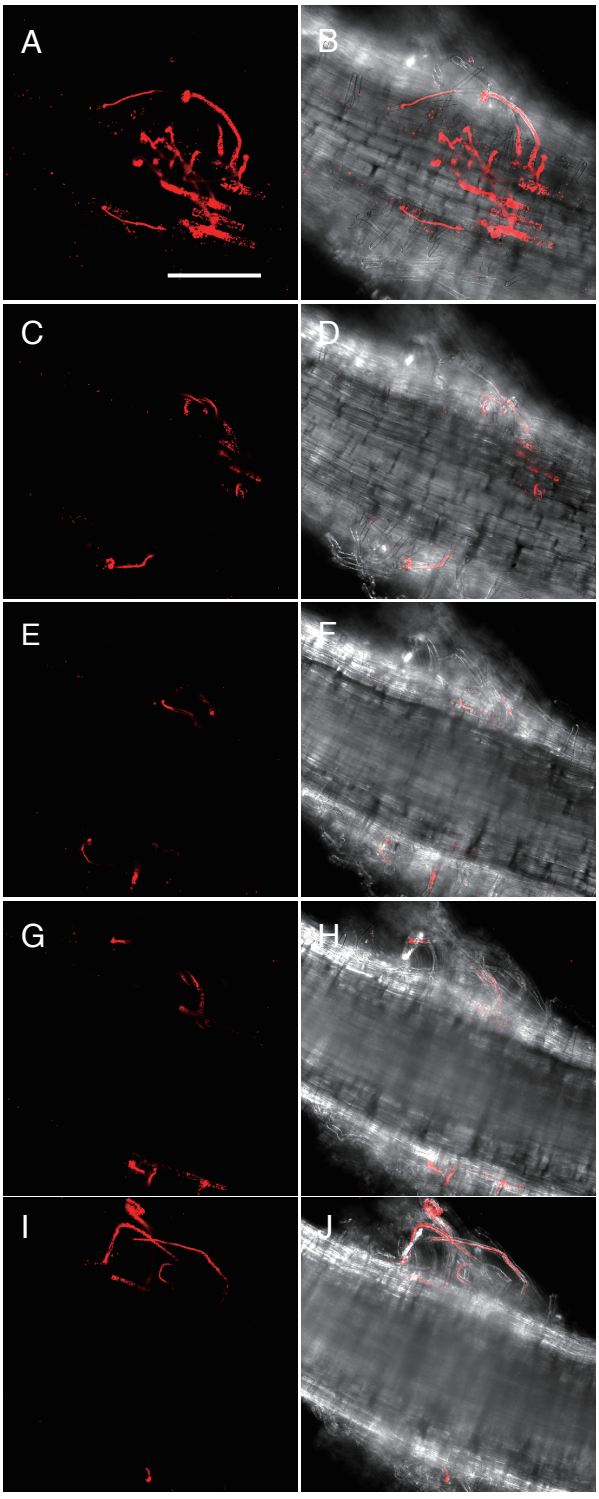

Figure 2-3. Z-stack images of the same area of *daphne* root.

daphne mutant root with *M. loti* MAFF303099 constitutively expressing *DsRed* at 7 DAI. Z distances between each image are 25 μm, from epidermal cell layer (A,B) to inner cellular tissues (I,J). Red fluorescence images are rhizobia included in infection threads (left column) and merged images with transmitted light images (right column). All images were captured in the same area of the root using confocal microscopy. Scale bars = 100 μm.

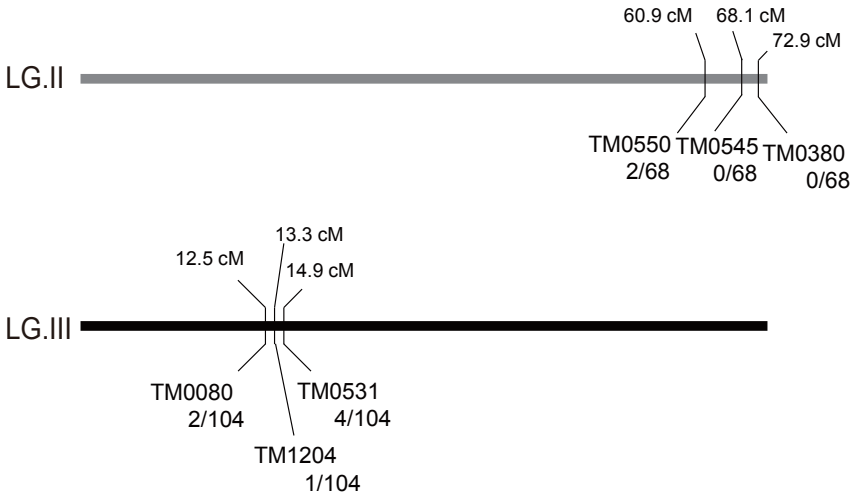

Figure 2-4. The two loci responsible for non-nodulation of *daphne* by rough mapping.
The *daphne* locus was roughly mapped using F_2 progeny of *daphne* and Gifu B-129. The two loci responsible for *daphne* on linkage group (LG) II (gray) and LG III (black) are indicated with the number of recombination events (events / total chromosomes).

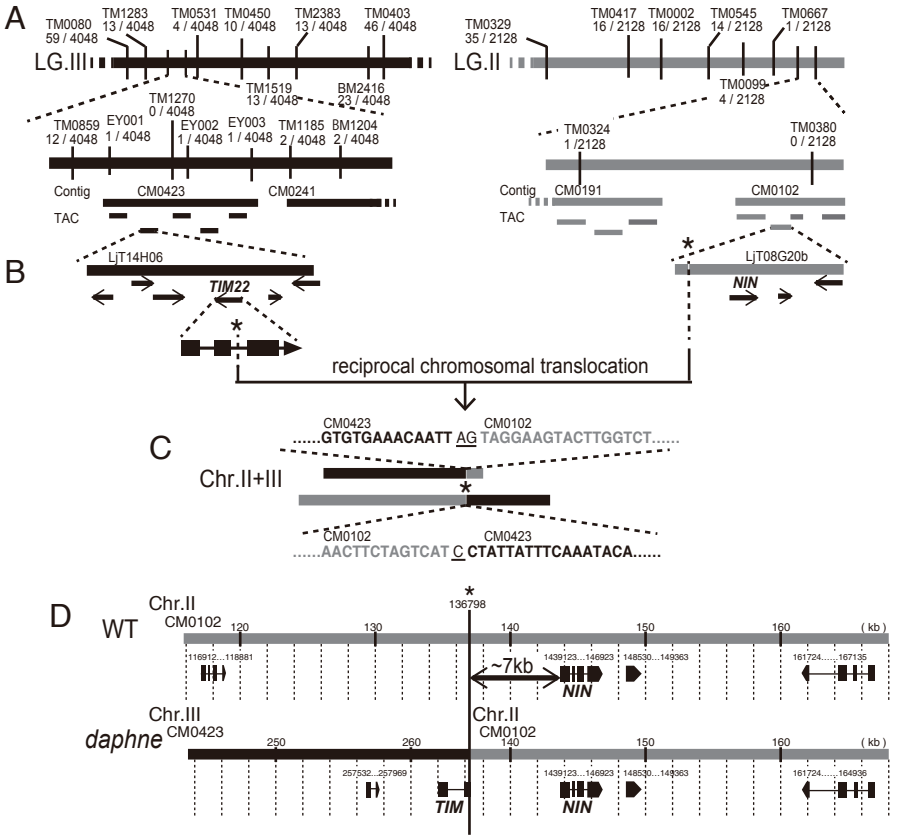

Figure 2-5. Identification of the *daphne* mutation.

A, Two genetic linkage maps of the regions of *daphne* loci in LG III (black, left) and LG II (gray, right). The newly developed markers (EY001-3) are shown in Table 2-2. The number of recombination events (events / total chromosomes) is indicated. B, Physical maps of TAC clone LjT14H06 (black, left) and TAC clone LjT08G20b (gray, right). Arrows indicate the annotations from miyakogusa.jp release 2.5 (http://www.kazusa.or.jp/lotus/; Sandal et al., 2006). C, Outline of chromosomal translocation between chromosomes (Chr.) II and Chr. III with sequences at the fusion point identified by inverse PCR amplified from the *daphne* genome. Black letters indicate the bases from CM0423 (Chr. III) and gray letters indicate the bases from CM0102 (Chr. II). Bases of unknown chromosomal origin are indicated by underlined letters. D, The location of translational fusion point in the contigs with gene annotations (exon shown as block and intron shown as thin line). Numbers on a ruler indicate the exact points (kb) in each contig. Asterisks (*) indicate the reciprocal chromosomal translocation points of each locus.

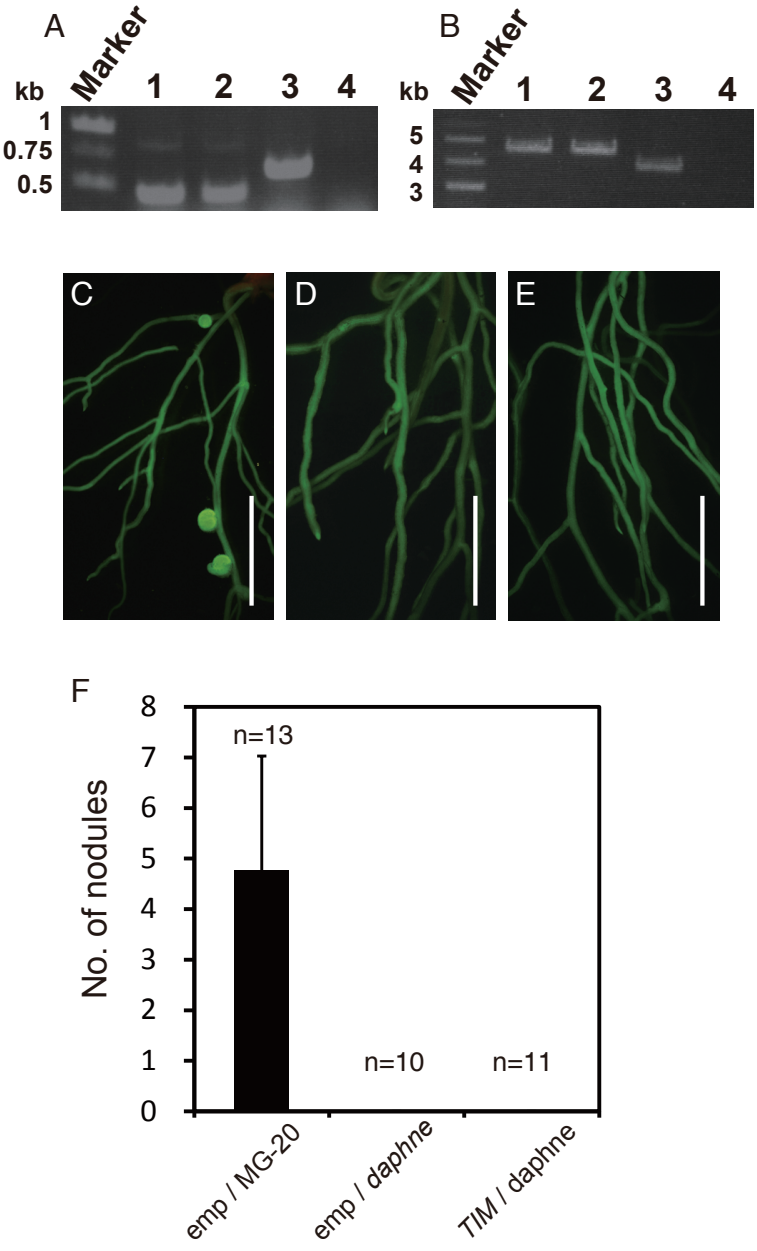

Figure 2-6. The result of complementation tests by the constitutive expression of *TIM*. Agarose gel electrophoresis of RT-PCR (A) and genomic PCR (B) products. The cDNA or DNA template are MG-20 (Lane 1,3) and *daphne* (Lane 2,4). The DNA fragment amplified with forward and reverse primer of a control gene (Lane 1,2) and *TIM* (chr3.CM0423.360.r2.d) (Lane 3,4). Primer sequences are shown in Table 2-4. B-D, The complementation test of non-nodulation phenotype of *daphne*; the control empty vector (C,D) and T-DNA containing *ProLjUBQ::TIM* (E) were introduced in MG-20 (C) and *daphne* (D,E) by hairy root transformation. F, The number of nodules was counted at 21 DAI.

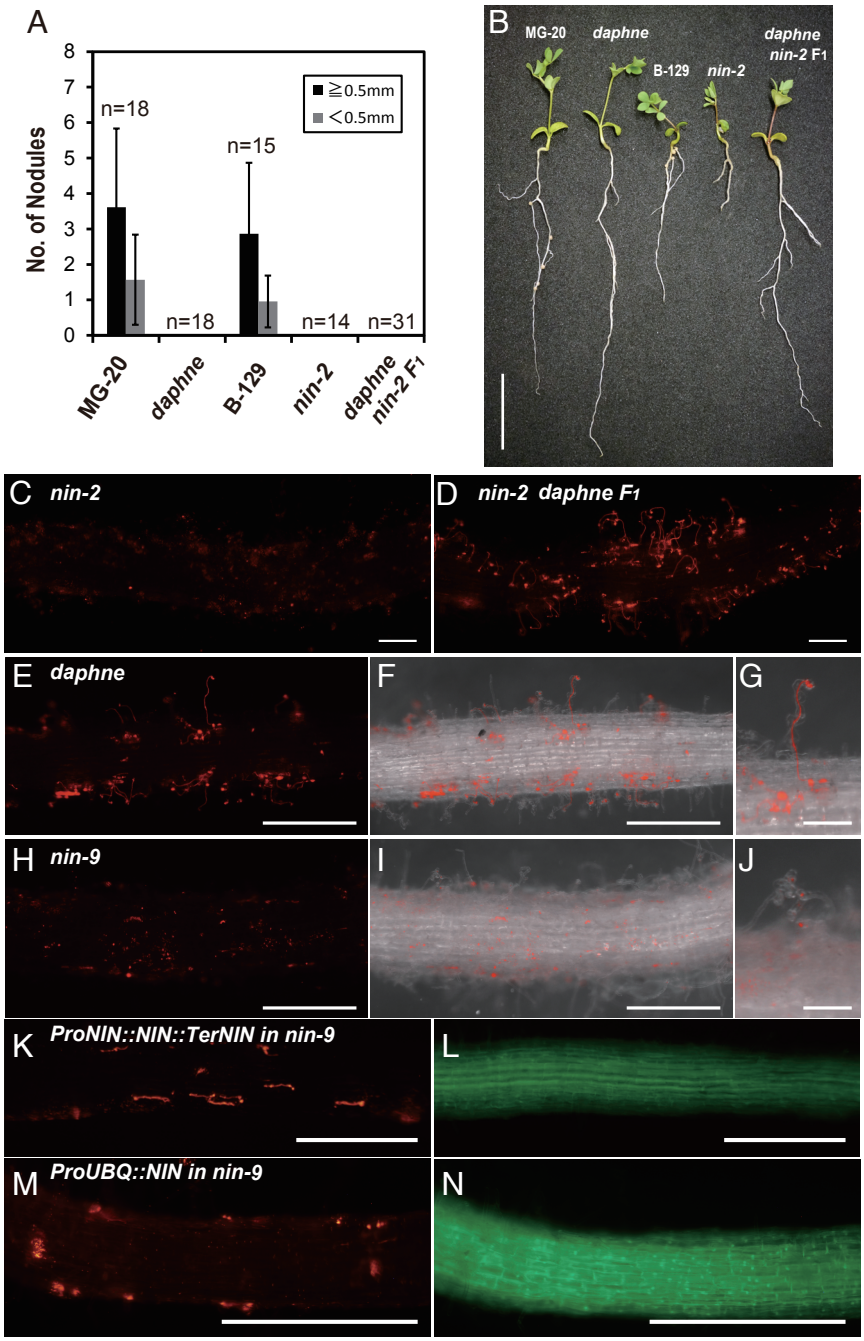

Figure 2-7. *daphne* is a novel *nin* mutant allele.

Allelism tests by crossing *daphne* and *nin-2* mutants. Nodules were counted at 14 DAI on each plant root (A,B). The anthocyanin accumulations on stems were observed in Gifu B-129 background, including *nin-2* and *daphne* × *nin-2* F_1. C-J, Root images inoculated with *M. loti* MAFF303099 constitutively expressing *DsRED*. Red fluorescence images (C,D,E,H) and red fluorescence images merged with transmitted light images (F,G,I,J). T-DNA containing *ProNIN::NIN::TerNIN* (K,L) and *ProLjUBQ::NIN* (M,N) were introduced in *nin-9* by hairy root transformation. GFP fluorescence was checked as a marker for transformation. Each genotype or transgene is shown in each panel. Scale bars = 2 cm in B; 200 μm in C,D; 500 μm in E,F,H,I,K-N; 50 μm in G,J.

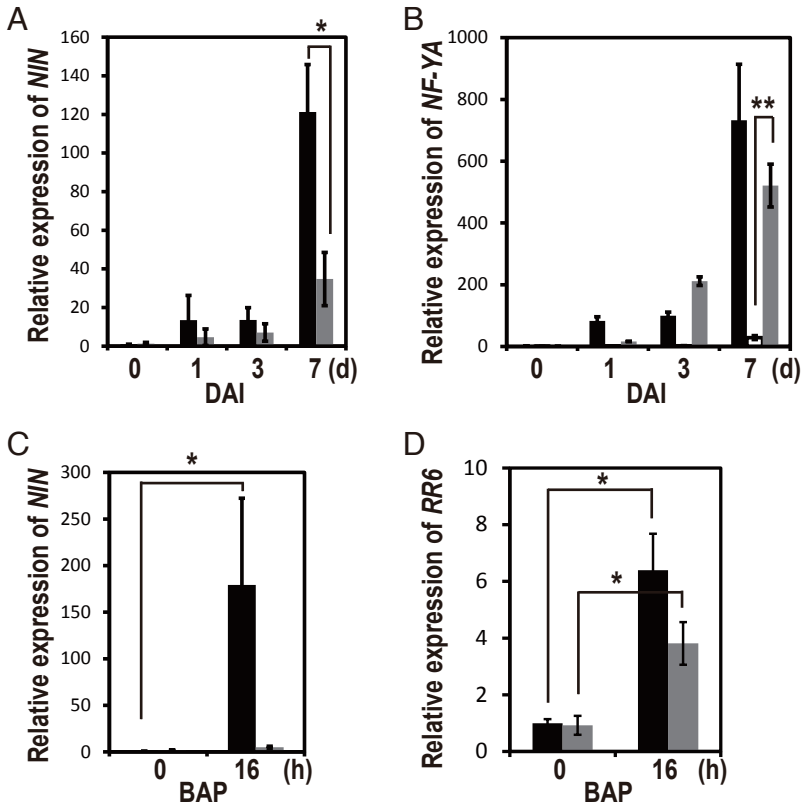

Figure 2-8. The altered expression patterns of *NIN* in *daphne.*

Quantitative real-time RT-PCR analysis of *NIN* (A,C), *NF-YA* (B) and *RR6* (D) expression in the MG-20 wild type (black bars), in *daphne* (gray bars) and in *nin-9* (white bars) at non-inoculated (0), 1, 3, and 7 DAI (A,B), or dependent on cytokinin treatment (10^{-7} M benzylaminopurine (BAP) for 16 h (C,D). Each cDNA was prepared from total RNA derived from whole root. Fold changes in expression are shown relative to roots at 0 DAI (A,B) or before cytokinin treatment (C,D). Error bars indicate S.D. of three biological replicates. **P* < 0.05, ***P* < 0.01, Student's *t*-test.

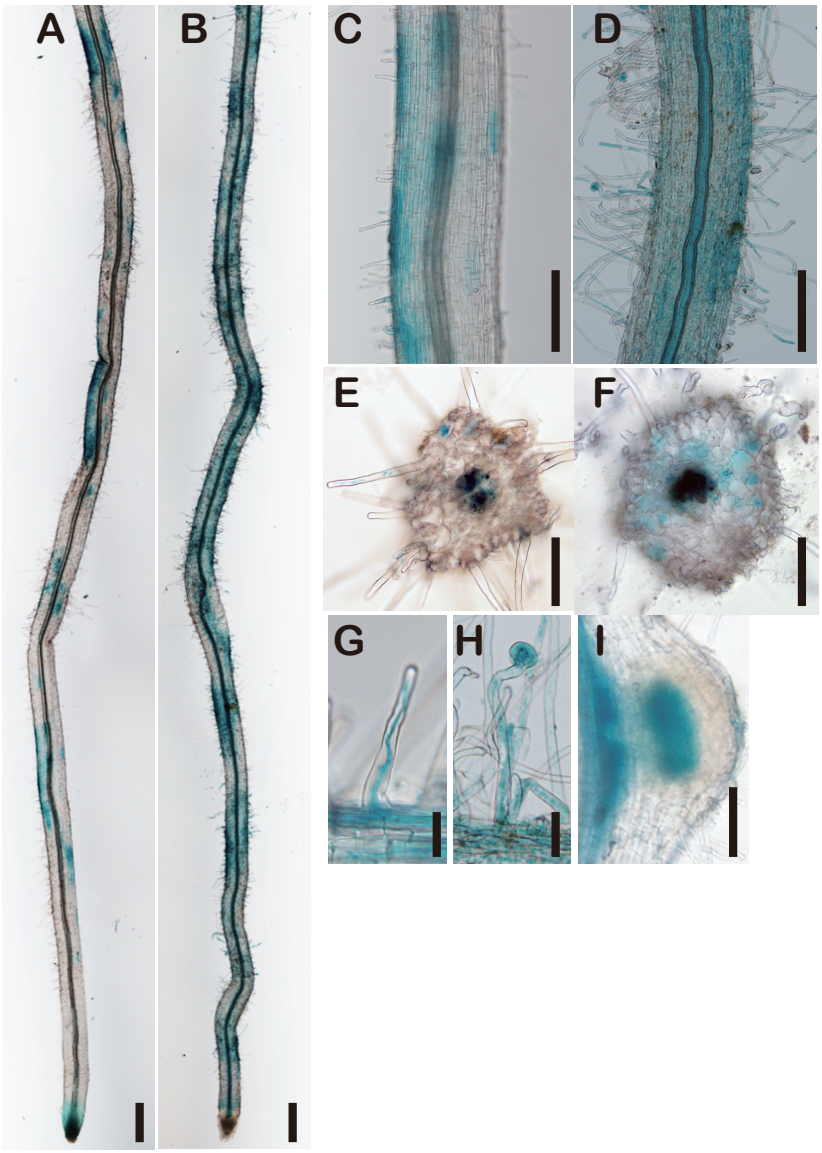

Figure 2-9. Spatial expression analysis of the *NIN* gene.

GUS staining images of *Agrobacterium rhizogenes*-mediated transformed roots with *ProNIN::GUS::TerNIN* at 7 DAI (with *M. loti* MAFF303099) on MG-20 wild type (A,C,E,G) and *daphne* (B,D,F,H). Blue staining was observed with transformed (GFP-positive) hairy roots in susceptible zones (A-F), including root hair cells (G,H) and immature nodule in wild type (I). Scale bars = 0.5 mm in A-D; 0.1 mm in E-I.

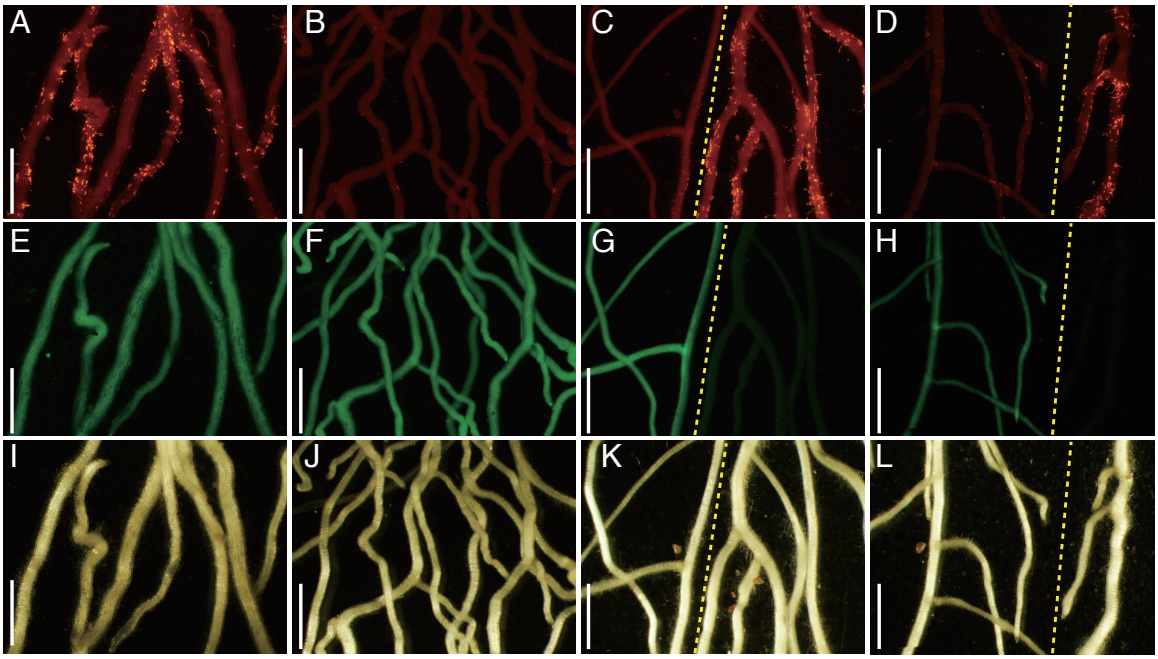

Figure 2-10. Overexpression of the *NIN* gene strongly suppresses excessive IT formation in *daphne*.

Red fluorescence images (A-D), GFP fluorescence images (E-H), and transmitted light images (I-L) of *A. rhizogenes*-mediated transformed *daphne* roots at 21 DAI. Transformed with negative control vector *ProLjUBQ::GUS* (A,E,I), *ProLjUBQ::NIN* (B,C,F,G,J,K), *ProLjUBQ::NIN::SRDX* (D,H,L). ITs were observed by inoculating *M. loti* MAFF303099 constitutively expressing *DsRED* (A-D). Green fluorescent protein fluorescence showed transformed roots (E-H). Yellow dashed lines indicate the border between transformed and non-transformed roots. Scale bars = 2 cm.

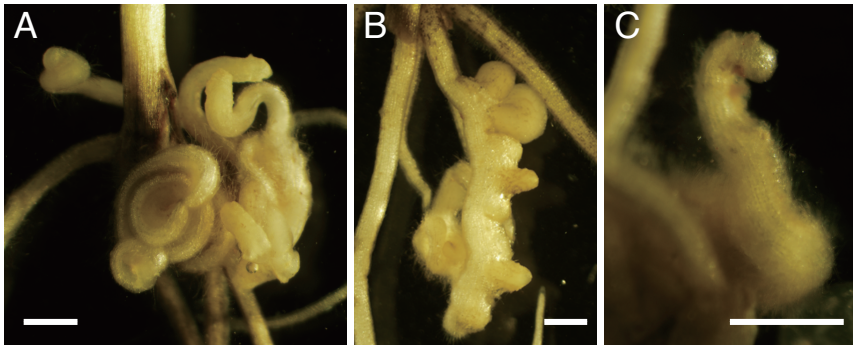

Figure 2-11. Enlarged bumps and tips were induced by over-expressing *NIN* in both MG-20 and *daphne.*

Transmitted light images of enlarged bumps and tips of transformed roots with *ProLjUBQ::NIN* in MG-20 (A), *nin-9* (B) and *J0571>>NIN* in *daphne* (C). Scale bars = 1 mm in A-C. Those structures were observed by inoculating *M. loti* MAFF303099 constitutively expressing *DsRED*.

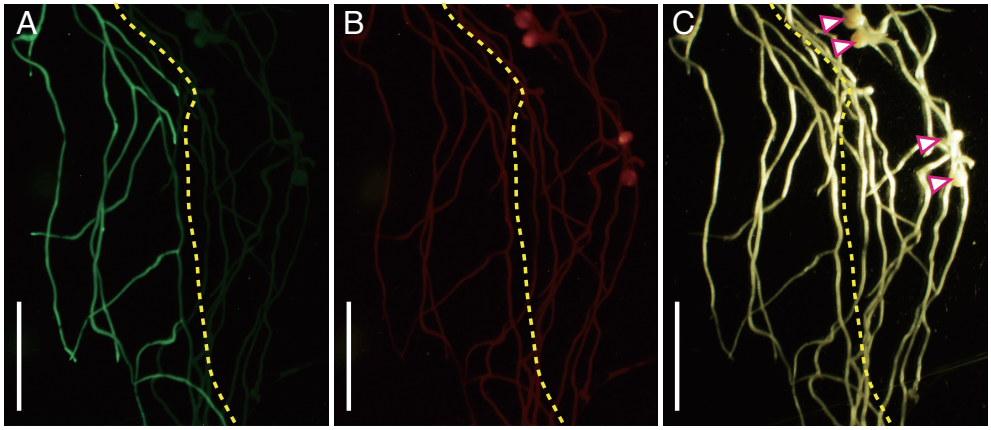

Figure 2-12. Nodule organogenesis was decreased in *ProLjUBQ::NIN::SRDX*-expressing roots.

GFP fluorescence images (A), red fluorescence images (B), and transmitted light images (C) showed nodulation phenotype of the MG-20 wild type inoculated with *M. loti* MAFF303099 constitutively expressing *DsRED*. T-DNA containing *ProLjUBQ::NIN::SRDX* were introduced in MG-20 by hairy root transformation. GFP fluorescence showed transformed roots (A,D,G). Yellow dashed lines indicate the border between transformed and non-transformed roots. Arrowheads indicate nodules. Scale bars = 5 mm in A-C.

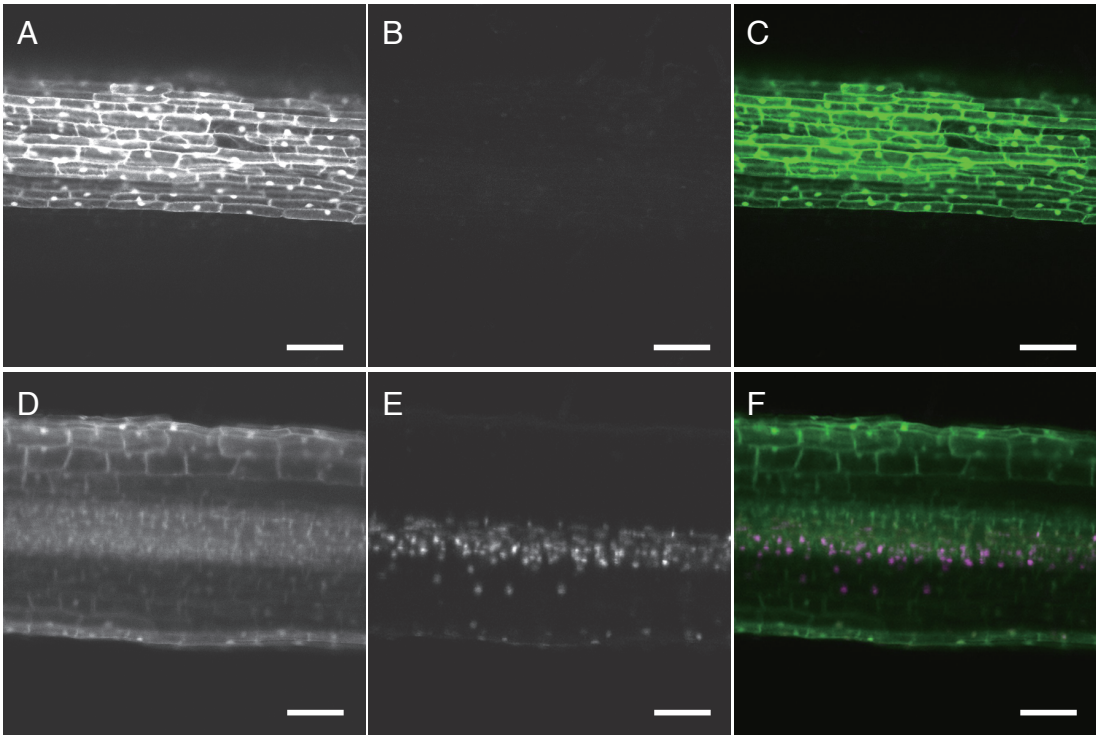

Figure 2-13. The expression pattern of a marker gene under the control of *J0571* enhancer. Confocal microscopic images of a transformed root with *Pro35S::GFP* and *J0571>>mCherry-NLS.* GFP fluorescence images (A,D), red fluorescence images (B,E), and merged images with transmitted light images (C,F) were acquired in the epidermis (A-C) and inner cell layers (D-F) of the same area. Scale bars = 100 μm in A-F.

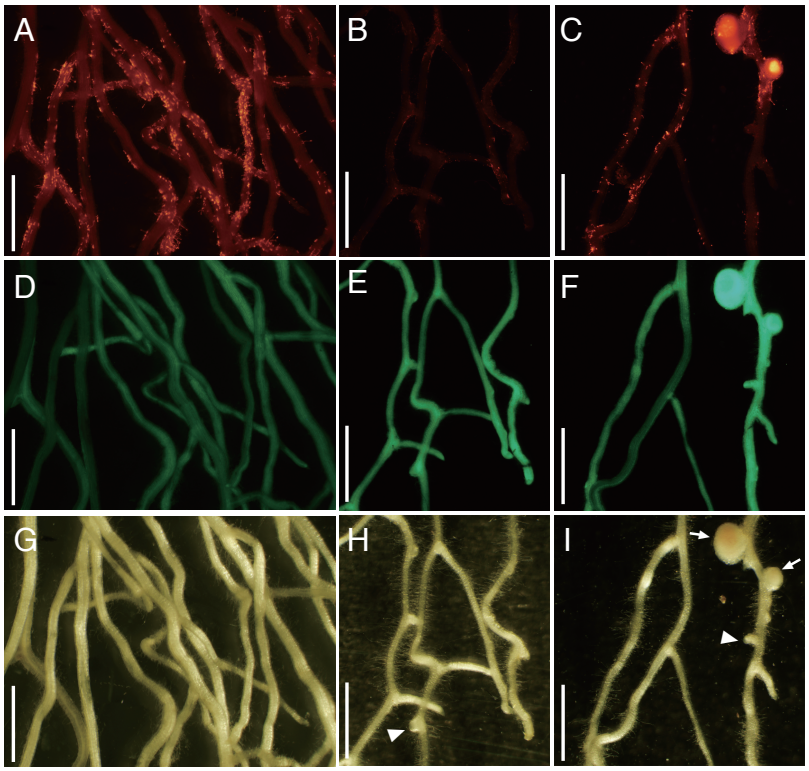

Figure 2-14. The non-nodulation phenotype in *daphne* is partially rescued by the cortical expression of *NIN*.

Red fluorescence images (A-C), GFP fluorescence images (D-F), and transmitted light images (G-I) of *A. rhizogenes*-mediated transformed *daphne* roots at 21 DAI. Transformed with *J0571>>NIN* (A-I). Excessive ITs (A,D,G), strongly suppressed ITs (B,E,H), and nodules (C,F,I) were observed by inoculating *M. loti* MAFF303099 constitutively expressing *DsRED*. GFP fluorescence showed transformed roots (F-J). Arrows and arrowheads indicate nodules and enlarged bumps, respectively. Scale bars = 2 cm.

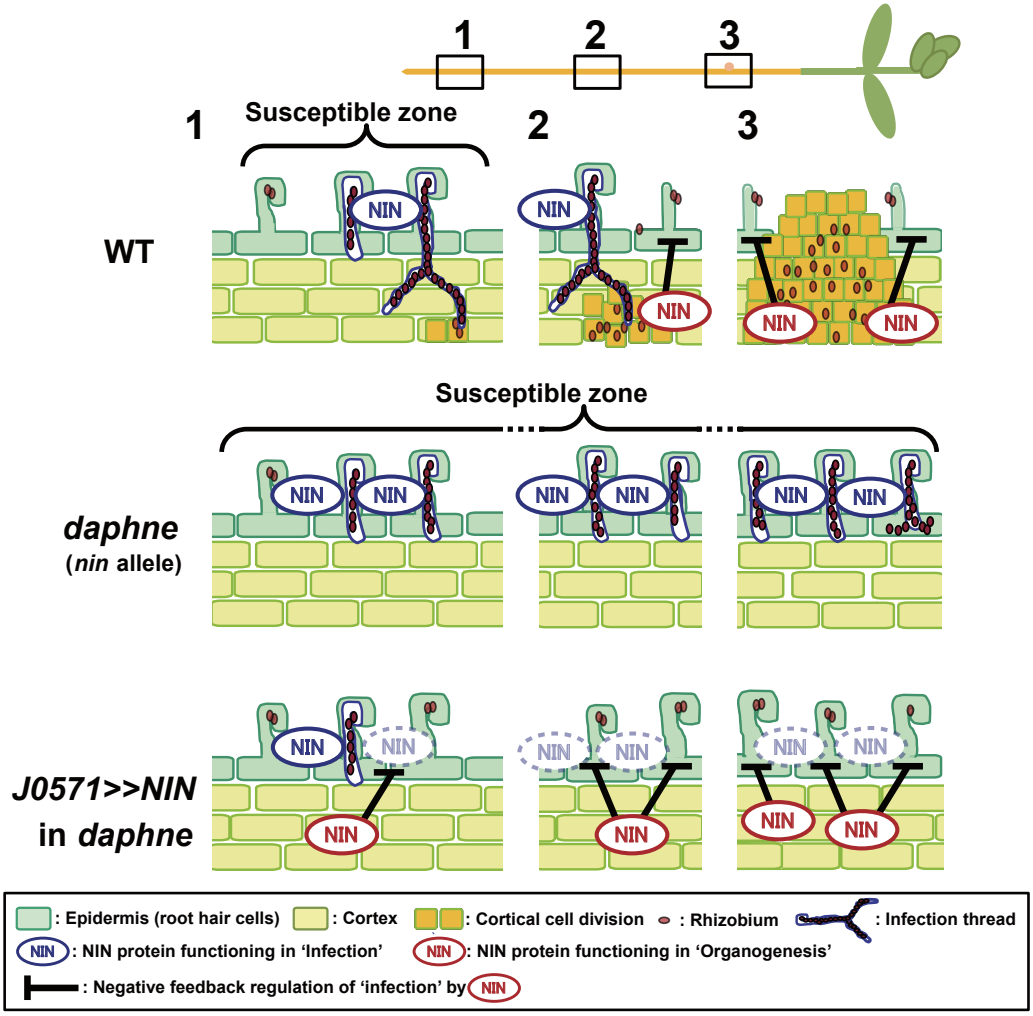

Figure 2-15. A model of inhibition of rhizobial infection processes mediated by NIN.
In the wild type, NIN functions in both rhizobial infection (blue, in the epidermis) and organogenesis (red, in the cortex). In the earlier stage (#1), NIN (blue) is predominant but in the later stage (#3), the proportion of NIN (red) has increased with nodule development. It is assumed that a potential negative correlation between organogenesis and infection pathway (black bars) regulates the amount of infection and restricts the region of rhizobial susceptibility. In the *daphne* mutant, NIN functions only in infection (blue) and not in organogenesis (red), resulting in no activation of cortical cell division. The loss of NIN (red) enhances rhizobial infection. When I induced the *NIN* expression in cortex in *daphne*, infection was strongly suppressed owing to the loss of a negative feedback loop (black bars) mediated by NIN (red). The numbers indicate the developmental stage of nodulation. NIN surrounded by dashed line indicates reduced gene expression or protein function of NIN, induced by a negative feedback loop described above (black bars).

Chapter 3

NIN inhibits rhizobial infection both locally and systemically

3.1. Introduction

In the previous **Chapter 2**, from the study of *daphne*, a specific allele of the *nin* mutant, I suggested the possible mechanism that once a nodule is formed, subsequent rhizobial infection tends to be inhibited. This regulatory mechanism has been supported not only by my study, but also by several studies of hyper-response of root hairs or hyper-formation of ITs in no or low nodulation mutants, such as *nin*, *hit1*, *vag1* and *ccamk-14* [**1.2.**, Table 1-1(f,g)]. In particular, the study of *daphne* demonstrates that cortical expression of *NIN* induced by the organogenesis pathway has a negative role in rhizobial infection, the NIN-mediated IT suppression (**2.3.1.**).

In contrast, a hyper-formation of IT with increased nodulation [Table 1-1(h)] indicates a common mechanism for controlling both IT numbers and nodule numbers. The possible common factor is ethylene which negatively regulates both infection and nodulation (**1.4.**, **2.3.**). Although IT formation in the *har1* mutant is similar to that in wild-type (Wopereis et al., 2000), an increased number of ITs observed in some hypernodulation mutants, *tml*, *klv*, and *plenty*; indicating the common mechanism (Magori et al., 2009; Miyazawa, 2010; Yoshida et al., 2010). Very recently, *CLE-RS1/2* genes, encoding root-derived inhibitors functioning in the long-distance control of nodulation (**1.4.**) were reported as direct targets of NIN transcriptional factor (Soyano et al., 2014). This direct molecular interaction between the long-distance control of nodulation pathway and NIN encourages further exploration of the similarity between nodulation control and IT control.

In this chapter, I investigated whether the NIN-mediated IT suppression is related to the HAR1-mediated long-distance control of nodulation, in order to predict the signaling molecules downstream of NIN. First, I analyzed the involvement of the components of long-distance control, CLE-RS1/2 peptides, HAR1, and KLV, in an IT control. Then, I examined the genetic overlap between long-distance control and NIN-mediated IT suppression.

3.2. Results

3.2.1. *CLE-RS1/2* peptide genes strongly inhibit hyper-formation of ITs in *daphne*, and are dependent on HAR1 receptor kinase

I suspected that the lower expression level of *NIN* in *daphne* is causal for the weakness in long-distance control, and follows the increased number of ITs. NIN regulates nodulation both positively and negatively, through its ability to bind the promoter of *CLE-RS1/2* genes (Soyano et al., 2014) and the subsequent induction of *CLE-RS1/2* expression (Okamoto et al., 2009). First, I checked the rhizobial inoculation-dependent gene induction level of *CLE-RS1/2* in *daphne*. The expression of both *CLE-RS1* and *CLE-RS2* was lower than in MG-20 wild type (Fig. 3-1). This prompted me to suspect that lower expression of *CLE-RS1/2* might be causal for the hyper-formation of ITs in *daphne.*

Next, to investigate whether CLE-RS1/2 peptides, root derived inhibitors of the HAR1-mediated long-distance control, are actually functional in an IT control, I made a hairy root transformed roots overexpressing *CLE-RS1/2* in a *daphne* mutant background (Fig. 3-2A-I). In transformed roots with negative control vector (*Pro35S::GUS*), the typical hyperinfection phenotype remained (Fig. 3-2A). In contrast,

CLE-RS1/2-overexpressing *daphne* roots showed strongly suppressed ITs in both GFP positive transformed roots and GFP negative untransformed roots (Fig. 3-2B,C). This indicates that overexpressed CLE-RS1/2 peptides systemically inhibit hyperinfection of *daphne*. Next, the same experiments were done in a *daphne har1-8* double mutant background in order to examine the possible involvement of HAR1 in the IT suppression pathway (Fig. 3-2J-R). No IT suppression effect was observed in transformed roots with *CLE-RS1/2*-overexpression (Fig. 3-2K,L). These results suggest that CLE-RS1/2 peptides strongly suppress IT formation via HAR1 as well as the well-known long-distance control of nodulation (Okamoto et al., 2009).

3.2.2. Strong suppression of ITs by *CLE-RS1/2* is mediated by HAR1 and KLV on shoot

In a previous study of the long-distance control of nodulation, HAR1 and KLV functioned in the shoot but not in the root. This shoot/root genetic dependency has been demonstrated by grafting experiments (**1.4.**) (Nishimura et al., 2002a; Oka-Kira et al., 2005). To determine the shoot/root dependency of *har1*and *klv* in the IT suppression pathway, I performed grafting experiments with *CLE-RS1*-overexpressing plants in a *daphne* mutant background. First, by grafting between *daphne* and MG-20 wild type, the shoot/root dependency of the hyper-IT phenotype of *daphne* was explored (Fig. 3-3A). The results indicate that the hyper-formation of ITs is determined by the root genotype, which means the *daphne* mutation only in the root is sufficient for displaying the hyper-IT phenotype. Then, I made *CLE-RS1*-overexpressing *daphne* by crossing with a stable transformants overexpressing *CLE-RS1* (Sasaki et al., 2014). I performed a series of further grafting experiments (Fig. 3-3B-Q). The combination of a

CLE-RS1-overexpressing *daphne* root and a shoot of MG-20 wild type confirmed the IT suppression effect (Fig. 3-3B,D) as previously shown in the hairy root experiments (Fig. 3-2A-C). In contrast, in grafting combinations with shoots of *har1* and *klv*, the IT-suppression effect of *CLE-RS1* overexpression was abolished, and typical *daphne*-like hyper-formation of ITs were observed (Fig. 3-3B,E,F). These observations suggest that IT-suppression by *CLE-RS1* overexpression is dependent on *HAR* and *KLV* expressed in the shoot as well as the long-distance control of nodulation pathway.

In addition, although expressions of *CLE-RS1/2* are specifically induced in the root (Okamoto et al., 2009), *CLE-RS1/2* overexpressed in the shoot are also functional for inhibition of nodulation (Sasaki et al., 2014). Therefore, to examine the same effect for inhibiting formation of ITs, I grafted normal *daphne* roots with *CLE-RS1*-overexpressing shoots of MG20 wild type (Fig. 3-3B,G). The result indicated that shoot-derived CLE-RS1/2 can suppress formation of ITs, similarly to the nodule suppression effect.

3.2.3. NIN systemically and locally inhibits hyper-formation of ITs in *daphne*

The IT suppression effects of *CLE-RS1*-overexpression are abolished in the presence of *har1* or *klv* in the shoot. Recently, it was reported that the expression of *CLE-RS1/2* genes is directly induced by NIN (Soyano et al., 2014), indicating that NIN-overexpression at least partially induces the *CLE-RS1/2* expression and the following long-distance inhibition of formation of ITs. Next, I determined whether the NIN-mediated IT suppression that I observed (**Chapter 2**, Fig. 2-10, Fig. 2-14) is fully explained by the effect of long-distance control. I introduced the NIN-overexpressing vector into the *daphne har1-8* double mutant and observed the hyper-IT phenotype (Fig.

3-4). Similar to the *CLE-RS1* overexpression experiments (Fig. 3-2, Fig. 3-3), some of the transgenic roots (8/18) still showed hyper-formation of ITs (Fig. 3-4B,F,J). On the other hand, differently from the *CLE-RS1* overexpression experiments (Fig. 3-2, Fig. 3-3), even in the presence of the *har1-8* mutation, the abnormally high number of ITs was strongly decreased in some transgenic roots (10/18) (Fig. 3-4C,G,K). Furthermore, in this case, IT suppression was restricted to the transgenic (GFP positive) roots. GFP-negative roots originated from the same plant shoot showed no IT suppression. This is consistent with my previous observation of local IT suppression by NIN overexpression (**Chapter 2**, Fig. 2-10). In addition, in *daphne har1-8*, the strong suppression of ITs also occurred in nearby nodule-like or bump-like structures rarely induced by NIN overexpression (Fig. 3-4D,H,L). These bumps depend on the cell division activity of NIN, as previously mentioned (**Chapter 2**, Fig 2-11). This observation explains the correlation between cortical cell division and IT suppression well.

3.3. Discussion

3.3.1. Consistency and inconsistency between the known long-distance control of nodulation and NIN-mediated IT inhibition

Although the receptor genes of CLE-RS1/2 peptides, *HAR1* and *KLV*, are expressed in different kinds of tissues, HAR1 and KLV expressed in the shoot were also indispensable to the suppression of the hyper-IT phenotype of *daphne* by *CLE-RS1/2* overexpression (Fig. 3-2, Fig. 3-3) as well as nodulation control (**1.4.**). This indicates that HAR1-mediated long-distance control is functional in both IT inhibition and nodule inhibition. In addition, according to a recent report that *CLE-RS1* and *CLE-RS2* are both

direct targets of NIN transcription factor (Soyano et al., 2014), at least part of the IT suppression observed in NIN-overexpressing roots (**Chapter 2**) may be derived from the shoot-mediated long-distance pathway. Further, *CLE-RS1*-overexpressing shoots were also functional in inhibiting the hyper-formation of ITs (Fig. 3-3B,G), as well as nodule suppression (Sasaki et al., 2014). Taken together, these observations suggest complete consistency of IT control and nodulation controls (Fig. 3-5, the long-distance pathway), although I have not yet checked the involvement of the rest of the components functioning in HAR1-mediated long-distance control, such as IPT3, cytokinin (SDI), and TML (**1.4.**).

However, consistent with the observation of a strong suppression of ITs only in GFP-positive transformed roots (**Chapter 2**, Fig. 2-10), the local suppression of hyper-formation of ITs by NIN overexpression remained in *daphne har1-8* double mutant. These results indicate that the local effect of NIN is clearly independent from HAR1-mediated long-distance control (Fig. 3-5, the local pathway). Curiously, this local effect was not always observed. Approximately half of transgenic plants (10/18) retained HAR1-independent local suppression. This might have been related to the expression level of the transgene or the chimeric nature of the transformed hairy roots. Moreover, the slightly different expression patterns of transgene may affect the ratio between NINs as an inducer of long-distance systemic pathway and NINs as an inducer of unknown local IT suppression pathway. The candidates for the molecules downstream of NIN in this local suppression pathway are further discussed below (**5.2.**).

3.3.2. The *daphne* mutant as a tool for studying IT control

CLE-RS1/2 overexpression strongly suppressed hyper-formation of ITs in *daphne*, but

this effect was lost in the presence of the *har1*and *klv* mutations, especially in shoots. Usually, it tends to be more difficult to evaluate the suppression effect on IT formation, rather than on nodulation, due to the difficulty of observation and quantification of IT numbers. In wild type, the number of ITs is usually less than approximately 20 per plant, especially in the MG-20 accession. Therefore, it is harder to observe the IT suppression effect. Further, it is even more difficult to investigate the effect only on infection or IT numbers because of the formation of nodules in wild type, assuming several possible common mechanisms for regulating both IT numbers and nodule numbers. In fact, the effect of *CLE-RS1/2* overexpression on IT inhibition was not detected in a previous report (Suzaki et al., 2012); however, the markedly increased number of ITs phenotype of *daphne* enabled me to clearly evaluate the effect. In this sense, the *daphne* mutant has demonstrable advantages for studying inhibitory signals involved in IT formation.

As some of the mutants involved in the long-distance control of nodulation in pea or soybean were originally identified as a series of *nitrate tolerant symbiosis* (*nts*) mutants (Jacobsen and Feenstra, 1984; Carroll et al., 1985), high nitrate is known as an inhibitor of nodulation. Likewise, nitrate and ammonium have been identified as negative factors for rhizobial infection processes (Malik et al., 1987; Barbulova et al., 2007). In addition, ethylene itself can downregulate initial symbiotic events in root hairs and subsequent rhizobial infection (Oldroyd et al., 2001; Lohar et al., 2009) as well as the control of nodule numbers as described above (**1.4**, **3.3.**). However, due to the difficulties of observation and quantification of ITs compared to nodules, the direct signaling molecules of these inhibitory pathway are still largely unknown. Thus, the clear hyper-IT phenotype of *daphne* could be a tool for evaluating these effects on inhibiting rhizobial infection in future studies.

3.4. Materials and Methods

Plant materials and growth conditions

Seeds were sown in sterilized vermiculite soaked in autoclaved vermiculite supplied with Broughton and Dilworth (B&D) solution (Broughton and Dilworth, 1971) containing 0.5 mM KNO_3 with *M. loti* MAFF 303099 constitutively expressing *DsRed* under 16-h light/8-h dark cycles. The *daphne* mutant is the same as in **Chapter 2** (**2.4.**). *har1-8* and *klv* were isolated in our laboratory (Miyazawa et al., 2010; Suzaki et al., 2012); genotyping primers for *har1-8* were 5'-CCCGGAGAGCTTCTCAAAACTG-3' and 5'-TCCCGCTTTTGCATAGATCCTGC-3' (dCAP genotyping with PstI digestion), and the genotyping primers for *klv* were previously described (Miyazawa et al., 2010). A *CLE-RS1*-overexpressing stable transformant was reported (Sasaki et al., 2014), and to select *CLE-RS1*-overexpressing *daphne* plants from the F_2 plants of crosses between *daphne* and the *CLE-RS1*-overexpressing transformant, I chose a plant that showed non-nodulation (*daphne* mutation) and GFP fluorescence (*CLE-RS1* overexpression).

Gene expression analysis

The method was the same as in **Chapter 2** (**2.4.**). The primers used for analyzing the expression of *CLE-RS1/2* genes were previously reported (Okamoto et al., 2009).

Grafting experiments

The method used in the grafting experiment was previously described (Yoshida et al., 2010). Grafted plants were kept on moistened filter paper for 7 days and successfully grafted plants were transplanted to vermiculite inoculated with *M. loti* constitutively

expressing *DsRed*. The number of ITs was measured at 7 DAI for combinations between *daphne* and MG-20 wild type, or at 21 DAI for a series of combinations with *CLE-RS1*-overexpressing *daphne* roots. ITs on all parts of the root were counted under the microscope, and root images were acquired form 5 grafted plants.

Microscopic observation

Bright-field and fluorescence images were viewed with an SZX12 stereomicroscope (Olympus). Images were acquired with a DP Controller (Olympus).

Plant transformation

A series of constructs for hairy root transformation, *Pro35S::GUS*, *Pro35S::CLE-RS1*, and *Pro35S::CLE-RS2* were provided by Dr. Okamoto (Okamoto et al., 2009). The series of constructs used for NIN overexpression and the method for hairy root transformation were the same as in **Chapter 2** (**2.4.**).

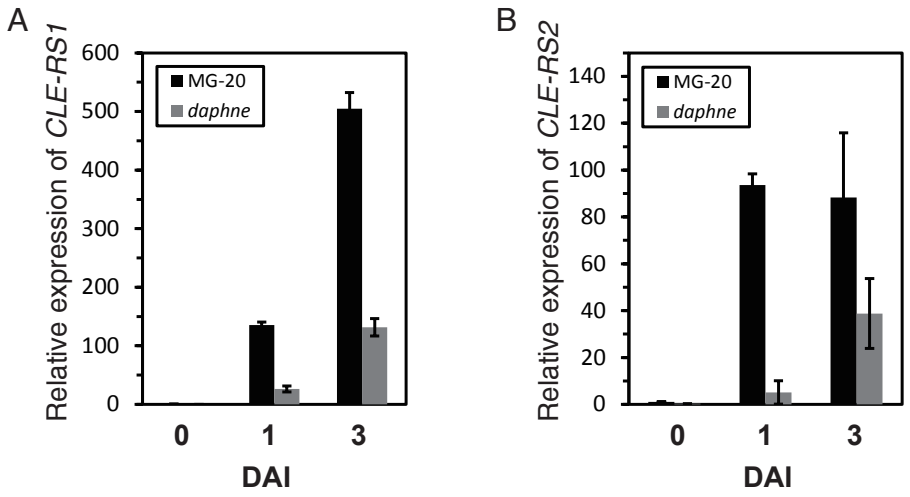

Figure 3-1. Gene expression analysis of *CLE-RS1/2*.

Quantitative real-time RT-PCR analysis of *CLE-RS1* (A) and *CLE-RS2* (B) in Miyakojima MG-20 wild type (black bars) and in *daphne* (gray bars) at non-inoculated (0), 1, and 3 DAI. Fold changes in expression are shown relative to at 0 DAI (A,B). Error bars indicate S.D. of three biological replicates.

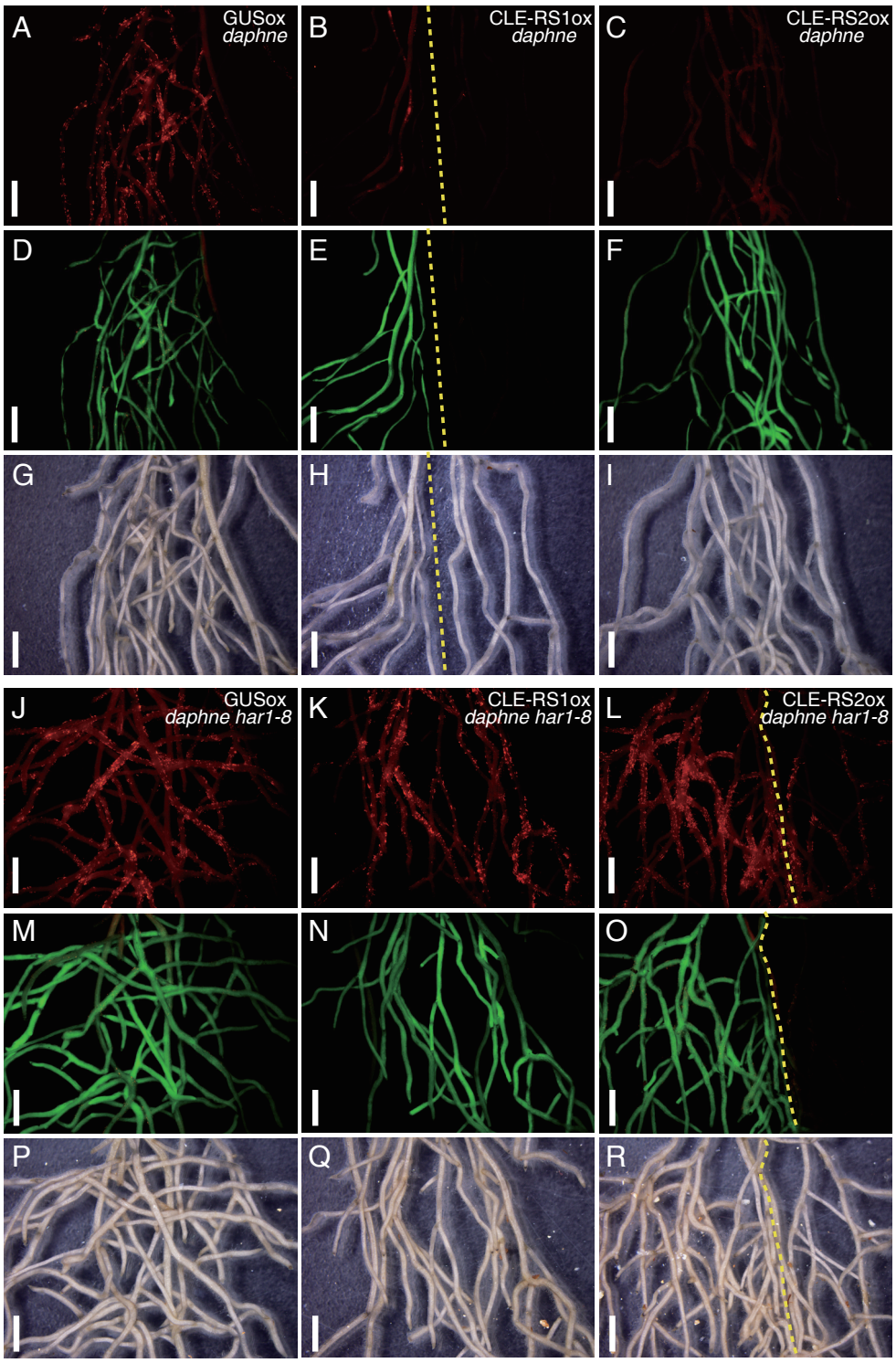

Figure 3-2. The IT suppression effect of *CLE-RS1/2* in *daphne* and *daphne har1-8*.

Red fluorescence images (A-C,J-L), GFP fluorescence images (D-F,M-O), and transmitted light images (G-I,P-R) of *A. rhizogenes*-mediated transformed roots of *daphne* and *daphne har1-8* at 21 DAI. Transformed with negative control vector *Pro35S::GUS* (A,D,G,J,M,P), *Pro35S::CLE-RS1* (B,E,H,K,N,Q), *Pro35S::CLE-RS2* (C,F,I,L,O,R). ITs were observed by inoculating *M. loti* MAFF303099 constitutively expressing *DsRED* (A-C,J-L). Green fluorescent protein fluorescence showed transformed roots (D-F,M-O). Yellow dashed lines indicate the border between transformed and non-transformed roots. Scale bars = 5 mm.

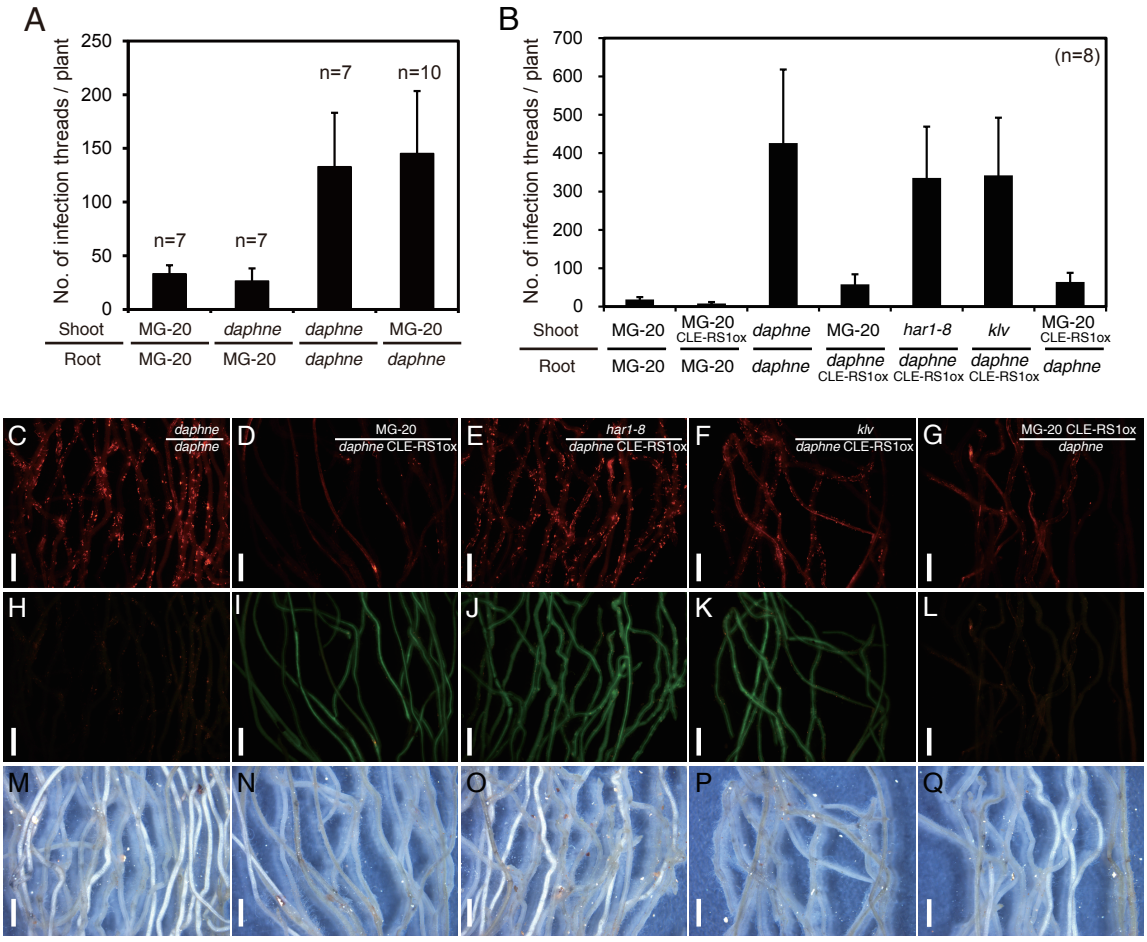

Figure 3-3. Grafting experiments with *daphne* or *CLE-RS1*-overexpressing *daphne*.

A, The number of ITs in grafting plants between MG-20 wild type and *daphne* at 7 DAI. B, The number of ITs in grafted plants between MG-20 wild type, *CLE-RS1*-overexpressing MG-20, *daphne*, *CLE-RS1*-overexpressing *daphne*, *har1-8*, *klv* at 21 DAI. Red fluorescence images (C-G), GFP fluorescence images (H-L), and transmitted light images (M-Q) of roots from 5 grafted plants. ITs were observed by inoculating *M. loti* MAFF303099 constitutively expressing *DsRED* (C-G). Green fluorescent protein fluorescence showed *CLE-RS1*-overexpressing stably transformed roots (H-L). Scale bars = 5 mm. Error bars indicate S.D.

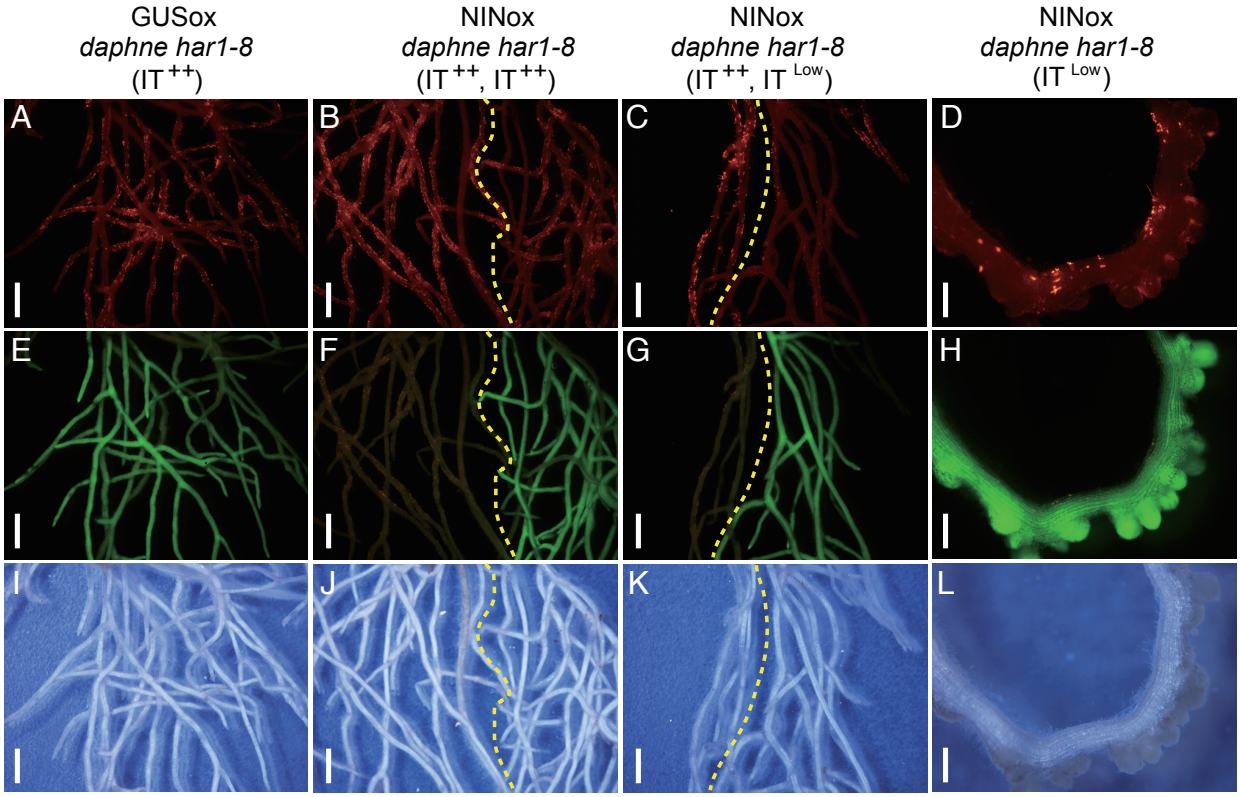

Figure 3-4. The IT suppression by NIN-overexpression in *daphne har1-8*.

Red fluorescence images (A-D), GFP fluorescence images (E-H), and transmitted light images (I-L) of *A. rhizogenes*-mediated transformed roots of *daphne har1-8* at 21 DAI. Transformed with negative control vector *ProLjUBQ::GUS* (A,E,I), *ProLjUBQ::NIN* (B-D,F-H,J-L). No IT suppression effects (IT^{++}) and strongly IT suppression effects (IT^{Low}) are shown in each panels. ITs are suppressed in the nodule-like bump structures (D,H,L). ITs were observed by inoculating *M. loti* MAFF303099 constitutively expressing *DsRED* (A-D). Green fluorescent protein fluorescence showed transformed roots (E-H). Yellow dashed lines indicate the border between transformed and non-transformed roots. Scale bars = 5 mm in A-C,E-G,J-K; 500 μm in D,H,L.

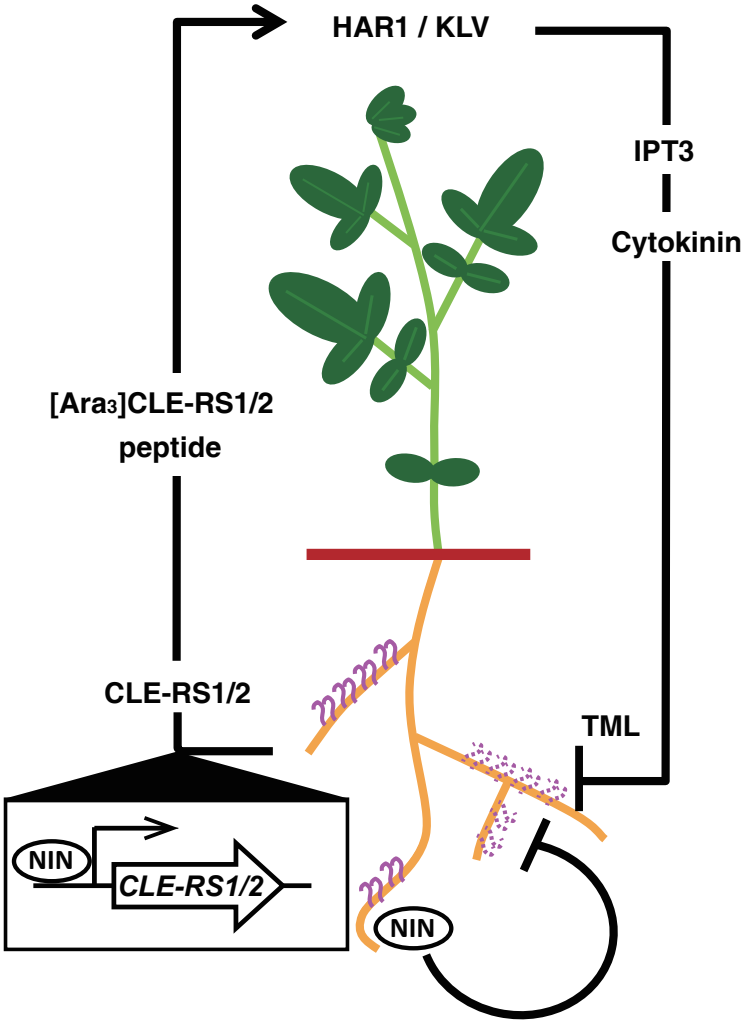

Figure 3-5. A model for the two local and systemic NIN-mediated IT suppression pathways. The some components of the long-distance control of nodulation, CLE-RS1/2 peptides, HAR1, and KLV are functional for the IT suppression in *daphne*. It is also shown that *CLE-RS1/2* genes are direct target of NIN transcription factor (Soyano et al., 2014). These indicate the pathway of the long-distance control of IT numbers. On the other hand, the local effect of IT suppression by NIN-overexpression is still observed even in the presence of *har1-8*. This suggests that NIN also locally functions in the IT suppression.

Chapter 4

Identification of *PLENTY* gene adds a new player for controlling nodule numbers

4.1. Introduction

As I described above (**1.4.**), the number of nodules is strictly controlled by host plant response to their nitrogen requirement. Among those controls, the molecular mechanisms for the long-distance control of nodulation have been gradually elucidated based on the identification of the genes responsible for hypernodulation mutants, *LjHAR1* (Krusell et al., 2002; Nishimura et al., 2002a), *GmNARK* (Searle et al., 2003), *MtSUNN* (Schnabel et al., 2005), *SYMBIOSIS 29* (*PsSYM29)* (Krusell et al., 2002), *LjKLV* (Oka-Kira et al., 2005; Miyazawa et al., 2010), and *LjTML* (Magori et al., 2009; Takahara et al., 2013). *LjHAR1/MtSUNN/GmNARK/PsSYM29* and *LjKLV* encode LRR-RLKs functioned in the shoot, but *LjTML* encodes F-box protein functioned in the root. In addition, reverse genetic approaches enable to find a ligand of HAR1, CLE-RS1/2 peptide. Recently, a post-translational modification of CLE-RS1/2, tri-arabinosylation, and its crucial role for its activity has been demonstrated [**1.4.**, Fig. 1-2(2)] (Okamoto et al., 2013a).

plenty mutant had been isolated from *L. japonicus* Miyakojima MG-20 wild type seeds mutagenized by ion beam, as a fourth hypernodulation mutant in our laboratory. However, the responsible gene has not yet been identified (Yoshida et al., 2010). In this chapter, I identified the *PLENTY* gene as being orthologous to *Mt ROOT DETERMINED NODULATION1 (RDN1)* and *Ps NODULATION3 (NOD3)* (Schnabel et al., 2011). In contrast to *har1* or *klv*, the hypernodulation of *plenty* was determined by the root genotype, suggesting that PLENTY functions in the root but not in the shoot

(Yoshida et al., 2010). This finding is consistent with the grafting results of *Mtrdn1* and *Psnod3* (Postma et al., 1988; Novak, 2010; Schnabel et al., 2011).

A few previous studies of *Lj*PLENTY/*Mt*RDN1/*Ps*NOD3 suggested that *Ps*NOD3 is involved in the generation of an unknown systemic signal for the long-distance control of nodulation (Li et al., 2009; Novak, 2010). Furthermore, since the inhibitory effect of *Mt*CLE12/13 overexpression on nodulation was abolished in *Psnod3* as well as in *Pssym29* (Osipova et al., 2012), *Ps*NOD3 possibly acts in the same genetic pathway as the *LjHAR1/MtSUNN/GmNARK/PsSYM29*-mediated long-distance control of nodulation. Very little was known about the *Lj*PLENTY/*Mt*RDN1/*Ps*NOD3 protein function, except for a putative transmembrane domain, putative secretory signal peptides at their N-termini, and broad sequence conservation throughout the plant kingdom including angiosperms, gymnosperms, mosses, and green algae (Schnabel et al., 2011). However, very recently Arabidopsis homologs of *Lj*PLENTY/*Mt*RDN1/*Ps*NOD3 were identified based on their biochemical activity and found to be HPATs, including HPAT1 (At2g25260), HPAT2 (At5g13500), and HPAT3 (At5g25265), (Ogawa-Ohnishi et al., 2013). This finding has provided new hints about potential molecular functions of the HPATs. *At*HPATs are thought to be enzymes that transfer an L-arabinosyl residue to the hydroxyl group of hydroxyproline residues in secretory peptides. This reaction is reminiscent of the arabinosylation of the CLE-RS2 peptide acting in the HAR1-mediated long distance control of nodulation (Ogawa-Ohnishi et al., 2013; Okamoto et al., 2013a).

Here, I cloned and analyzed the subcellular localization of PLENTY, and did phylogenetic analysis of PLENTY family in plants. Further I investigate the involvement of PLENTY in the arabinosylation of CLE-RS1/2 peptides, and the genetic

relationship between *plenty* and *har1*. Lastly, I will discuss several possible functions of PLENTY through comparison of previous functional predictions for *Ps*NOD3 and *Mt*RDN1.

4.2. Results

4.2.1. Identification of the *PLENTY* gene

The *plenty* mutant mainly has two characteristic root phenotypes, namely, slightly increased nodulation and short roots in both the presence and absence of rhizobia (Yoshida et al., 2010). Yoshida et al. previously reported that the locus for *plenty* is located between markers TM0002 and TM0324 on the long arm of chromosome II. Thus, I started further map-based cloning using a larger mapping population (1087 F_2 plants) to delineate better the chromosomal region (Fig. 4-1). By genomic PCR between markers TM0308 and EY005 (a newly developed marker in this chapter, Table 4-1), a deleted region was detected that included two protein-coding genes, CM0308.590.r2.d and CM0308.600.r2.d (http://www.kazusa.or.jp/lotus/). Phylogenetic analysis using the same amino acid sequence data set originating from the study of *Mt*RDN1 (Schnabel et al., 2011) revealed that the latter coding region, which I named *PLENTY*, is exactly orthologous to *MtRDN1* (Fig. 4-2). In the genome of *L. japonicus*, there are two other *PLENTY* homologs, named *PLENTY2* and *PLENTY3* that are also orthologous to *Mt*RDN2 and *Mt*RDN3, respectively. As previously reported, there is no homolog of Brassicaceae in Group 1 including *Lj*PLENTY and *Mt*RDN1, and specifically the Brassicaceae homologs are in another clade nearby Group 3 instead (Schnabel et al., 2011; Fig. 4-2). To examine the evolution of PLENTY genes in the Brassicaceae, I added the homologous sequences of *Brassica rapa*, *Carica papaya* (papaya),

Gossypium raimondii (cotton), and *Eucalyptus grandis* (eucalypt) from the Phytozome database (http://www.phytozome.net/) to the phylogenetic analysis. Among these plants, all PLENTY homologs from eudicots except for those from *Brassica rapa* are classified in Groups 1-3. Genes from *Carica papaya* in the order Brassicales, are notable for their exceptional evolution in the Brassicaceae family (Fig. 4-2).

4.2.2. Nodule numbers and short root phenotype of *plenty* were complemented by *PLENTY*

The *plenty* mutant primarily has an increased number of nodules and shorter roots in both symbiotic and non-symbiotic conditions (Yoshida et al., 2010). I made stably transformed plants expressing *PLENTY* cDNA under the control of the *ProUBQ* in the *plenty* mutant and performed complementation tests in both inoculated and non-inoculated conditions. There were significantly fewer nodules and primary root length was elongated in inoculated *PLENTY*-expressing roots in different T3 plant lines (Fig. 4-3A-F). Furthermore, primary root length was also rescued by introducing *PLENTY* in the non-inoculated condition (Fig. 4-3G,H). These results indicate that *PLENTY* functions in controlling nodule numbers and root growth even in the absence of rhizobia. As previously reported, the hypernodulation phenotype of *plenty* is milder than *har1*, *klv*, *tml*, but *plenty* tends to form increased numbers of mature nodules greater than 0.5 mm in diameter rather than small nodules (Yoshida et al., 2010). In good agreement with this previous report, the number of mature nodules was significantly reduced in *PLENTY*-transformed plants (Fig. 4-3E).

4.2.3. PLENTY is localized to the Golgi complex

To gain insights into the potential molecular function of *PLENTY*, I next investigated the subcellular localization of this uncharacterized protein gene using a series of constructs expressing PLENTY-GFP fusion proteins. Since the N-terminal amino acid sequence of *Mt*RDN1 was previously predicted as a signal peptide (SP) leading to the secretory pathway, I constructed three kinds of vectors: full length PLENTY (Full-PLENTY-GFP), PLENTY without an N-terminal region (deltaN-PLENTY-GFP), and only the N-terminal region of PLENTY (SP-GFP) (Fig. 4-4A). I first tested Full-PLENTY-GFP localization by particle bombardment of onion epidermal cells and *L. japonicu*s root cells (Fig. 4-4B-F). Full-PLENTY-GFP was visible in intracellular punctate structures. For high efficiency of transformation, I tested *Agrobacterium* infiltration of *Nicotiana benthamiana* leaves (Fig. 4-4G-J) and observed the same punctate localization of Full-PLENTY-GFP and SP-GFP. On the contrary, GFP and deltaN-PLENTY-GFP were clearly localized in nuclei and the cytoplasm, suggesting that the N-terminal regions are essential and sufficient for proper subcellular localization of PLENTY. To analyze these localization patterns in greater detail, I compared PLENTY localization with the localization of a *cis*-Golgi marker, soybean alpha-1,2-mannosidase I (Nebenfuhr et al., 1999; Saint-Jore-Dupas et al., 2006; Nelson et al., 2007) in *N. benthamiana*. The subcellular localization of PLENTY overlapped completely with that of the *cis*-Golgi marker, suggesting that PLENTY is a component of Golgi complexes (Fig. 4-4K-P). Considering the Golgi localization of *At*HPAT1 (Ogawa-Ohnishi et al., 2013), PLENTY may be involved in post-translational modifications in the Golgi, similar to the *At*HPATs glycosylation enzymes.

4.2.4. Genetic relationships between *PLENTY* and CLE-RS1/2 peptides, the

systemic signal for HAR1-mediated long-distance control of nodulation

To reveal whether PLENTY acts in the known HAR1-mediated long-distance control of nodulation, I next focused on the nodulation phenotype of *plenty* affected by CLE-RS1/2 overexpression. Although under natural conditions the expression of *CLE-RS1/2* is specifically induced by rhizobial inoculation or high nitrate levels in roots (Okamoto et al., 2009), the grafting experiments showed that artificially overexpressed *CLE-RS1/2* in the shoot function in inhibition of nodulation in a HAR1-dependent manner (Sasaki et al., 2014). Therefore, at first, I examined the suppression of nodulation in *plenty* grafted with CLE-RS1/2-overexpressing shoots (Fig. 4-5A,B). The CLE-RS1/2-mediated suppression of nodulation in *plenty* excludes the possibility that PLENTY functions downstream of CLE-RS1/2 peptides as a receiver of SDI in the HAR1-mediated long-distance control of nodulation. This result agrees with a previous prediction that *Ps*NOD3 may be involved in producing a root-derived inhibitor, but not a receiver of SDI (Li et al., 2009; Novak, 2010). Since the specific localization of PLENTY to the Golgi led us to speculate that PLENTY modifies CLE-RS1/2 peptides, I next investigated whether PLENTY is involved in the generation of active CLE-RS1/2 peptides by hairy root transformation with *CLE-RS1/2* overexpressing vectors. For CLE-RS2, arabinosylaion is essential for its inhibitory effect on nodulation (Okamoto et al., 2013a). I hypothesized that if PLENTY mediates the arabinosylation of CLE-RS1/2, then the nodule suppression effect by *CLE-RS1/2* overexpression would be aborted in *plenty*, as observed in *har1* (Okamoto et al., 2009). In fact, the hypernodulation of *plenty* and wild type were both strongly suppressed by *CLE-RS1/2* overexpression (Fig. 4-5C-I). Thus, even in *plenty*, overexpressed *CLE-RS1/2* maintains sufficient biological activity to inhibit nodulation.

Then, I examined the inoculation-dependent gene expression of *CLE-RS1/2* in *plenty*, in order to rule out the possibility that PLENTY induces *CLE-RS1/2* expression. Relative transcript levels of *CLE-RS1/2* in *plenty* were nearly the same as that of the wild type (Fig. 4-6). Thus, it is unlikely that the hypernodulation of *plenty* is caused by loss of *CLE-RS1/2* gene expression.

4.2.5. The *plenty har1* double mutant produced more mature nodules than the *har1* single mutant

CLE-RS1/2 gene products, root-derived inhibitors in the HAR1-mediated long-distance control of nodulation, were still functional in *plenty* when it overexpressed. To further investigate the genetic interaction between the *HAR1* receptor and *PLENTY*, I made the *plenty har1-7* double mutant and measured nodule numbers normalized to total root length (Fig. 4-7). In good agreement with previous results of grafting experiments with *har1-7* shoots (Yoshida et al., 2010), the number of nodules in *plenty har1-7* was increased in comparison to that of the *har1-7* or the *plenty* single mutants. Remarkably, *plenty har1-7* had more mature nodules with diameters greater than 0.5 mm compared to the *har1-7* single mutant (Fig. 4-7F). These results also demonstrate that the *plenty* mutation is genetically independent from *har1-7* in the control of nodulation. This finding also confirmed the additive nodulation demonstrated by the *plenty tml* double mutant (Takahara et al., 2013). In addition, the lateral root length of *plenty har1-7* was markedly reduced (Fig. 4-7G), indicating that the additional nodulation might be caused by lateral root suppression in *plenty har1-7*.

On the other hand, in terms of the short primary root phenotype in the non-inoculated condition, *plenty har1-7* had no additive effect in comparison to the

har1-7 single mutant, indicating that the short root phenotype in the absence of rhizobia might be controlled by the same genetic pathway (Fig. 4-8).

4.2.6. The *plenty snf2* double mutant had more spontaneous nodules than *snf2*

Assuming that PLENTY plays a role in a novel pathway for controlling nodulation, the site of action could be different from the HAR1-mediated long-distance control of nodulation. The genetic interactions between the nodule organogenesis pathway and the HAR1-mediated long-distance control of nodulation were demonstrated by crossing with *snf2* (Tirichine et al., 2007) (**1.3.**). As previously reported, the increased spontaneous nodulation of *har1-8 snf2*, *klv snf2*, and *tml snf2* compared to the *snf2* single mutant indicated that the downstream of cytokinin signaling during nodule organogenesis is targeted by the HAR1-mediated pathway to inhibit nodulation (Miyazawa et al., 2010; Takahara et al., 2013) [**Chapter 1**, Fig. 1-2(5)]. To assess the target site of the PLENTY-mediated nodule suppression pathway, I made the *plenty snf2* double mutant and measured the number of spontaneous nodules in comparison with that of *snf2* (Fig. 4-9). The *plenty snf2* double mutant had significantly more spontaneous nodules than *snf2*. This result suggests that even if a novel PLENTY-mediated pathway for controlling nodulation exists, the site of action is also downstream of cytokinin signaling (Fig. 4-10).

4.3. Discussion

4.3.1. Several possible PLENTY-mediated pathways for inhibiting nodulation

First, in this study I cloned the *LjPLENTY* gene, which is orthologous to *MtRDN1* or *PsNOD3* and homologous to *AtHPATs*. *Lj*PLENTY localizes to the Golgi complex as

does *At*HPAT which plays a role in the arabinosylation of small peptides (Ogawa-Ohnishi et al., 2013). Although I have not yet directly assayed the biochemical activity of PLENTY, the possible functions of PLENTY proposed below relies on the assumption that PLENTY function is similar to *At*HPAT function with respect to the post-translational modification of small peptides. Importantly, the post-translational arabinosylation of *Lj*CLE-RS2, which functions in the HAR1-mediated long-distance control of nodulation, is essential for the inhibitory effect on nodulation (Okamoto et al., 2013a). Results from my investigation of the genetic interaction between PLENTY and CLE-RS1/2 peptides and HAR1 suggest the possibility that the PLENTY-mediated pathway may be completely independent from the known HAR1-mediated long-distance control of nodulation. Furthermore, PLENTY probably modifies an unknown root-derived inhibitor, other than CLE-RS1/2, that acts in the long-distance control of nodulation or in the local inhibition of nodulation (Fig. 4-10, red dashed lines). The putative inhibitor might be related to a different regulatory pathway for inhibiting nodulation through jasmonic acid (Nakagawa et al., 2006; Seo et al., 2007; Kinkema and Gresshoff, 2008), abscisic acid (Ding et al., 2008; Biswas et al., 2009), ethylene (Penmetsa and Cook, 1997; Penmetsa et al., 2003; Lohar et al., 2009; Miyata et al., 2013), brassinosteroid (Terakado et al., 2006), or photomorphogenesis (Nishimura et al., 2002b).

Although these results showing the genetic independence between *plenty* and *har1* are consistent with a previous report of *plenty tml* (Takahara et al., 2013), I cannot rule out the possibility that PLENTY mediates the arabinosylation of CLE-RS2 peptides because of the functional redundancy among the other PLENTY paralogs. The expression patterns of *PLENTY2* and *PLENTY3* during the course of nodulation and in

different plant tissues are almost the same as *PLENTY* (Fig. 4-2, Fig. 4-11), and the broad expression patterns of all three *PLENTY* genes are similar to those of *Mt*RDN1 and *At*HPATs (Schnabel et al., 2011; Ogawa-Ohnishi et al., 2013). To investigate this redundancy, I suppressed the expression of *PLENTY2* and *PLENTY3* by RNA interference, but the plants did not exhibit a hypernodulation phenotype (data not shown). Furthermore, I also suspect another possibility that arabinosylated CLE-RS peptides bind to other receptors besides HAR1 and KLV, achieving partial genetic independence between PLENTY and HAR1 (Fig. 4-10, blue dashed line). A receptor complex of *Lj*CLAVATA2 (*Lj*CLV2)/*Ps*SYMBIOSIS28 and *Lj*CORYNE (*Lj*CRN) is a strong candidate for contributing to the parallel pathway based on a study of Arabidopsis stem cell maintenance (Muller et al., 2008); however, the additive effect on nodulation has not been detected in the *har1 clv2* double mutant in *L. japonicus*, probably due to the weak mutation of *clv2* (Krusell et al., 2011).

Lastly, although all of these putative PLENTY-mediated novel pathways may exist, the target site for nodule inhibition would be the same as that of the HAR1-mediated pathway, downstream of cytokinin signaling (Fig. 4-10). This inhibition site could be linked to a recent study about cross-talk between the nodulation signaling pathway and *Mt*CLE12/13-mediated nodule inhibition (Saur et al., 2011). This study indicates that *Mt*EFD and *Mt*RR8 might negatively regulate nodulation via down-regulation of cytokinin signaling. Further studies of TML or the other components are needed to identify most of the steps downstream of both the HAR1-mediated and PLENTY-mediated pathways for nodule inhibition.

4.3.2. Comparisons with previous studies of *PLENTY* orthologs, *MtRDN1* and

PsNOD3

Grafting experiments using inoculated sensor roots that generate a systemic inhibitor and reporter roots whose nodulation could be affected by the sensor roots (Caetano-Anollés and Gresshoff 1990) were important for defining *nod3* (Li et al., 2009). The sensor roots of *nod3* had less of an inhibitory effect on nodule suppression of the reporter roots compared to wild type sensor roots, even though *nod3* had an abundance of nodules. This finding was explained by hypothesizing that *nod3* produced less inhibitor for suppressing nodules than wild type. Moreover, the observation that hypernodulation of adventitious roots originated from wild type shoots and not from *nod3* roots indicated the involvement of *Ps*NOD3 in the generation of an unknown root-derived systemic signal for inhibiting nodulation (Novak, 2010). In combination with these previous reports, these results indicate that *Lj*PLENTY/*Mt*RDN1/*Ps*NOD3 participates in the modification of a novel, systemic mobile signal that inhibits nodulation other than the known CLE peptides. On the other hand, the hypernodulation of *Psnod3* was not suppressed by *MtCLE13* gene overexpression (Osipova et al., 2012). The authors proposed that *Mt*RDN1 might act downstream or alongside *Mt*CLE12/13 during *Mt*SUNN-mediated long-distance control of nodulation, a result that is completely inconsistent with my results of *Lj*CLE-RS1/2 overexpression in *plenty*. Although I could not rule out that *Lj*PLENTY/*Mt*RDN1/*Ps*NOD3 contributes to the arabinosylation of *Lj*CLE-RS1/2/*Mt*CLE12/13, genetic analysis in my study clearly provided evidence for the existence of an *Lj*PLENTY-mediated *Lj*HAR1-independent pathway. This inconsistency might be caused by different contributions or substrate specificities between *Lj*PLENTY/*Mt*RDN1/*Ps*NOD3 and their homologs in each species. In fact, in Arabidopsis it seems that HPAT activity varies among substrates

(Ogawa-Ohnishi et al., 2013). Another reason why my result was inconsistent with that of *Mt*CLE13 overexpression is that arabinosylation may no longer be needed due to the overproduction of *Lj*CLE-RS1/2 peptides. Identification of the molecular activities and substrates for *Lj*PLENTY/*Mt*RDN1/*Ps*NOD3 and their homologs is necessary for accounting for the apparent inconsistencies in the functions of these proteins among legumes.

4.4. Materials and Methods

Growth conditions

Seeds were sown in sterilized vermiculite to which Broughton and Dilworth (B&D) solution (Broughton and Dilworth 1971) containing 0.5 mM KNO_3 or no KNO_3 (in the case of spontaneous nodulation) was added. Seeds were inoculated with *M. loti* MAFF 303099, and control seedlings were not inoculated. Seedlings were grown under 16-h light/8-h dark cycles at 24℃.

Map-based cloning and genomic PCR, and 5'/3'-RACE

The *plenty* mutants were backcrossed three times with the parental plant accession Miyakojima MG-20, and then crossed with another accession Gifu B-129. The genomes of 1087 F_2 progeny with the *plenty* mutant phenotype were used to detect DNA polymorphisms using a series of genetic markers (http://www.kazusa.or.jp/lotus/markerdb_index.html; Sandal et al., 2006) and two genetic markers newly developed in this study, EY004 and EY005 (Table 4-1). The deleted locus of the *PLENTY* gene was determined by genomic PCR (Fig. 4-1), using sets of primers shown in Table 4-2. Genomic DNA was extracted with a DNeasy Plant

Mini Kit (Qiagen). The 5’ and 3’ ends of *PLENTY*, *PLENTY2*, and *PLENTY3* are determined by SMARTer® RACE cDNA Amplification Kit (Clontech) using RNA extracted from whole roots at 5 DAI (accession number: LC010646, LC010647, and LC010648).

Plasmid construction

Full-length and a deletion series of *PLENTY* cDNA fragments were generated by reverse transcription using appropriate primer sets (Table 4-2), cloned into the pGEM®-T-Easy vector (Promega) by a TA strategy, and named pGEM-Full-PLENTY, pGEM-deltaN-PLENTY, and pGEM-SP-PLENTY. Next, each construct was digested with EcoRI and SpeI, inserted into the Gateway-based entry plasmid pJL-Blue (Suzaki et al., 2012), and named pJL-Blue-Full-PLENTY, pJL-Blue-deltaN-PLENTY, and pJL-Blue-SP-PLENTY. For the complementation test, the fragments of *Full-PLENTY* were inserted into the Gateway site of pUB-GW-HYG by an LR recombination reaction (Invitrogen), and named pUB-GW-Full-PLENTY (Maekawa et al., 2008). For making the PLENTY-GFP fusion, I mutagenized the stop codon of pJL-Blue-based entry vectors using circular PCR with a phosphorylated set of primers (Table 4-2), DpnI digestion, and self-ligation. For subcellular localization analysis, a series of *PLENTY* fragments from the mutagenized pJL-Blue-based entry vectors were inserted into pUGW5 for particle bombardment in onion epidermal cells and *L. japonicus* roots, and into pGWB5 for *A. tumefaciens* infiltration of *N. benthamiana* by an LR recombination reaction (Invitrogen). Two constructs, pUGW5 and pGWB5 (Nakagawa et al., 2007), were kindly provided by Dr. Mano (National institute for Basic Biology) and Dr. Nakagawa (Shimane University), respectively.

Hairy root and stable transformation of *L. japonicus*

Hairy root and stable transformation of *L. japonicus* were performed with *Agrobacterium rhizogenes* strain AR1193 alone or with *Agrobacterium rhizogenes* strain AR1193 and *Agrobacterium tumefaciens* strain AGL1 harboring respective plasmids by previously described methods (Okamoto et al., 2013b; Sasaki et al., 2013; http://www.bio-protocol.org/e795; http://www.bio-protocol.org/e796). In the case of hairy root transformation of *CLE-RS1/2* for overexpression, GFP fluorescence was checked as a marker for transformation, and transformed roots were inoculated with *M. loti* MAFF303099. Nodules and the other phenotypes of hairy roots and stably transformed roots were measured at 14 DAI.

Subcellular localization analysis

Onion epidermal cells and *L. japonicus* root cells were transformed by particle bombardment with each construct (pUGW5-based series) using a Helios Gene Gun (BIO-RAD) as described previously (Mano et al., 2006). In order to verify co-localization in Golgi complexes, *A. tumefaciens* AGL1 strains carrying each construct (pGWB5-based series) and a Golgi marker construct (G-rb) (Nelson et al., 2007) were mixed and co-infiltrated into *N. benthamiana* leaves with the p19-harboring strain as previously described (Voinnet et al., 2003; Kinoshita et al., 2010).

Microscopic observations

Bright-field and fluorescence images were viewed with an SZX12/16 stereomicroscope or a BX50 microscope (Olympus). Images were acquired with a DP Controller

(Olympus). Confocal images were viewed with an A1 confocal laser-scanning microscope (Nikon) using NIS Elements (Nikon).

Double mutant analysis

For selecting the *plenty har1-7* homozygous double mutant, each genotype was checked using an amplified polymorphic sequence marker for *har1-7* (Miyazawa et al., 2010) and primers for *PLENTY* (Table 4-2). Nodules and the other root phenotypes were counted and measured at 28 DAI. The *snf2* and *har1-8 snf2* double mutant in an MG-20 background were previously reported (Miyazawa et al., 2010; Suzaki et al., 2014). The homozygosity of the *plenty* and *snf2* genotypes were checked by PCR with appropriate sets of primers (Table 4-2).

Gene expression analysis

The method is the same as **Chapter 2** (**2.4.**). Primers for analysing the expression of *CLE-RS1/2* genes are previously reported (Okamoto et al., 2009). The other primers used in this chapter are shown in Table 4-2.

Grafting experiments

The method is the same as **Chapter 3** (**3.4.**), and inoculated with wild type *M. loti*. Nodule number and other phenotypes were measured at 14 DAI. *CLE-RS1/2* over-expressing plants were kindly provided by Takema Sasaki (Sasaki et al., 2014).

Phylogenetic analysis

Amino acid sequences used for the query were obtained from the study of *MtRDN1*

(Schnabel et al., 2011). I added the sequences of *Brassica rapa Chiifu-401 v1.2*, *Carica papaya*, *Gossypium raimondii*, and *Eucalyptus grandis* from the Phytozome website (http://www.phytozome.net/) by BLAST search. I aligned the sequences using MUSCLE (Edgar, 2004). The analysis involved 57 amino acid sequences. All positions containing gaps and missing data were eliminated. There were a total of 266 positions in the final dataset. Evolutionary analyses were conducted in MEGA6 (Tamura et al., 2013). The evolutionary history was inferred by using the Maximum Likelihood method based on the Le_Gascuel_2008 model (Le and Gascuel, 2008). The tree with the highest log likelihood (-7013.2051) is shown (Fig. 4-2). The initial tree for the heuristic search was obtained by applying the Neighbor-Joining method to a matrix of pairwise distances estimated using a JTT model. A discrete Gamma distribution was used to model evolutionary rate differences among sites [5 categories (+G, parameter = 0.4454)].

Table 4-1. The newly developed genetic markers for map-based cloning of *PLENTY*.

marker	clone	sequence before polymorphisms	polymorphisms		sequence after polymorphisms	primers for detecting polymorphism		restriction enzyme	length of fragment (bp)
			MG-20	B-129		direction	sequence		
EY004	LjT42O06	GCGGGTAAGGCAACAACTCA	CCTGAGACTAATTCCTCATC	-	ACACGCAATCTTACTTTGAA	F	TGGTGAGGTGGAAGTGTCAA	-	MG-20, 184
						R	CCAATGCCTGCTAGTTTGCT		B-129, 164
EY005	LjT42O06	AAACACACATACATCCCCTT	A	G	CACCTAAATTGTTCTCTAAG	F	CAAACACACATACATCCCGATC	PvuI	MG-20, 170
						R	GCAGAAATGAATTTGAATGG		B-129, 149+21

Table 4-2. Primers used in this chapter

Use	Primer Name	Sequence	Notes
Real-time RT-PCR	PLENTY_5UTR_F	GACTTTGCCCTTCCCATGTTTTT	
	PLENTY_5UTR_R	TTAGTTCTAAGCAATTGCTGATAGCAGA	
	PLENTY2_5UTR_F	AAGTAATGGTGAAGCTCGCGC	
	PLENTY2_5UTR_R	TCTTCTGCTGAAGTTGTGGGAAAATT	
	PLENTY3_5UTR_F	TTGCCACTACAACCCATGTTGATT	
	PLENTY3_5UTR_R	ATGTAAGGAACACCCCTCCAAC	
Construction	PLENTY_cDNA_F	ATGGGAAGGGCAAAGTCACTTC	
	PLENTY_cDNA_R	TCAGCTTCTATTTAATGAATCCCATTCAG	
	SP_PLENTY_cDNA_R	ATGGTATTTCGCATTAGTGCTTG	
	deltaN_PLENTY_cDNA_F	ATGTTGGGTTCGGCAAGCAC	
	mut_vector_F	GCGGCCGCCTGCAGGTCG	introduce mutations for GFP-fusion
	mut_PLENTY_tail_R	GCTTCTATTTAATGAATCCCATTCAGG	introduce mutations at tail of PLENTY and deltaN-PLENTY for GFP-fusion
	mut_SP-PLENTY_tail_R	GTGATTATGGTATTTCGCATTAGTGC	introduce mutations at tail of SP-PLENTY for GFP-fusion
Genotyping	plenty_F	ATGGGAAGGGCAAAGTCACTTC	
	plenty_R	CCATCAACTGGTCTGTCCTT	
	snf2_wt_F	TCCCTTGTGGAGAATTTGCT	forward primer for amplification of wild type *LHK1*
	snf2_snf2_F	TCCCTTGTGGAGAATTTGTT	forward primer for amplification of *snf2* type *LHK1*
	snf2_R	GGAATGCCGTGGTATATGCT	
	HPTII_F	GGCGAGTACTTCTACACAGC	for genotyping stabely transformed plants
	HPTII_R	CATGTGTATCACTGGCAAAC	for genotyping stabely transformed plants

Table 4-2. Primers used in this chapter (continued)

Deleted region detection	PLENTY_del_down_F	CATAAGGCATCCCTGC
	PLENTY_del_down_R1	AAGACTCCTGGACTGCAAGA
	PLENTY_del_down_R2	AAGATATGTGCCTTGTACGAGTG
	PLENTY_del_down_R3	ATCCATGCCGAAATTCAGC
	PLENTY_del_down_R4	AAGGATCCTGCAGCTGCAA
	PLENTY_del_up_F1	TTCACAGGTGTAGCCCTGT
	PLENTY_del_up_F2	TAACATCCTAATAATGAAATTTATAACTTATCAATC
	PLENTY_del_up_F3	CACAGGCCAAGTTAGTGACG
	PLENTY_del_up_F4	CGCTCCGAGATTAATTCTCACTTA
	PLENTY_del_up_R	TTTGAGGTTTGCCATGGTTGAGAT
5' or 3'RACE	3RACE_PLENTY_1st	GTAAATCCTTTGCCTAATTTGGCT
	3RACE_PLENTY_2nd	CTAGAACCCAACCAGCAGG
	5RACE_PLENTY_2nd	CAGTAACGGGACCCTTGTC
	5RACE_PLENTY_1st	GGAGAATTGCCAATCGGATC
	3RACE_PLENTY2_1st	GCCTGATCACGTATTTGTACG
	3RACE_PLENTY2_2nd	TCCCAATCTGGCTTATGGAG
	5RACE_PLENTY2_2nd	TGTTACTGGTCCTTTCTCCTC
	5RACE_PLENTY2_1st	GAGAATTGCCAATCGGATCAATA
	3RACE_PLENTY3_1st	GCCCGATCATATAATTGTCAAAC
	3RACE_PLENTY3_2nd	TACCCAACTTAGCTAAAGATGGG
	5RACE_PLENTY3_2nd	CCATTGGGACACTCCGTAA
	5RACE_PLENTY3_1st	CCAACAATAACTGGTGAATTTCC

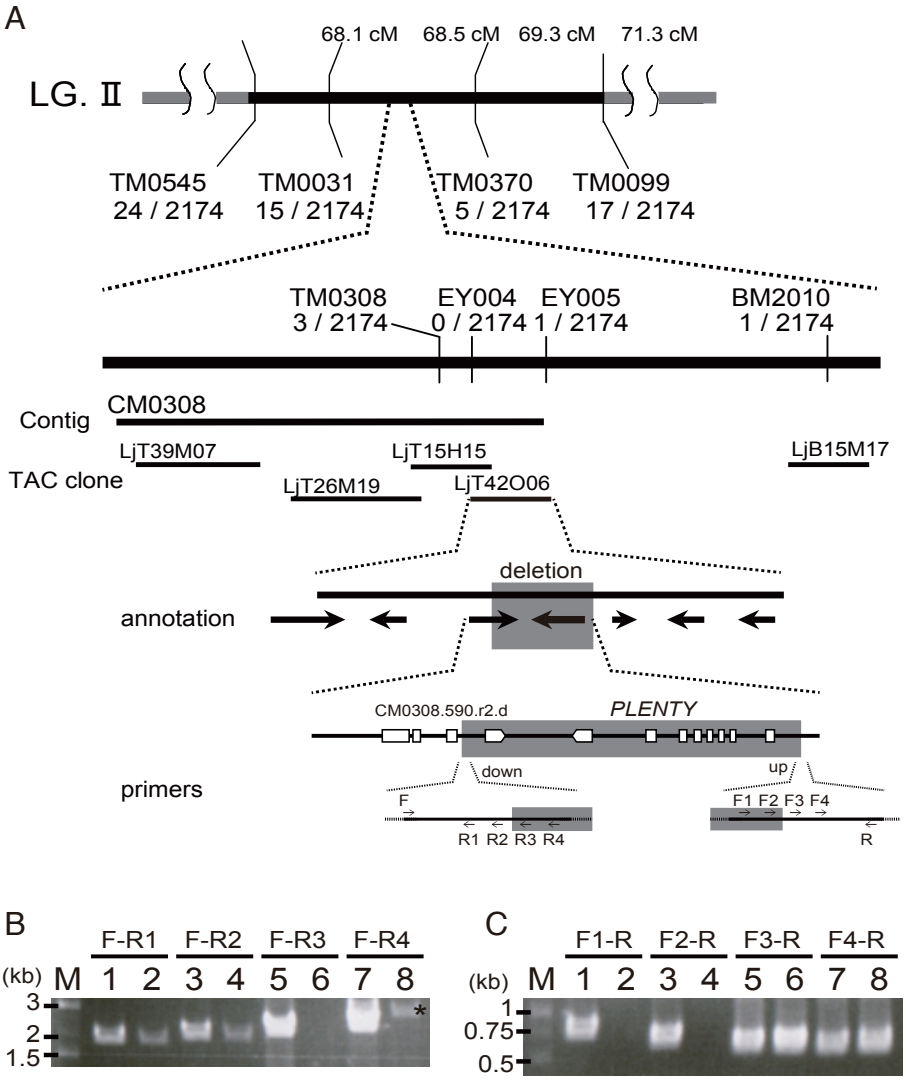

Figure 4-1. Identification of the *plenty* locus and the deletion site in the *plenty* genome.

A, The locus responsible for *plenty* on LG II is indicated with the number of recombination events (events / total chromosomes), and physical map with names of TAC/BAC clones are indicted above the lines. The large deletion (shaded in grey) including CM0308.590.r2.d and CM0308.600.r2.d which we named *PLENTY*, was detected by genomic PCR in the chromosomal region between TM0308 and EY005 (a newly developed marker in this chapter, Table 4-1). Arrows indicate primers used to identify the deletion (Table 4-2). B, C, Agarose gel electrophoresis of DNA markers (M) and PCR products of genomic DNA templates of MG-20 (Lanes 1,3,5,7) and *plenty* (Lanes 2,4,6,8). The DNA fragments were amplified with sets of primers as shown in each lane and these positions are shown in A.

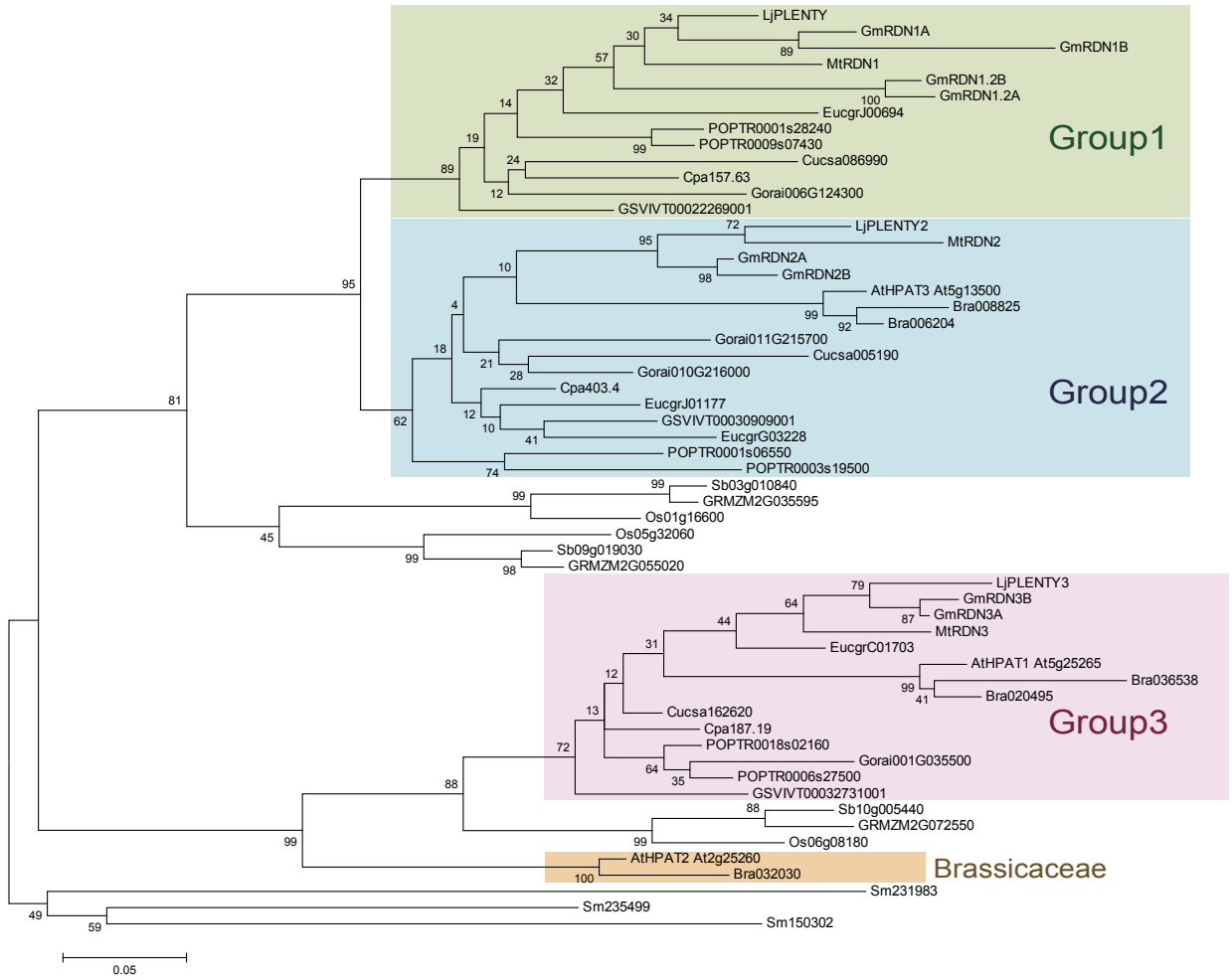

Figure 4-2. Phylogenetic tree of the *Lj*PLENTY family in land plants.

The percentage of trees in which the associated taxa clustered together is shown next to the branches after bootstrapping (1,000 replicates). The tree is drawn to scale with branch lengths measured in the number of substitutions per site. The 57 amino acid sequences used for this analysis consist of the same data set from the study of *Mt*RDN1 (Schnabel et al., 2011) including the eudicots *Lotus japonicus* (Lj), *Medicago truncatula* (Mt), soybean (*Glycine max* Gm), grape (*Vitus vinifera*, GSVIVT), cucumber (*Cucumus sativus*, Cucsa), poplar (*Populus trichocarpa*, POPTR), and *Arabidopsis thaliana* (*At*); the monocots rice (*Oryza sativa*, Os), sorghum (*Sorghum bicolor*, Sb), and maize (*Zea mays*, GRMZM); and the lycophyte *Selaginella moellendorfii* (Sm) and the newly added sequences from Phytozome (http://www.phytozome.net/) including *Brassica rapa Chiifu-401* (Bra), papaya (*Carica papaya*, Cpa), cotton (*Gossypium raimondii*, Gorai), and eucalypt (*Eucalyptus grandis*, Eucgr). All positions containing gaps and missing data were eliminated. There were a total of 270 positions in the final dataset. Evolutionary analyses were conducted in MEGA6 (Tamura et al., 2013).

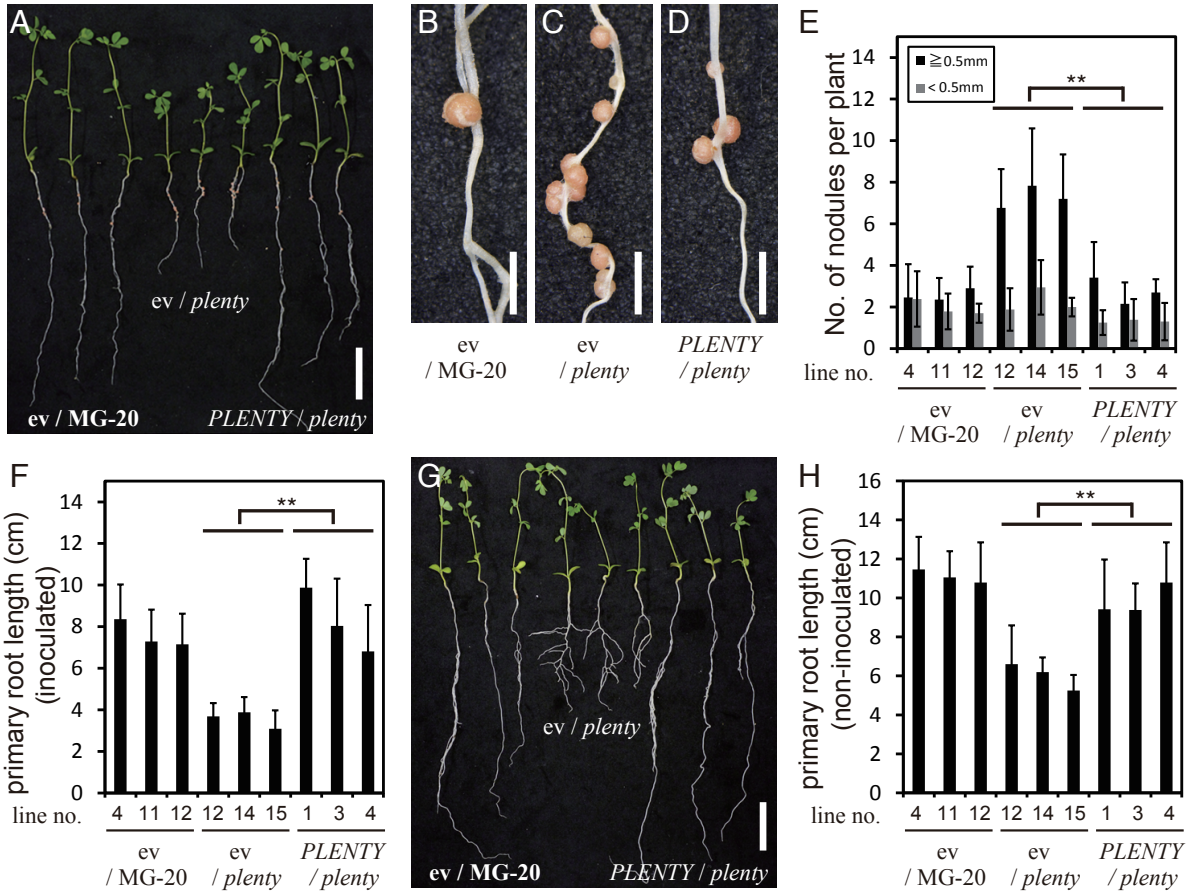

Figure 4-3. Complementation test of *plenty* with *PLENTY*-expressing T3 lines.

A, Rhizobium-inoculated plants of a wild type (MG-20) stably transformed with empty vector pUB-GW-GFP (ev/MG-20), a *plenty* mutant transformed with empty vector (ev/*plenty*), and a *plenty* mutant transformed with pUB-GW-Full-PLENTY (*PLENTY*/*plenty*) at 14 DAI with *M. loti* MAFF303099. Magnified images of the nodulated region of ev/MG-20 (B), ev/*plenty* (C), and *PLENTY*/*plenty* (D) are shown. Nodule numbers (≧0.5 mm diameter in black bars, and <0.5 mm diameter in grey bars) per plant (E) and primary root length (F) of each inoculated T3 transgenic line (n > 10) were counted and measured, respectively. G, Non-inoculated plants of ev/MG-20, ev/*plenty*, and *PLENTY*/*plenty* are shown. H, Primary root length of each T3 transgenic line was measured at 21 DAG. Scale bars = 2 cm in A,G and 2 mm in B-D; Error bars indicate the S.D. $^{**}P < 0.01$, Student's *t*-test. Values of total nodule numbers were used for statistical analysis in E.

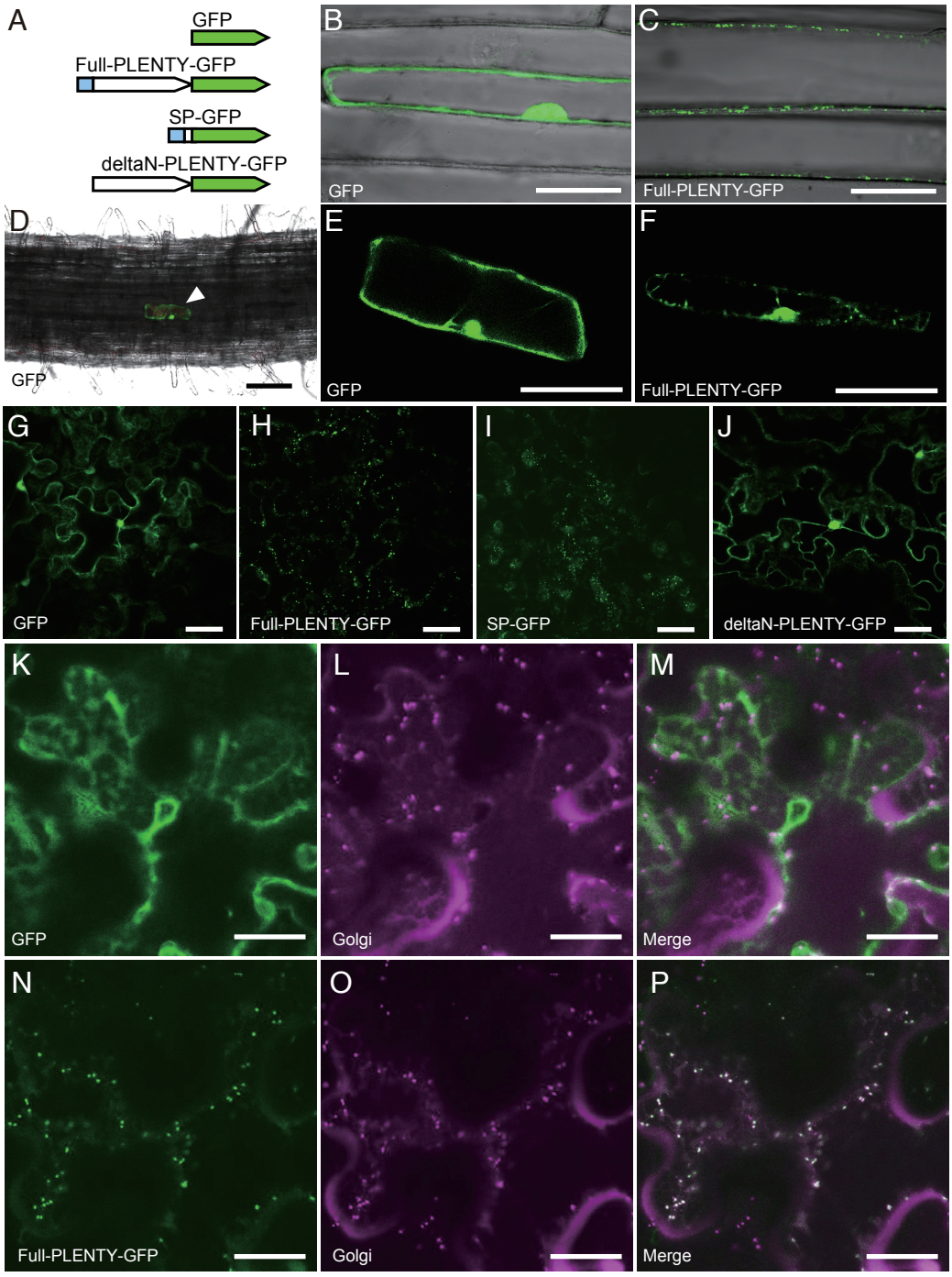

Figure 4-4. Subcellular localization of PLENTY-GFP fusion proteins.

A, Overview of the four GFP-fusion protein constructs used in this analysis, GFP, Full-PLENTY-GFP, SP-GFP, and deltaN-PLENTY-GFP. PLENTY includes a putative secretory signal peptide at the N-terminus (shown in blue). The confocal microscopic GFP florescence images of GFP-fusion proteins in onion epidermal cells (B,C) and *Lotus japonicus* root cells (D-F) transformed by particle bombardment, and *N. benthamiana* leaves (G-P) transformed by agroinfiltration. Merged images (M,P) showing the transient co-expression of GFP (G,K) or full-length PLENTY-GFP (H,N), and the *cis*-Golgi marker (mannosidase I)-mCherry (L,O). Constructs used for the analysis are shown in each panel (B-P). Arrowhead in D indicates rarely observed transformed cell in *L. japonicus* by particle bombardment. Scale bars = 100 μm in D; 50 μm in B,C,E-J; 25 μm in K-P.

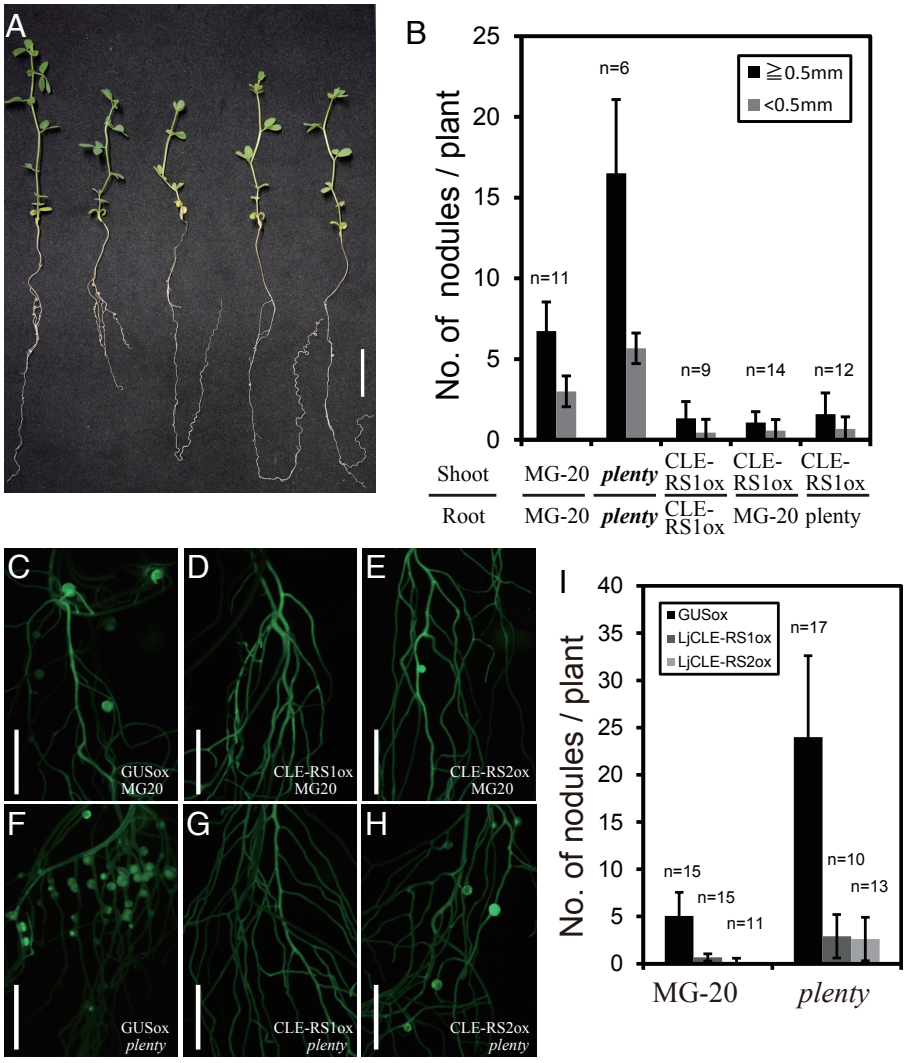

Figure 4-5. Suppression of hypernodulation in *plenty* by *CLE-RS1*/*2* overexpression.

A, Plant images of different grafting combinations (Shoot/Root), shown from left to right [MG20/MG20, *plenty*/*plenty*, *CLE-RS1*-overexpressing plant (CLE-RS1ox)/CLE-RS1ox, CLE-RS1ox/MG-20, and CLE-RS1ox/*plenty*]. B, Nodule numbers (≧0.5 mm diameter in black bars, and <0.5 mm diameter in grey bars) per plant was counted in different grafting combinations at 14 DAI with *M. loti* MAFF303099. C-H, Images of hairy root-transformed roots with over-expressing *GUS* (as a control), *CLE-RS1*, or *CLE-RS2*. GFP fluorescence was checked as a marker for transformation. The genotypes and introduced constructs are indicated in each panel. I, Nodules per transformed plant was counted at 14 DAI. Error bars indicate the S.D. Scale bars = 5 mm in C-H.

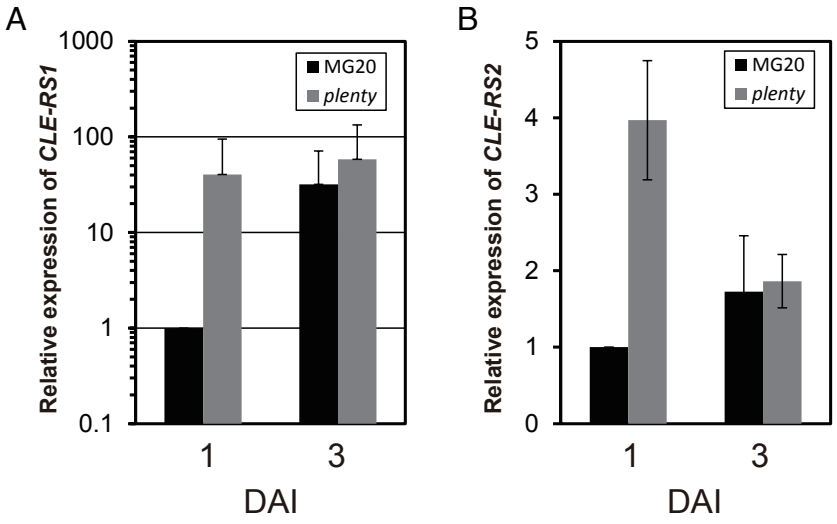

Figure 4-6. Gene expression levels of *CLE-RS1* and *CLE-RS2* in *plenty.*

Real-time RT-PCR analysis of *CLE-RS1* (A) and *CLE-RS2* (B) normalized by the expression levels of *EF-1a* in Miyakojima MG-20 wild type (black bars) and *plenty* (gray bars) at 1 day or 3 DAI with *M. loti* MAFF303099. Fold changes in expression are shown relative to that of MG-20 wild type at 1 DAI. Data are the mean ± S.D. of three biological replicates.

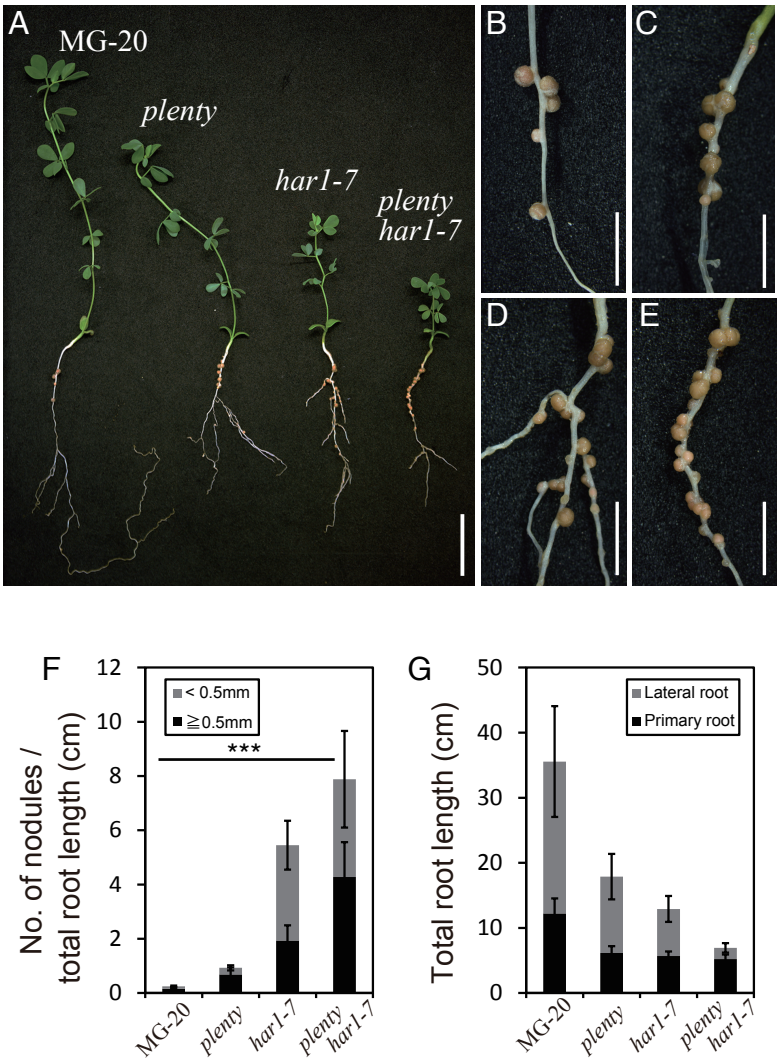

Figure 4-7. Additional nodulation of *plenty har1-7*.

A, Nodulated plants of wild type (MG-20), *plenty*, *har1-7*, and the *plenty har1-7* double mutant. Magnified images of nodulated roots of wild type (MG-20) (B), *plenty* (C), *har1-7* (D), and the *plenty har1-7* double mutant (E). F, Nodule numbers (≧0.5 mm diameter in black bars, and <0.5 mm diameter in grey bars) normalized by the total root length (primary root length in black bars, and lateral loot length in grey bars) of each plant (G) was counted at 21 DAI with *M. loti* MAFF303099. Error bars indicate the S.D. Scale bars = 2 cm in A; 5 mm in B-E. Values of total nodule numbers were used for statistical analysis in (f). ***$P < 0.0001$, Kruskal-Wallis test.

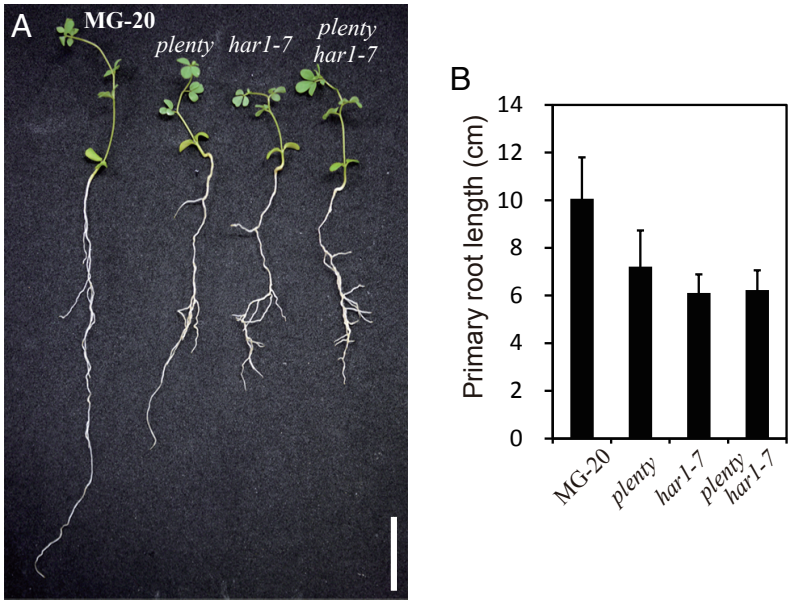

Figure 4-8. No additional primary root length phenotype of *plenty har1-7*.

A, Non-inoculated plants at 28 DAG. The genotype of each plant is shown inside the panel. B Primary root lengths of MG-20, *plenty*, *har1-7*, and the *plenty har1-7* double mutant were measured. Scale bar = 2 cm in A. Error bars indicate the S.D.

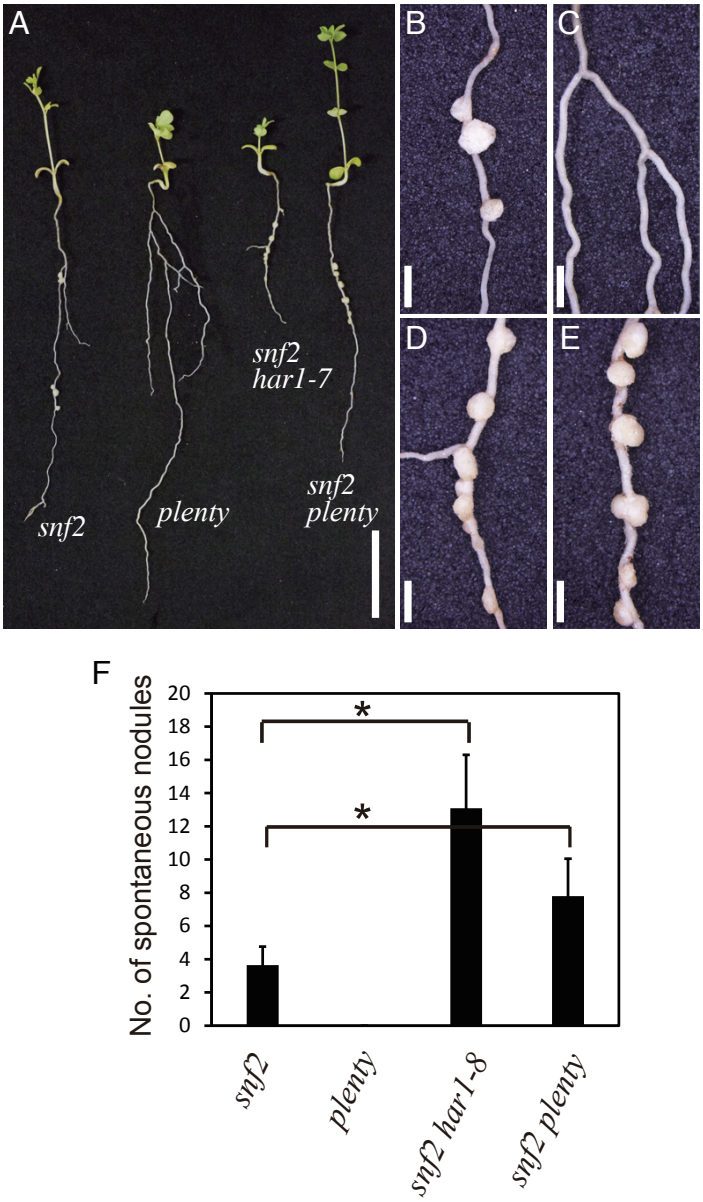

Figure 4-9. The increased spontaneous nodules of *plenty snf2*.

A, Non-inoculated plants of *snf2*, *plenty*, the *snf2 har1-7* double mutant, and the *snf2 plenty* double mutant grown in the absence of KNO_3 at 42 DAG. Magnified images of spontaneously nodulateds root of *snf2* (B), *plenty* (C), the *snf2 har1-8* double mutant (D), and the *snf2 plenty* double mutant (E). F, Spontaneous nodule numbers per plant was counted at 42 DAG. Error bars indicate the S.D. Scale bars = 2 cm in A-E. $*P < 0.05$, Student's *t*-test.

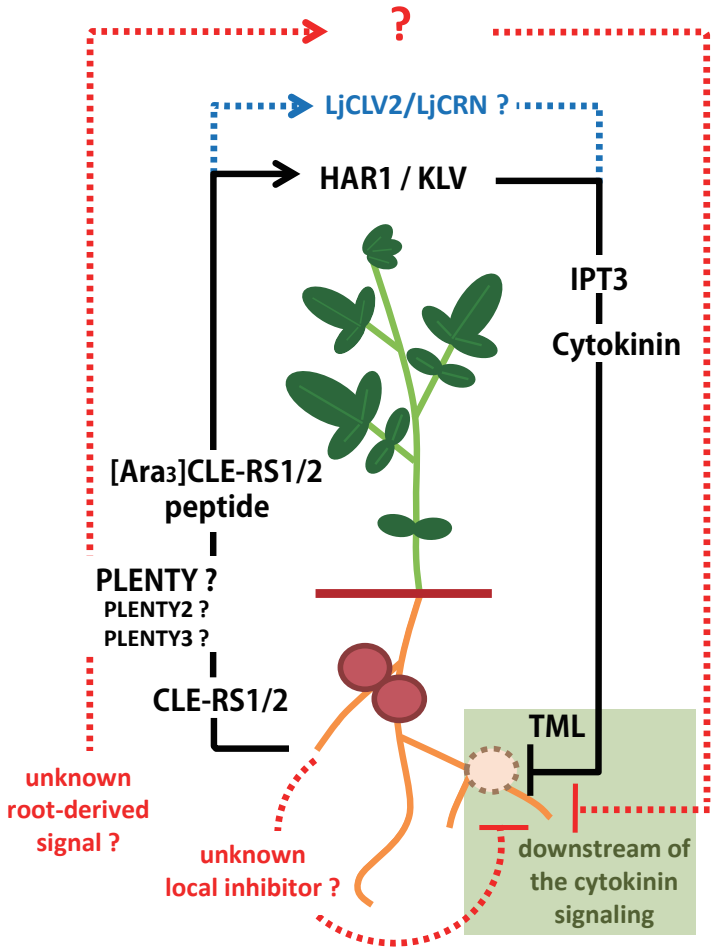

Figure 4-10. A model of several possible pathways for PLENTY-mediated control of nodulation.

The well-characterized pathway for HAR1-meditated long-distance control of nodulation features; *CLE-RS1/2* gene induction, post-translational arabinosylation of CLE-RS1/2 pepides perception of CLE-RS1/2 peptides by HAR1 and KLV receptors, production of a shoot-derived inhibitor, and degradation of an unknown positive factor for nodulation mediated by TML (black solid line). My results support two different hypotheses that PLENTY controls nodule numbers independently from the HAR1-mediated pathway. One proposed pathway presumes that PLENTY mediates the production of a completely unknown root-derived systemic signal or local inhibitor other than CLE-RS1/2 (red dashed lines). Another possibility is that PLENTY mediates the arabinosylation of CLE-RS1/2 peptides that can bind to other receptors besides HAR1or KLV, thereby providing a partially HAR1-independent pathway (blue dashed lines). Both the HAR1- and the PLENTY-mediated pathways inhibit downstream of cytokinin signaling during nodule organogenesis (green box).

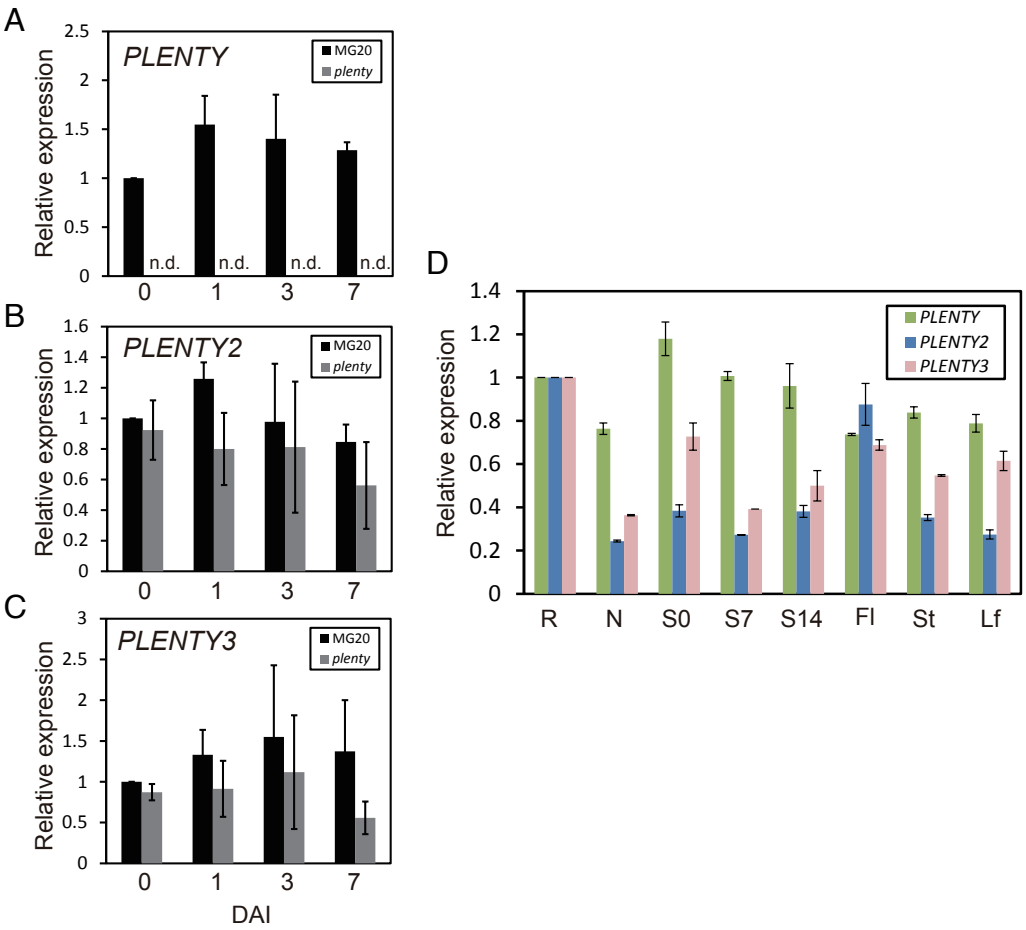

Figure 4-11. The expression patterns of *PLENTY* and *PLENTY* paralogs.

Real-time RT-PCR analysis of *PLENTY* (A), *PLENTY2* (B) and *PLENTY3* (C) normalized by the expression levels of *EF-1a* in Miyakojima MG-20 wild type (black bars) and *plenty* (grey bars) at non-inoculated (0), 1, 3, and 7 DAI with *M. loti* MAFF303099. Fold changes in expression are shown relative to that of MG-20 wild type at 0 DAI. Data are the mean ± S.D. of three biological replicates. D, Real-time RT-PCR analysis of *PLENTY* (green bars), *PLENTY2* (blue bars), and *PLENTY3* (pink bars) in different tissues including whole roots at 14 DAI (R), nodules at 14 DAI (N), whole shoots at 0 DAI (S0), whole shoots at 7 DAI (S7), whole shoots at 14 DAI (S14), flowers at 8 weeks after germination (Fl), stems at 8 weeks after germination (St), and leaves at 8 weeks after germination (Lf) of Miyakojima MG-20 wild type normalized by the expression levels of *EF-1a*. Fold changes in expression are shown relative to that of whole roots (R). Data are the mean ± S.D. of three technical replicates. n.d. means non-detected.

Chapter 5

GENERAL DISCUSSION

In this chapter, first, I describe the possible molecular mechanisms underlying the NIN transcription factor-mediated IT suppression, which are found in **Chapter 2**, focusing on several studies of transcription factors of Arabidopsis or known factors involved in IT inhibition (**5.1.**, **5.2.**). Secondly, I describe perspectives for future studies of rhizobial infection (**5.3.**). Thirdly, I discuss both similarities and dissimilarities between the well-known long-distance control of nodulation (**Chapter 4**) and NIN-mediated IT suppression (**Chapters 2, 3**) (**5.4.**). Then, I add findings from recent studies on the positive long-distance control of nodulation, in order to discuss the future direction of studies on systemic signals and non-symbiotic root development (**5.5.**). Lastly, I offer perspectives for future studies of PLENTY family proteins.

5.1. NIN-mediated IT suppression as a novel means of intercellular communication in legume-rhizobial symbiosis

Rhizobial infection in the epidermis and nodule organogenesis are tightly coupled, and several players required for cross-talk between the two pathways have been identified, *Lj*NFR5/*Mt*NFP, *Lj*SYMRK/*Mt*DMI2, *Lj*CYCLOPS/*Mt*IPD3, and *Lj*CCaMK/*Mt*DMI3 (**2.1.**, **3.1.**). These proteins are expressed in both epidermis and cortex; however, how they behave in the different root cell layers to transduce cross-signaling remains unclear. The specific post-translational elimination of the ectodomain of SYMRK protein, and the strength of phosphorylation activity of CCaMK, provide their important functions as hub proteins between the infection and organogenesis pathways (**2.1.**, **3.1.**). Although in

this dissertation I proposed a new cross-talking mechanism mediated by NIN transcriptional factor between the two pathways, how can two different biological events, infection and organogenesis, be controlled by the same transcription factor, NIN? Moreover, how can NIN act both positively and negatively in a stage- or tissue-dependent manner during nodule organogenesis? I further discuss the potential functions of NIN as a putative bifunctional transcription factor. Recent reports in Arabidopsis indicate that a single transcription factor may act as a multifunctional transcription factor and mediate a wide variety of biological events.

NIN transcription factor itself has both positive and negative roles in manners that depend on multiple domains. In fact, WUSCHEL acts as both a repressor and an activator in a protein domain-dependent manner (Ikeda et al., 2009; Daum et al., 2014). At least in my study, however, a NIN chimeric repressor can repress IT formation in the epidermis (**Chapter 2**, Fig. 2-10, Table 2-3), so I expect that NIN functions only as an activator in both the infection and organogenesis pathways. If NIN functions as a repressor of infection, a NIN chimeric repressor will not show strong suppression of IT formation.

Another possibility is that different actions of NIN are dependent on tissue- or stage-specific downstream targets, including co-transcriptional regulators. Putative cortex- or late nodule-specific downstream factors might suppress the function of NIN for IT formation transcriptionally or post-transcriptionally. This potential mechanism is supported by several studies. Studies of LEAFY and ACTIVATOR PROTEIN1 transcription factors indicate that a single transcription factor can bind to different groups of targets by interacting with individual *cis*-regions or co-factors, depending on the particular developmental stages (Gregis et al., 2008; Liu and Mara, 2010). Moreover,

several reports of cross-talk in defense signaling propose a potential mechanism by which single transcription factors, such as WRKYs and TGAs (bZIP-type transcription factors), play both positive roles in the salicylic acid (SA)-dependent pathway and negative roles in the jasmonic acid-dependent pathway (Li et al., 2004; Gao et al., 2011; Van der Does et al., 2013).

5.2. Potential downstream targets of novel NIN-mediated local suppression of IT

Previously, a few hyperinfection mutants, *Ljhit1-1*, *Mtsickle* and *Mtefd* [Table 1-1(g,h)] (Penmetsa et al., 2003; Murray et al., 2007; Vernie et al., 2008) have suggested the existence of regulatory mechanisms controlling rhizobial infection processes. However, the molecular mechanisms behind this control are far less well known than those involved in nodulation control, due to technical difficulties in measurement of IT numbers as described above (**3.3.2**). Furthermore, although *Ljhit1-1* exhibits low nodulation, *Mtsickle* and *Mtefd* exhibit an increased number of nodules, leaving the putative cross-talk between the infection and organogenesis pathways mysterious. According to my study, the phenotype of *Ljhit1-1* is caused by lower expression of *NIN*, functioning in organogenesis and inhibiting infection, similar to *daphne*. In contrast, in *Mtsickle* and *Mtefd*, *NIN* may be more highly expressed, but the inhibitory mechanisms of infection mediated by NIN may be lost.

In any case, the identification of the downstream targets of NIN will be crucial for further understanding of the control of development of ITs. In terms of the downstream targets of NIN in its role as a positive factor for organogenesis (cell proliferation activity), NSP2 and NF-YA/YB have been identified (Soyano et al., 2013). My study also demonstrated that CLE-RS1/2 peptides, as the direct downstream targets

of NIN (Soyano et al., 2014), induce the long-distance systemic inhibition of ITs (**Chapter 3**, Fig. 3-2, Fig. 3-3). However, the components of the pathway involved in NIN-mediated local inhibition of ITs are unknown. This novel pathway is predicted by the observation that NIN overexpression is still effective for IT suppression in the *daphne har1-8* double mutant (**Chapter 3**, Fig. 3-4).

Previous studies of negative regulators of rhizobial infection suggest one of the possible downstream candidates, an ethylene-signaling factor. *Mt*SICKLE and *Lj*EIN1/2, which are orthrogous to Arabidopsis EIN2, are involved in nodule suppression (**1.4.**) (Penmetsa and Cook, 1997; Penmetsa et al., 2003; Miyata et al., 2013). In particular, an aberrantly expanded radial pattern of nodules in *Mtsickle* indicate that the suppression induced by ethylene signaling has extremely local action. In addition, it has been shown that an accumulation of ethylene near the protoxylem pole negatively regulates both infection and cortical cell division, mediated by the specific spatial expression of aminocyclopropane-1-carboxylic acid oxidase which catalyzes the final step of ethylene biosynthesis (Heidstra et al., 1997). More importantly, the genetic independence of the *Lj*HAR1/*Mt*SUNN-mediated long-distance pathway and the *Mt*SICKLE-mediated ethylene pathway also supports the possibility of an involvement of ethylene in the novel NIN-mediated suppression of IT (Penmetsa et al., 2003).

5.3. Future studies in the control of rhizobial infection

The biological meaning of controlling the susceptibility of rhizobial infection has not yet been established. At least under my experimental conditions, excessive IT-forming *daphne* exhibited no significant growth delay compared to no-IT-forming *daphne* (Fig. 5-1), unlike observations of hypernodulation mutants (Wopereis et al., 2000; Nishimura

et al., 2002a; Oka-Kira et al., 2005). This may indicate that IT formation is a less energy-consuming process compared to nodule formation or nitrogen fixation (Tjepkema and Winship, 1980; Udvardi et al., 1988; Udvardi and Poole, 2013). Thus, it may be not necessary for a plant to control ITs for energy saving.

An alternative role of IT control might be as a mechanism for preventing infection by other non-beneficial bacteria. In natural conditions, even during an interaction with symbiotic bacteria, plants may be in danger of pathogenic bacterial infection. In this sense, *daphne* may be at a higher risk of pathogen invasion. Several studies show common phenomena in both plant-symbiont and plant-pathogen interactions, such as ROS production, SA accumulation, and the hypersensitive response (Vasse et al., 1993; Bozso et al., 2009; Soto et al., 2009). In particular, reduced accumulation of SA in *L. japonicus* results in a high frequency of IT formation as well as nodulation (Stacey et al., 2006). For successful infection, several rhizobial factors contribute to the suppression of host immune responses (reviewed in Soto et al., 2009). In fact, a significant decrease in ROS accumulation via downregulation of *Mt*RBOH2/3 (membrane-associated NADPH oxidases) is induced by Nod factor treatment, and ROS reduction is required for root hair deformation (Lohar et al., 2007). Another recent study provides strong evidence: even in Arabidopsis, rhizobial Nod factor can suppress the host immune response, depending on an ortholog of Nod factor receptor (Liang et al., 2013). Further study of the molecular interaction that is involved between the control of symbiotic bacterial infection and general plant defense responses will provide new insight into its biological function.

Although I did not mention rhizobial factors in this dissertation, IT formation is also affected by them. ExoO, NodE, NodF, and NodL have positive effects on infection

based on observation of phenotypes of rhizobial mutants lacking these genes, which are responsible for production of exopolisaccarides and modification of Nod factors (Ardourel et al., 1994; Gage, 2004; Jones et al., 2007). In particular, in alfalfa, cortical cell activation for nodule organogenesis is also affected by structural differences in Nod factors as well as IT initiation (Ardourel et al., 1994). Thus, these authors propose a negative feedback regulatory mechanism for organogenesis accomplished by putatively different types of Nod factor receptors. Recently, in the *S. meliloti–Medicago* symbiosis, it is reported that inactivation of the signaling cascade of cAMP, one of the most popular molecules for quorum sensing in bacterial communication, result in a hyperinfection phenotype (Tian et al., 2012). These results indicate that rhizobia themselves also contribute to the regulation of infection processes. Of course, IT progression is accompanied by division of rhizobia. Though the driving force of IT elongation is proposed to be plant-side IT membrane synthesis, based on observation of a bacterial-free zone in the tip of growing ITs [**1.2.**, Fig. 1-1(3)] (Fournier et al., 2008), IT numbers can be coordinately controlled by the efficiency of rhizobia colonization in the lumen of IT.

Until now, most knowledge of rhizobial factors required for symbiosis has been gained separately from that of host plant factors. Except for the two combinations involved in early recognition of each other (**1.1.**), (1) rhizobial *nod* genes and plant flavonoids, and (2) rhizobial Nod factor and plant Nod factor receptors, the direct molecular interactions between symbiont and host plant remain largely unidentified. Recent advances regarding the interaction between host defense response and rhizobial entry indicate the importance of other molecular interactions during establishment of the symbiosis (Soto et al., 2009; Okazaki et al., 2013). Future corroborative research studies

on both the rhizobial side and plant side should offer breakthroughs to understand the complicated interactions between rhizobia and host plants.

5.4. Mechanisms for controlling IT numbers and nodule numbers

Several molecules are certainly shared between pathways involved in nodulation control and IT control. My study showed that several components of the HAR1-mediated pathway are also functional in inhibiting excessive ITs in *daphne* (**Chapter 3**). Assuming a direct negative regulator that inhibits both ITs and nodules, the marked difference in the machinery involved in IT formation and nodulation should not be ignored. IT formation require a kind of tip growth, including degradation and reorganization of cell wall or membrane, cytoskeletal rearrangement, and vesicle trafficking; the molecules involved in these phenomena can be recruited by the machinery used for root hair or pollen tube growth (**1.2.**). On the other hand, organogenesis in the root cortex is required for dedifferentiation or activation of cortical cells and reentering the cell cycle. These processes are thought to be primarily mediated by cytokinin signaling, auxin signaling, and endoreduplication (**1.3.**). Therefore, I suspect that the inhibition signal would be transduced differently into appropriate signals for each pathway. This means that the target molecules for IT control and nodulation control can be different.

The next important question is what kinds of molecules are targeted by these inhibition pathways. At least in terms of the long-distance control of nodulation, the target may function downstream of positive cytokinin signaling, based on the increased spontaneous nodules of *snf2* in the presence of the mutations *har1*, *klv*, *tml*, and *plenty* (**Chapter 4**) (Miyazawa et al., 2010; Takahara et al., 2013). Another study proposes the

same genetic site, because initial cortical cell division together with auxin accumulation, which occurs downstream of cytokinin signaling, is observed even in *CLE-RS1/2*-overexpressing roots (Suzaki et al., 2012). Inconsistent with this prediction, in *M. truncatula* it is proposed that the long-distance control of nodulation directly down regulate the cytokinin signaling to suppress nodulation. This is explained by the decreased expression level of *MtEFD* and *MtRR8* in *MtCLE-12*-overexpressing roots (Saur et al., 2011).

Additionally, identification of TML, an F-box protein, prompts me to predict that at the site furthest downstream of the long-distance control, an unknown positive factor for nodulation might be degraded in a TML-dependent manner (Takahara et al., 2013). Identification of the target molecules in future studies will answer the exact site of action in the long-distance control.

5.5. More complicated mechanisms for long-distance control of nodulation and non-symbiotic root development

Looking back at the history of research into long-distance systemic control in nodulation, the main focus has been on negative regulation of nodulation, because the nodulation phenotypes of a series of isolated hypernodulation mutants in different legumes are frequently dependent on their shoot genotype (**1.4.**). Very recently, however, positive long-distance control of nodulation was discovered in *M. truncatula* (Huault et al., 2014). The mutant *compact root architecture 2* (*cra2*) showed low nodulation and short roots with a dramatically increased number of lateral roots, and harbors a mutation in a *LRR-RLK* gene, *MtCRA2*, which is orthologous to Arabidopsis XYLEM INTERMIXED IN PHLOEM 1 (XIP1) (Bryan et al., 2012). *At*XIP1 was also recently

identified as a receptor of *At*CEP1 peptide, which belongs to the C-terminally encoded peptide (CEP) family (Tabata et al., 2014). Furthermore, consistent with these recently identified pieces of molecular evidence, it had already been proposed that *Mt*CEP1 positively regulates nodulation in response to low nitrogen conditions (Imin et al., 2013). Taken together, these studies predict that a combination of *Mt*CEP1 peptide and *Mt*CRA2 receptor may positively regulate nodulation and negatively regulate root growth and lateral root formation in legumes, at least in *M. truncatula*, similarly to *Lj*HAR1/*Mt*SUNN and *Lj*CLE-RS1/2/*Mt*CLE12/13 in long-distance control (**1.4.**, **Chapter 4**).

More surprisingly, grafting experiments with *Mtcra2* showed that the phenotype showing a lower number of nodules was determined by shoot genotype, but the compact root phenotype was determined by root genotype. This result strongly suggests that *Mt*CRA2 functions differently depending on the pathway involved in nodulation control or root development. The different pathways may be determined by distinct ligands.

In my study, PLENTY was also required for negative regulation of nodulation and non-symbiotic primary root growth (**Chapter 4**, Fig. 4-3). Intriguingly, the *plenty har1* double mutant phenotype indicated that nodulation control was independent of HAR1; conversely, primary root growth regulation by PLENTY used the same genetic pathway as HAR1 (Fig. 4-7, Fig. 4-8). These distinct contributions of PLENTY to nodulation control and root development may be explained by differences between unidentified substrates of PLENTY, putatively small peptides functioning in the two processes. In addition, the different contributions remind me of that of *Mt*CRA2.

Most nodulation mutants affect root architecture, indicating shared mechanisms for regulating both nodulation and root development. Knowledge of *Mt*CRA2 provided

insight into the far more complicated systemic and local regulatory pathways involved in nodulation and root growth development than I expected. Even if genes are common between the two phenomena, their functional tissues, upstream, or downstream may be completely different. Identification of systemic or local signaling molecules and understanding for the mechanisms controlling their production, transportation, and reception in response to various conditions will be crucial issues in this research field.

5.6. Further characteristics of the PLENTY family proteins

In **Chapter 4**, I identified a putative protein-modifying enzyme, PLENTY, as a new player for nodule inhibition, based on a recent identification of its three Arabidopsis homologs, HPATs, which mediate post-translational modification, hydroxyproline O-arabinosylation. This modification is widely found in secreted plant peptides, some of which play important roles in stem cell maintenance, cell proliferation, and defense responses (Amano et al., 2007; Ohyama et al., 2009; Shinohara and Matsubayashi, 2010). *At*EXT3 (extensin), *At*PSY1 (plant peptide containing sulfated tyrosine 1), and *At*CLE2 are certainly arabinosylated by *At*HPATs; however, the substrate specificities are a little different between three homologs (Ogawa-Ohnishi et al., 2013). A Loss-of-function mutant of *At*HPATs, the *Athpat1-1 Athpat1-2* double mutant, show impaired pollen tube growth, thicker cell walls, early flowering, early senescence, and longer hypocotyls (Ogawa-Ohnishi et al., 2013). These abnormalities suggest the existence of other unidentified substrates of *At*HPATs that are involved in various aspects of plant development and signaling. Among these phenotypes observed in the *Athpat1-1 Athpat1-2* double mutant, at least the short hypocotyl phenotype of *plenty* seedlings was opposite to that of *Athpat1-1 Athpat1-2* (Ogawa-Ohnishi et al., 2013) (Fig.

5-2). This difference may be derived from distinct enzyme-substrate combinations among different plant species.

In the end, I refined the previous phylogenetic analysis of the PLENTY gene family by adding sequences from other plant species, such as a eucalypt, cotton, and papaya. My results confirmed that the distribution of *At*HPATs in the Brassicaceae is very different from that of the other eudicots (Schnabel et al., 2011; Fig. 4-2). Most notably, papaya which belongs to Brassicales, has an ortholog in the same group as PLENTY (Group 1), indicating that gene loss in Group 1 specifically occurred in the Brassicaceae. Perhaps homologs in Group 1, including PLENTY, have unknown molecular functions that members of the Brassicaceae have lost. Actually, in *L. japonicus*, CLE-RS2 peptide functioning in the long-distance control of nodulation, is an only identified arabinosylated peptide; however, my study showed that CLE-RS2 may not be substrate of PLENTY. Further studies of PLENTY families in legumes and other plants may shed new light on the roles of different glycopeptides, not only in nodule symbiosis but also in other aspects of plant development or signaling.

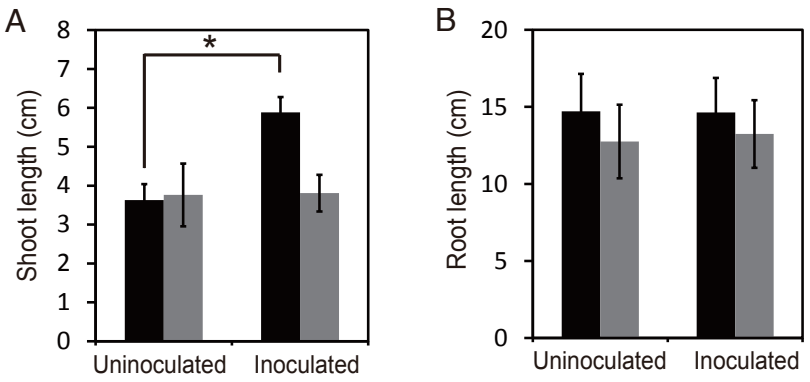

Figure 5-1. The plant growth difference between non-inoculated and inoculated conditions. The plant shoot (A) and root (B) length of MG-20 (black bar) and *daphne* (gray bar) were measured at 21 DAG inoculated with or without *M. loti* MAFF303099. **P* < 0.01, Student's *t*-test. n = 13.

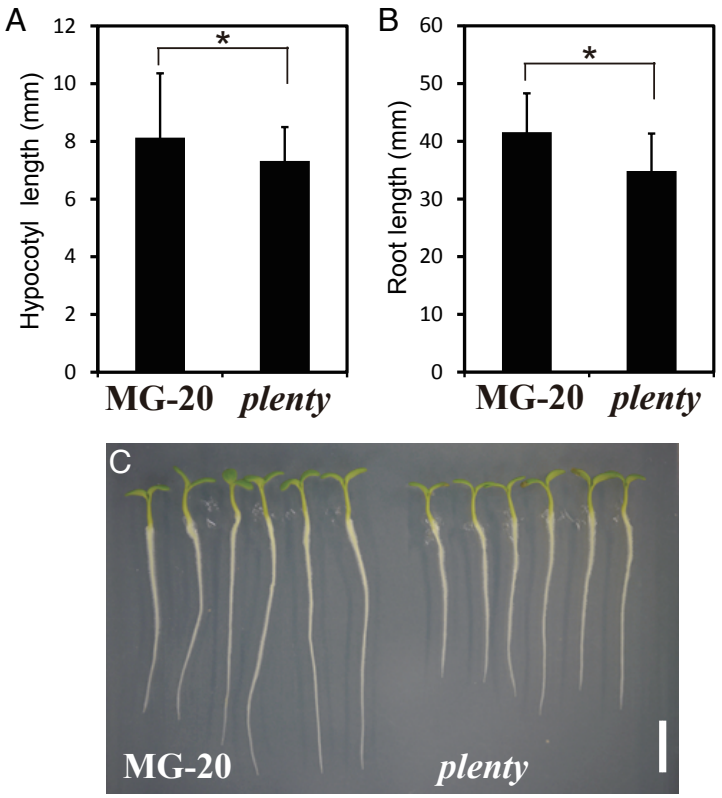

Figure 5-2. The seedling phenotypes of *plenty*.

A, Hypocotyl length of MG-20 wild type and *plenty* seedlings. B, Root lengths of MG-20 wild type and *plenty* seedlings. C, Plant images of seedlings at 3 DAG. Genotypes are shown inside of the panel. Scale bar = 1 cm. *$P < 0.05$, Student's *t*-test.

ACKNOWLEDGEMENTS

First of all, I deeply appreciate my supervisor, Dr. Masayoshi Kawaguchi [The Graduate University for Advanced Studies (SOKENDAI) and National Institute for Basic Biology (NIBB)], for his generous guidance and support. I sincerely appreciate, Dr. Takuya Suzaki (SOKENDAI and NIBB) for his helpful suggestions and discussion during my 5 years of study. I appreciate the current and former members of the Division of Symbiotic Systems in NIBB for lots of useful advice during my daily research life. I would like to especially thank former members Dr. Chie Yoshida for her preliminary work leading up to my study and Dr. Satoru Okamoto (Nagoya University) and Mr. Takema Sasaki (NIBB) for their work and providing vectors or transformed plant seeds of CLE-RS1/2-overexpression.

I express my gratitude to the advisors of NIBB, Dr. Kiyoshi Tatematsu, Dr. Shoji Mano, Dr. Masanao Sato, Dr. Mikio Nishimura, and Dr. Mitsuyasu Hasebe for their valuable comments.

I appreciate Dr. Jens Stougaard (Aarhus University, Denmark) for mutant seeds of *nin-2*, Dr. Krzyztof Szczyglowski (University of Western Ontario, Canada) for mutant seeds of *hit1-1*, Dr. Detlef Weigel (the Max Planck Institute for Developmental Biology, German) for the *GUS* construct, Dr. Makoto Hyashi (RIKEN) for *M. loti* MAFF303099 expressing *DsRED*, Dr. Shusei Sato (Tohoku University) for genomic data on *L. japonicus*, Dr. Masaru Ohme-Takagi (National Institute of Advanced Industrial Science and Technology) for the *SRDX* construct, and Dr. Tsuyoshi Nakagawa (Shimane University) for various plant transformation vectors.

I would like to thank former members of the Department of Cell Biology of NIBB Dr. Shoji Mano, Dr. Michitaro Shibata, Dr. Kenji Yamada, and Dr. Shino

Goto-Yamada for technical support of protein localization analysis. I also thank Dr. Kentaro Tamura (Kyoto University) and Dr. Ikuko Hara-Nishimura (Kyoto University) for providing vectors for organelle markers.

I also thank the Functional Genomics Facility and Spectrography and Bioimaging Facility and Model Plant Facilities of NIBB for technical support.

My study is also supported by the Japan Society for the Promotion of Science (JSPS) Grant-in-Aid for JSPS Fellow (grant number 25-3940 to Emiko Yoro), the Ministry of Education, Culture, Sports, Science and Technology Grants-in-Aid for Scientific Research [grant number 25114519 to Takuya Suzaki, and 25291066 and 22128006 to Masayoshi Kawaguchi], and the Yoshida Scholarship Foundation (to Emiko Yoro).

Finally, I express my sincere gratitude to my family.

LIST OF REFERENCES

Amano Y, Tsubouchi H, Shinohara H, Ogawa M, Matsubayashi Y (2007) Tyrosine-sulfated glycopeptide involved in cellular proliferation and expansion in *Arabidopsis*. *P Natl Acad Sci USA* **104:** 18333-18338

Ane JM, Kiss GB, Riely BK, Penmetsa RV, Oldroyd GED, Ayax C, Levy J, Debelle F, Baek JM, Kalo P, Rosenberg C, Roe BA, Long SR, Denarie J, Cook DR (2004) *Medicago truncatula* DMI1 required for bacterial and fungal symbioses in legumes. *Science* **303:** 1364-1367

Antolin-Llovera M, Ried MK, Parniske M (2014) Cleavage of the SYMBIOSIS RECEPTOR-LIKE KINASE ectodomain promotes complex formation with nod factor receptor 5. *Curr Biol* **24:** 422-427

Ardourel M, Demont N, Debelle FD, Maillet F, Debilly F, Prome JC, Denarie J, Truchet G (1994) Rhizobium-Meloloti Lipooligosaccharide nodulation factors – different structural requirements for bacterial entry into target root hair-cells and induction of plant symbiotic developmental responses. *Plant Cell* **6:** 1357-1374

Ariel F, Brault-Hernandez M, Laffont C, Huault E, Brault M, Plet J, Moison M, Blanchet S, Ichante JL, Chabaud M, Carrere S, Crespi M, Chan RL, Frugier F (2012) Two direct targets of cytokinin signaling regulate symbiotic nodulation in *Medicago truncatula*. *Plant Cell* **24:** 3838-3852

Arrighi J-F, Godfroy O, de Billy F, Saurat O, Jauneau A, Gough C (2008) The RPG gene of *Medicago truncatula* controls Rhizobium-directed polar growth during infection. *P Natl Acad Sci USA* **105:** 9817-9822

Barbulova A, Rogato A, D'Apuzzo E, Omrane S, Chiurazzi M (2007) Differential effects of combined N sources on early steps of the nod factor-dependent transduction pathway in Lotus japonicus. *Mol Plant-Microbe Interact* **20:** 994-1003

Battaglia M, Ripodas C, Clua J, Baudin M, Mario Aguilar O, Niebel A, Eugenia Zanetti M, Antonio Blanco F (2014) A nuclear factor Y interacting protein of the GRAS family is required for nodule organogenesis, infection thread progression, and lateral root growth. *Plant Physiol* **164:** 1430-1442

Bauer P, Ratet P, Crespi MD, Schultze M, Kondorosi A (1996) Nod factors and cytokinins induce similar cortical cell division, amyloplast deposition and *MsEnod12A* expression patterns in alfalfa roots. *Plant J* **10:** 91-105

Ben Amor B, Shaw SL, Oldroyd GED, Maillet F, Penmetsa RV, Cook D, Long SR, Denarie J,

Gough C (2003) The NFP locus of *Medicago truncatula* controls an early step of Nod factor signal transduction upstream of a rapid calcium flux and root hair deformation. *Plant J* **34:** 495-506

Bersoult A, Camut S, Perhald A, Kereszt A, Kiss GB, Cullimore JV (2005) Expression of the *Medicago truncatula DMI2* gene suggests roles of the symbiotic nodulation receptor kinase in nodules and during early nodule development. *Mol Plant-Microbe Interact* **18:** 869-876

Biswas B, Chan PK, Gresshoff PM (2009) A novel ABA insensitive mutant of *Lotus japonicus* with a wilty phenotype displays unaltered nodulation regulation. *Molecular Plant* **2:** 487-499

Borisov AY, Madsen LH, Tsyganov VE, Umehara Y, Voroshilova VA, Batagov AO, Sandal N, Mortensen A, Schauser L, Ellis N, Tikhonovich IA, Stougaard J (2003) The *Sym35* gene required for root nodule development in pea is an ortholog of *Nin* from *Lotus japonicus*. *Plant Physiol* **131:** 1009-1017

Bozso Z, Maunoury N, Szatmari A, Mergaert P, Ott PG, Zsiros LR, Szabo E, Kondorosi E, Klement Z (2009) Transcriptome analysis of a bacterially induced basal and hypersensitive response of *Medicago truncatula*. *Plant Mol Biol* **70:** 627-646

Brewin NJ (2004) Plant cell wall remodelling in the rhizobium-legume symbiosis. *Crit Rev Plant Sci* **23:** 293-316

Bright LJ, Liang Y, Mitchell DM, Harris JM (2005) The *LATD* gene of *Medicago truncatula* is required for both nodule and root development. *Mol Plant-Microbe Interact* **18:** 521-532

BroughtonWJ, Dilworth MJ (1971) Control of leghaemoglobin synthesis in snake beans. *Biochem J* **125:** 1075-1080

Bryan AC, Obaidi A, Wierzba M, Tax FE (2012) XYLEM INTERMIXED WITH PHLOEM1, a leucine-rich repeat receptor-like kinase required for stem growth and vascular development in *Arabidopsis thaliana*. *Planta* **235:** 111-122

Caetano-Anollés G, Gresshoff PM (1990) Early induction of feedback regulatory responses govering nodulation in soybean. *Plant Sci* **71:** 69-81

Caetano-Anollés G, Gresshoff PM (1991) Efficiency of nodule initiation and autoregulatory responses in supernodulating soybean mutant. *Appl Environ Microbiol* **57:** 2205-2210

Campanoni P, Blatt MR (2007) Membrane trafficking and polar growth in root hairs and pollen tubes. *J Exp Bot* **58:** 65-74

Capoen W, Goormachtig S, De Rycke R, Schroeyers K, Holsters M (2005) *SrSymRK*, a plant receptor essential for symbiosome formation. *P Natl Acad Sci USA* **102:** 10369-10374

Carroll BJ, McNeil DL, Gresshoff PM (1985) A supernodulation and nitrate-tolerant symbiotic (*nts*) soybean mutant. *Plant Physiol* **78:** 34-40

Catoira R, Galera C, de Billy F, Penmetsa RV, Journet EP, Maillet F, Rosenberg C, Cook D,

Gough C, Denarie J (2000) Four genes of *Medicago truncatula* controlling components of a nod factor transduction pathway. *Plant Cell* **12:** 1647-1665

Combier JP, Frugier F, de Billy F, Boualem A, El-Yahyaoui F, Moreau S, Vernie T, Ott T, Gamas P, Crespi M, Niebel A (2006) *Mt*HAP2-1 is a key transcriptional regulator of symbiotic nodule development regulated by microRNA169 in *Medicago truncatula*. *Genes Dev* **20:** 3084-3088

Cooper JE (2004) Multiple responses of rhizobia to flavonoids during legume root infection. *Advances in Botanical Research Incorporating Advances in Plant Pathology* **41:** 1-62

Crespi M, Frugier F (2008) De novo organ formation from differentiated cells: root nodule organogenesis. *Science Signaling* **1:** re11

Daum G, Medzihradszky A, Suzaki T, Lohmann JU (2014) A mechanistic framework for noncell autonomous stem cell induction in Arabidopsis. *P Natl Acad Sci USA* **111:** 14619-14624

Delves AC, Mathews A, Day DA, Carter AS, Carroll BJ, Gresshoff PM (1986) Regulation of the soybean-rhizobium nodule symbiosis by shoot and root factors. *Plant Physiol* **82:** 588-590

den Camp R, De Mita S, Lillo A, Cao Q, Limpens E, Bisseling T, Geurts R (2011) A phylogenetic strategy based on a legume-specific whole genome duplication yields symbiotic cytokinin type-A response regulators. *Plant Physiol* **157:** 2013-2022

Den Herder G, De Keyser A, De Rycke R, Rombauts S, Van de Velde W, Clemente MR, Verplancke C, Mergaert P, Kondorosi E, Holsters M, Goormachtig S (2008) Seven in absentia proteins affect plant growth and nodulation in *Medicago truncatula*. *Plant Physiol* **148:** 369-382

Ding YL, Kalo P, Yendrek C, Sun JH, Liang Y, Marsh JF, Harris JM, Oldroyd GED (2008) Abscisic acid coordinates Nod factor and cytokinin signaling during the regulation of nodulation in *Medicago truncatula*. *Plant Cell* **20:** 2681-2695

Doyle JJ (2011) Phylogenetic perspectives on the origins of nodulation. *Mol Plant-Microbe Interact* **24:** 1289-1295

Edgar RC (2004) MUSCLE: Multiple sequence alignment with high accuracy and high throughput. *Nucleic Acids Res* **32:** 1792-1797

Edwards A, Heckmann AB, Yousafzai F, Duc G, Downie JA (2007) Structural implications of mutations in the pea *SYM8* symbiosis gene, the *DMI1* ortholog, encoding a predicted ion channel. *Mol Plant-Microbe Interact* **20:** 1183-1191

Esseling JJ, Lhuissier FGP, Emons AMC (2003) Nod factor-induced root hair curling: Continuous polar growth towards the point of Nod factor application. *Plant Physiol* **132:** 1982-1988

Eugenia Zanetti M, Blanco FA, Pia Beker M, Battaglia M, Mario Aguilar O (2010) A C subunit of the plant nuclear factor NF-Y required for rhizobial infection and nodule development afects partner selection in the common bean-*Rhizobium etli* Symbiosis. *Plant Cell* **22:**

4142-4157

Ferguson BJ, Indrasumunar A, Hayashi S, Lin M-H, Lin Y-H, Reid DE, Gresshoff PM (2010) Molecular analysis of legume nodule development and autoregulation. *J Integr Plant Biol* **52:** 61-76

Fletcher LC, Brand U, Running MP, Simon R, Meyerowitz EM (1999) Signaling of cell fate decisions by CLAVATA3 in *Arabidopsis* shoot meristems. *Science* **283:** 1911-1914

Foucher F, Kondorosi E (2000) Cell cycle regulation in the course of nodule organogenesis in Medicago. *Plant Mol Biol* **43:** 773-786

Fournier J, Timmers ACJ, Sieberer BJ, Jauneau A, Chabaud M, Barker DG (2008) Mechanism of infection thread elongation in root hairs of *Medicago truncatula* and dynamic interplay with associated rhizobial colonization. *Plant Physiol* **148:** 1985-1995

Frank B (1889) Ueber die Pilzsymbiose der Leguminosen. *Bet Dtsch Bot Ges* **7:** 332–346

Gage DJ (2004) Infection and invasion of roots by symbiotic, nitrogen-fixing rhizobia during nodulation of temperate legumes. *Microbiol Mol Biol Rev* **68:** 280-300

Gao QM, Venugopal S, Navarre D, Kachroo A (2011) Low oleic acid-derived repression of jasmonic acid-inducible defense responses requires the WRKY50 and WRKY51 Proteins. *Plant Physiol* **155:** 464-476

Goh T, Joi S, Mimura T, Fukaki H (2012) The establishment of asymmetry in *Arabidopsis* lateral root founder cells is regulated by LBD16/ASL18 and related LBD/ASL proteins. *Development* **139:** 883-893

Gonzalez-Rizzo S, Crespi M, Frugier F (2006) The *Medicago truncatula* CRE1 cytokinin receptor regulates lateral root development and early symbiotic interaction with *Sinorhizobium meliloti*. *Plant Cell* **18:** 2680-2693

Goormachtig S, Capoen W, James EK, Holsters M (2004) Switch from intracellular to intercellular invasion during water stress-tolerant legume nodulation. *P Natl Acad Sci USA* **101:** 6303-6308

Gregis V, Sessa A, Colombo L, Kater MM (2008) AGAMOUS-LIKE24 and SHORT VEGETATIVE PHASE determine floral meristem identity in Arabidopsis. *Plant J* **56:** 891-902

Groth M, Takeda N, Perry J, Uchida H, Draxl S, Brachmann A, Sato S, Tabata S, Kawaguchi M, Wang TL, Parniske M (2010) NENA, a *Lotus japonicus* homolog of Sec13, is required for rhizodermal infection by arbuscular mycorrhiza fungi and rhizobia but dispensable for cortical endosymbiotic development. *Plant Cell* **22:** 2509-2526

Guan D, Stacey N, Liu C, Wen J, Mysore KS, Torres-Jerez I, Vernie T, Tadege M, Zhou C, Wang Z-y, Udvardi MK, Oldroyd GED, Murray JD (2013) Rhizobial infection is associated with the development of peripheral vasculature in nodules of *Medicago*

truncatula. *Plant Physiol* **162:** 107-115

Haney CH, Long SR (2010) Plant flotillins are required for infection by nitrogen-fixing bacteria. *P Natl Acad Sci USA* **107:** 478-483

Haney CH, Riely BK, Tricoli DM, Cook DR, Ehrhardt DW, Long SR (2011) Symbiotic rhizobia bacteria trigger a change in localization and dynamics of the *Medicago truncatula* receptor kinase LYK3. *Plant Cell* **23:** 2774-2787

Hayashi T, Shimoda Y, Sato S, Tabata S, Imaizumi-Anraku H, Hayashi M (2014) Rhizobial infection does not require cortical expression of upstream common symbiosis genes responsible for the induction of Ca^{2+} spiking. *Plant J* **77:** 146-159

Heckmann AB, Lombardo F, Miwa H, Perry JA, Bunnewell S, Parniske M, Wang TL, Downie JA (2006) *Lotus japonicus* nodulation requires two GRAS domain regulators, one of which is functionally conserved in a non-legume. *Plant Physiol* **142:** 1739-1750

Heckmann AB, Sandal N, Bek AS, Madsen LH, Jurkiewicz A, Nielsen MW, Tirichine L, Stougaard J (2011) Cytokinin induction of root nodule primordia in *Lotus japonicus* is regulated by a mechanism operating in the root cortex. *Mol Plant-Microbe Interact* **24:** 1385-1395

Heidstra R, Yang WC, Yalcin Y, Peck S, Emons AM, vanKammen A, Bisseling T (1997) Ethylene provides positional information on cortical cell division but is not involved in Nod factor-induced root hair tip growth in *Rhizobium*-legume interaction. *Development* **124:** 1781-1787

Held M, Hossain MS, Yokota K, Bonfante P, Stougaard J, Szczyglowski K (2010) Common and not so common symbiotic entry. *Trends Plant Sci* **15:** 540-545

Held M, Hou H, Miri M, Huynh C, Ross L, Hossain MS, Sato S, Tabata S, Perry J, Wang TL, Szczyglowski K (2014) *Lotus japonicus* cytokinin receptors work partially redundantly to mediate nodule formation. *Plant Cell* **26:** 678-694

Hepler PK, Vidali L, Cheung AY (2001) Polarized cell growth in higher plants. *Annu Rev Cell Dev Biol* **17:** 159-187

Higashi S, Kushiyama K, Abe M (1986) Electron-microscopic observations of infection threads in driselase treated nodules of *Astragalus sinicus*. *Canadian Journal of Microbiology* **32:** 947-952

Hirsch AM, Bhuvaneswari TV, Torrey JG, Bisseling T (1989) Early nodulin genes are induced in alfalfa root outgrowths elicited by auxin transport inhibitors. *P Natl Acad Sci USA* **86:** 1244-1248

Honma MA, Asomaning M, Ausubel FM (1990) *Rhizobium meliloti nodD* genes mediate host-specific activation of *nodABC*. *J Bacteriol* **172:** 901-911

Horvath B, Yeun LH, Domonkos A, Halasz G, Gobbato E, Ayaydin F, Miro K, Hirsch S, Sun

JH, Tadege M, Ratet P, Mysore KS, Ane JM, Oldroyd GED, Kalo P (2011) *Medicago truncatula* IPD3 is a member of the common symbiotic signaling pathway required for rhizobial and mycorrhizal symbioses. *Mol Plant-Microbe Interact* **24:** 1345-1358

Hossain MS, Liao J, James EK, Sato S, Tabata S, Jurkiewicz A, Madsen LH, Stougaard J, Ross L, Szczyglowski K (2012) *Lotus japonicus* ARPC1 is required for rhizobial infection. *Plant Physiol* **160:** 917-928

Huault E, Laffont C, Wen J, Mysore SK, Ratet P, Duc G, Frugier F (2014) Local and systemic regulation of plant root system architecture and symbiotic nodulation by a receptor-like kinase. *PLoS Genet* **10:** e1004891

Ikeda M, Mitsuda N, Ohme-Takagi M (2009) *Arabidopsis* WUSCHEL is a bifunctional transcription factor that acts as a repressor in stem cell regulation and as an activator in floral patterning. *Plant Cell* **21:** 3493-3505

Imaizumi-Anraku H, Kouchi H, Syono K, Akao S, Kawaguchi M (2000) Analysis of *ENOD40* expression in *alb1*, a symbiotic mutant of *Lotus japonicus* that forms empty nodules with incompletely developed nodule vascular bundles. *Mol Gen Genet* **264:** 402-410

Imaizumi-Anraku H, Takeda N, Charpentier M, Perry J, Miwa H, Umehara Y, Kouchi H, Murakami Y, Mulder L, Vickers K, Pike J, Downie JA, Wang T, Sato S, Asamizu E, Tabata S, Yoshikawa M, Murooka Y, Wu GJ, Kawaguchi M, Kawasaki S, Parniske M, Hayashi M (2005) Plastid proteins crucial for symbiotic fungal and bacterial entry into plant roots. *Nature* **433:** 527-531

Imin N, Mohd-Radzman NA, Ogilvie HA, Djordjevic MA (2013) The peptide-encoding CEP1 gene modulates lateral root and nodule numbers in *Medicago truncatula*. *J Exp Bot* **64:** 5395-5409

Ishida K, Niwa Y, Yamashino T, Mizuno T (2009) A genome-wide compilation of the two-component systems in *Lotus japonicus*. *DNA Res* **16:** 237-247

Jacobsen E, Feenstra WJ (1984) A new pea mutant with efficient nodulation in the presence of nitrate. *Plant Science Letters* **33:** 337-344

Jefferson RA, Kavanagh TA, Bevan MW (1987) GUS fusions: beta-glucuronidase as a sensitive and versatile gene fusion marker in higher plants. *EMBO J* **6:** 3901-3907

Jones KM, Kobayashi H, Davies BW, Taga ME, Walker GC (2007) How rhizobial symbionts invade plants: the *Sinorhizobium-Medicago* model. *Nat Rev Microbiol* **5:** 619-633

Kalo P, Gleason C, Edwards A, Marsh J, Mitra RM, Hirsch S, Jakab J, Sims S, Long SR, Rogers J, Kiss GB, Downie JA, Oldroyd GED (2005) Nodulation signaling in legumes requires NSP2, a member of the GRAS family of transcriptional regulators. *Science* **308:** 1786-1789

Kanamori N, Madsen LH, Radutoiu S, Frantescu M, Quistgaard EMH, Miwa H, Downie JA,

James EK, Felle HH, Haaning LL, Jensen TH, Sato S, Nakamura Y, Tabata S, Sandal N, Stougaard J (2006) A nucleoporin is required for induction of Ca^{2+} spiking in legume nodule development and essential for rhizobial and fungal symbiosis. *P Natl Acad Sci USA* **103:** 359-364

Karas B, Murray J, Gorzelak M, Smith A, Sato S, Tabata S, Szczyglowski K (2005) Invasion of *Lotus japonicus root hairless 1* by *Mesorhizobium loti* involves the nodulation factor-dependent induction of root hairs. *Plant Physiol* **137:** 1331-1344

Kawaguchi M, Imaizumi-Anraku H, Koiwa H, Niwa S, Ikuta A, Syono K, Akao S (2002) Root, root hair, and symbiotic mutants of the model legume *Lotus japonicus*. *Mol Plant-Microbe Interact* **15:** 17-26

Kiirika LM, Bergmann HF, Schikowsky C, Wimmer D, Korte J, Schmitz U, Niehaus K, Colditz F (2012) Silencing of the Rac1 GTPase MtROP9 in *Medicago truncatula* stimulates early mycorrhizal and oomycete root colonizations but negatively affects rhizobial infection. *Plant Physiol* **159:** 501-516

Kinkema M, Gresshoff PM (2008) Investigation of downstream signals of the soybean autoregulation of nodulation receptor kinase GmNARK. *Mol Plant-Microbe Interact* **21:** 1337-1348

Kinoshita A, Betsuyaku S, Osakabe Y, Mizuno S, Nagawa S, Stahl Y, Simon R, Yamaguchi-Shinozaki K, Fukuda H, Sawa S (2010) RPK2 is an essential receptor-like kinase that transmits the CLV3 signal in *Arabidopsis*. *Development* **137:** 3911-3920

Kistner C, Parniske M (2002) Evolution of signal transduction in intracellular symbiosis. *Trends Plant Sci* **7:** 511-518

Kosslak RM, Bohlool BB (1984) Suppression of nodule development of one side of a split-root system of soybeans caused by prior inoculation of the other Side. *Plant Physiol* **75:** 125-130

Kosuta S, Held M, Hossain MS, Morieri G, MacGillivary A, Johansen C, Antolin-Llovera M, Parniske M, Oldroyd GED, Downie AJ, Karas B, Szczyglowski K (2011) *Lotus japonicus symRK-14* uncouples the cortical and epidermal symbiotic program. *Plant J* **67:** 929-940

Krusell L, Madsen LH, Sato S, Aubert G, Genua A, Szczyglowski K, Duc G, Kaneko T, Tabata S, de Bruijn F, Pajuelo E, Sandal N, Stougaard J (2002) Shoot control of root development and nodulation is mediated by a receptor-like kinase. *Nature* **420:** 422-426

Krusell L, Sato N, Fukuhara I, Koch BEV, Grossmann C, Okamoto S, Oka-Kira E, Otsubo Y, Aubert G, Nakagawa T, Sato S, Tabata S, Duc G, Parniske M, Wang TL, Kawaguchi M, Stougaard J (2011) The *Clavata2* genes of pea and *Lotus japonicus* affect autoregulation of nodulation. *Plant J* **65:** 861-871

Kuppusamy KT, Endre G, Prabhu R, Penmetsa RV, Veereshlingam H, Cook DR, Dickstein R,

VandenBosch KA (2004) *LIN*, a *Medicago truncatula* gene required for nodule differentiation and persistence of rhizobial infections. *Plant Physiol* **136:** 3682-3691

Laloum T, Baudin M, Frances L, Lepage A, Billault-Penneteau B, Cerri MR, Ariel F, Jardinaud M-F, Gamas P, de Carvalho-Niebel F, Niebel A (2014) Two CCAAT-box-binding transcription factors redundantly regulate early steps of the legume-rhizobia endosymbiosis. *Plant J* **79:** 757-768

Laporte P, Lepage A, Fournier J, Catrice O, Moreau S, Jardinaud M-F, Mun J-H, Larrainzar E, Cook DR, Gamas P, Niebel A (2014) The CCAAT box-binding transcription factor NF-YA1 controls rhizobial infection. *J Exp Bot* **65:** 481-494

Laus MC, van Brussel AAN, Kijne JW (2005) Role of cellulose fibrils and exopolysaccharides of Rhizobium leguminosarum in attachment to and infection of *Vicia sativa* root hairs. *Mol Plant-Microbe Interact* **18:** 533-538

Le SQ, Gascuel O (2008) An improved general amino acid replacement matrix. *Mol Biol Evol* **25:** 1307-1320

Lefebvre B, Timmers T, Mbengue M, Moreau S, Herve C, Toth K, Bittencourt-Silvestre J, Klaus D, Deslandes L, Godiard L, Murray JD, Udvardi MK, Raffaele S, Mongrand S, Cullimore J, Gamas P, Niebel A, Ott T (2010) A remorin protein interacts with symbiotic receptors and regulates bacterial infection. *P Natl Acad Sci USA* **107:** 2343-2348

Levy J, Bres C, Geurts R, Chalhoub B, Kulikova O, Duc G, Journet EP, Ane JM, Lauber E, Bisseling T, Denarie J, Rosenberg C, Debelle F (2004) A putative Ca^{2+} and calmodulin-dependent protein kinase required for bacterial and fungal symbioses. *Science* **303:** 1361-1364

Li D, Kinkema M, Gresshoff PM (2009) Autoregulation of nodulation (AON) in *Pisum sativum* (pea) involves signalling events associated with both nodule primordia development and nitrogen fixation. *J Plant Physiol* **166:** 955-967

Li J, Brader G, Palva ET (2004) The WRKY70 transcription factor: A node of convergence for jasmonate-mediated and salicylate-mediated signals in plant defense. *Plant Cell* **16:** 319-331

Liang Y, Cao Y, Tanaka K, Thibivilliers S, Wan J, Choi J, Kang CH, Qiu J, Stacey G (2013) Nonlegumes respond to rhizobial Nod factors by suppressing the innate immune response. *Science* **341:** 1384-1387

Liao J, Singh S, Hossain MS, Andersen SU, Ross L, Bonetta D, Zhou Y, Sato S, Tabata S, Stougaard J, Szczyglowski K, Parniske M (2012) Negative regulation of CCaMK is essential for symbiotic infection. *Plant J* **72:** 572-584

Liebig J (1840) Organic chemistry in its application to agriculture and physiology. English edn edited by L. Playfair and W. Gregory, London: Taylor and Walton Press

Lim CW, Lee YW, Hwang CH (2011) Soybean nodule-enhanced CLE peptides in roots act as signals in GmNARK-mediated nodulation suppression. *Plant Cell Physiol* **52:** 1613-1627

Limpens E, Franken C, Smit P, Willemse J, Bisseling T, Geurts R (2003) LysM domain receptor kinases regulating rhizobial Nod factor-induced infection. *Science* **302:** 630-633

Limpens E, Mirabella R, Fedorova E, Franken C, Franssen H, Bisseling T, Geurts R (2005) Formation of organelle-like N_2-fixing symbiosomes in legume root nodules is controlled by *DMI2*. *P Natl Acad Sci USA* **102:** 10375-10380

Lin YH, Ferguson BJ, Kereszt A, Gresshoff PM (2010) Suppression of hypernodulation in soybean by a leaf-extracted, NARK- and Nod factor-dependent, low molecular mass fraction. *New Phytol* **185:** 1074-1086

Liu P, Li R-L, Zhang L, Wang Q-L, Niehaus K, Baluska F, Samaj J, Lin J-X (2009) Lipid microdomain polarization is required for NADPH oxidase-dependent ROS signaling in *Picea meyeri* pollen tube tip growth. *Plant J* **60:** 303-313

Liu ZC, Mara C (2010) Regulatory mechanisms for floral homeotic gene expression. *Semin Cell Dev Biol* **21:** 80-86

Lohar D, Stiller J, Kam J, Stacey G, Gresshoff PM (2009) Ethylene insensitivity conferred by a mutated *Arabidopsis* ethylene receptor gene alters nodulation in transgenic *Lotus japonicus*. *Ann Bot* **104:** 277-285

Lohar DP, Haridas S, Gantt JS, VandenBosch KA (2007) A transient decrease in reactive oxygen species in roots leads to root hair deformation in the legume-rhizobia symbiosis. *New Phytol* **173:** 39-49

Lombardo F, Heckmann AB, Miwa H, Perry JA, Yano K, Hayashi M, Parniske M, Wang TL, Downie JA (2006) Identification of symbiotically defective mutants of *Lotus japonicus* affected in infection thread growth. *Mol Plant-Microbe Interact* **19:** 1444-1450

Madsen EB, Madsen LH, Radutoiu S, Olbryt M, Rakwalska M, Szczyglowski K, Sato S, Kaneko T, Tabata S, Sandal N, Stougaard J (2003) A receptor kinase gene of the LysM type is involved in legume perception of rhizobial signals. *Nature* **425:** 637-640

Madsen LH, Tirichine L, Jurkiewicz A, Sullivan JT, Heckmann AB, Bek AS, Ronson CW, James EK, Stougaard J (2010) The molecular network governing nodule organogenesis and infection in the model legume *Lotus japonicus*. *Nat Commun* **1:** 10

Maekawa-Yoshikawa M, Mueller J, Takeda N, Maekawa T, Sato S, Tabata S, Perry J, Wang TL, Groth M, Brachmann A, Parniske M (2009) The temperature-sensitive *brush* mutant of the legume *Lotus japonicus* reveals a link between root development and nodule infection by rhizobia. *Plant Physiol* **149:** 1785-1796

Maekawa T, Kusakabe M, Shimoda Y, Sato S, Tabata S, Murooka Y, Hayashi M (2008) Polyubiquitin promoter-based binary vectors for overexpression and gene silencing in *Lotus*

japonicus. *Mol Plant-Microbe Interact* **21:** 375-382

Magori S, Oka-Kira E, Shibata S, Umehara Y, Kouchi H, Hase Y, Tanaka A, Sato S, Tabata S, Kawaguchi M (2009) TOO MUCH LOVE, a root regulator associated with the long-distance control of nodulation in *Lotus japonicus*. *Mol Plant-Microbe Interact* **22:** 259-268

Malik NSA, Calvert HE, Bauer WD (1987) Nitrate induced regulation of nodule formation in soybean. *Plant Physiol* **84:** 266-271

Mano S, Nakamori C, Nito K, Kondo M, Nishimura M (2006) The *Arabidopsis pex12* and *pex13* mutants are defective in both PTS1- and PTS2-dependent protein transport to peroxisomes. *Plant J* **47:** 604-618

Markmann K, Parniske M (2009) Evolution of root endosymbiosis with bacteria: How novel are nodules? *Trends Plant Sci* **14:** 77-86

Marsh JF, Rakocevic A, Mitra RM, Brocard L, Sun J, Eschstruth A, Long SR, Schultze M, Ratet P, Oldroyd GED (2007) *Medicago truncatula* NIN is essential for rhizobial-independent nodule organogenesis induced by autoactive calcium/calmodulin-dependent protein kinase. *Plant Physiol* **144:** 324-335

Mbengue M, Camut S, de Carvalho-Niebel F, Deslandes L, Froidure S, Klaus-Heisen D, Moreau S, Rivas S, Timmers T, Herve C, Cullimore J, Lefebvre B (2010) The *Medicago truncatula* E3 ubiquitin ligase PUB1 interacts with the LYK3 symbiotic receptor and negatively regulates infection and nodulation. *Plant Cell* **22:** 3474-3488

Messinese E, Mun J-H, Yeun LH, Jayaraman D, Rouge P, Barre A, Lougnon G, Schornack S, Bono J-J, Cook DR, Ane J-M (2007) A novel nuclear protein interacts with the symbiotic DMI3 calcium- and calmodulin-dependent protein kinase of *Medicago truncatula*. *Mol Plant-Microbe Interact* **20:** 912-921

Middleton PH, Jakab J, Penmetsa RV, Starker CG, Doll J, Kalo P, Prabhu R, Marsh JF, Mitra RM, Kereszt A, Dudas B, VandenBosch K, Long SR, Cook DR, Kiss GB, Oldroyd GED (2007) An ERF transcription factor in *Medicago truncatula* that is essential for nod factor signal transduction. *Plant Cell* **19:** 1221-1234

Miller DD, Leferink-ten Klooster HB, Emons AMC (2000) Lipochito-oligosaccharide nodulation factors stimulate cytoplasmic polarity with longitudinal endoplasmic reticulum and vesicles at the tip in vetch root hairs. *Mol Plant-Microbe Interact* **13:** 1385-1390

Mitra RM, Gleason CA, Edwards A, Hadfield J, Downie JA, Oldroyd GED, Long SR (2004) A Ca^{2+}/calmodulin-dependent protein kinase required for symbiotic nodule development: gene identification by transcript-based cloning. *P Natl Acad Sci USA* **101:** 4701-4705

Miwa H, Sun J, Oldroyd GED, Downie JA (2006) Analysis of nod-factor-induced calcium signaling in root hairs of symbiotically defective mutants of *Lotus japonicus*. *Mol*

Plant-Microbe Interact **19:** 914-923

Miyahara A, Richens J, Starker C, Morieri G, Smith L, Long S, Downie JA, Oldroyd GED (2010) Conservation in function of a SCAR/WAVE component during infection thread and root hair growth in *Medicago truncatula*. *Mol Plant-Microbe Interact* **23:** 1553-1562

Miyashima S, Koi S, Hashimoto T, Nakajima K (2011) Non-cell-autonomous microRNA165 acts in a dose-dependent manner to regulate multiple differentiation status in the *Arabidopsis* root. *Development* **138:** 2303-2313

Miyata K, Kawaguchi M, Nakagawa T (2013) Two distinct EIN2 genes cooperatively regulate ethylene signaling in *Lotus japonicus*. *Plant Cell Physiol* **54:** 1469-1477

Miyazawa H (2010) Molecular genetic analysis of *KLAVIER* mediating long-distance negative regulation of nodulation in *Lotus japonicus*. PhD thesis, The University of Tokyo

Miyazawa H, Oka-Kira E, Sato N, Takahashi H, Wu G-J, Sato S, Hayashi M, Betsuyaku S, Nakazono M, Tabata S, Harada K, Sawa S, Fukuda H, Kawaguchi M (2010) The receptor-like kinase KLAVIER mediates systemic regulation of nodulation and non-symbiotic shoot development in *Lotus japonicus*. *Development* **137:** 4317-4325

Moling S, Pietraszewska-Bogiel A, Postma M, Fedorova E, Hink MA, Limpens E, Gadella TWJ, Bisseling T (2014) Nod factor receptors form heteromeric complexes and are essential for intracellular infection in *Medicago* nodules. *Plant Cell* **26:** 4188-4199

Mortier V, Den Herder G, Whitford R, Van de Velde W, Rombauts S, D'Haeseleer K, Holsters M, Goormachtig S (2010) CLE peptides control *Medicago truncatula* nodulation locally and systemically. *Plant Physiol* **153:** 222-237

Mortier V, De Wever E, Vuylsteke M, Holsters M, Goormachtig S (2012a) Nodule numbers are governed by interaction between CLE peptides and cytokinin signaling. *Plant J* **70:** 367-376

Mortier V, Holsters M, Goormachtig S (2012b) Never too many? How legumes control nodule numbers. *Plant Cell Environ* **35:** 245-258

Muller R, Bleckmann A, Simon R (2008) The receptor kinase CORYNE of *Arabidopsis* transmits the stem cell-limiting signal CLAVATA3 independently of CLAVATA1. *Plant Cell* **20:** 934-946

Munoz JA, Coronado C, Perez-Hormaeche J, Kondorosi A, Ratet P, Palomares AJ (1998) *MsPG3*, a *Medicago sativa* polygalacturonase gene expressed during the alfalfa *Rhizobium meliloti* interaction. *P Natl Acad Sci USA* **95:** 9687-9692

Murakami Y, Miwa H, Imaizumi-Anraku H, Kouchi H, Downie JA, Kawaguchi M, Kawasaki S (2006) Positional cloning identifies *Lotus japonicus* NSP2, a putative transcription factor of the GRAS family, required for *NIN* and *ENOD40* gene expression in nodule initiation. *DNA Res* **13:** 255-265

Murray JD (2011) Invasion by invitation: rhizobial infection in legumes. *Mol Plant-Microbe*

Interact **24:** 631-639

Murray JD, Karas BJ, Sato S, Tabata S, Amyot L, Szczyglowski K (2007) A cytokinin perception mutant colonized by *Rhizobium* in the absence of nodule organogenesis. *Science* **315:** 101-104

Murray JD, Muni RRD, Torres-Jerez I, Tang Y, Allen S, Andriankaja M, Li G, Laxmi A, Cheng X, Wen J, Vaughan D, Schultze M, Sun J, Charpentier M, Oldroyd G, Tadege M, Ratet P, Mysore KS, Chen R, Udvardi MK (2011) *Vapyrin*, a gene essential for intracellular progression of arbuscular mycorrhizal symbiosis, is also essential for infection by rhizobia in the nodule symbiosis of *Medicago truncatula*. *Plant J* **65:** 244-252

Nakagawa T, Kouchi H, Kawaguchi M (2006) Shoot-applied MeJA suppresses root nodulation in *Lotus japonicus*. *Plant Cell Physiol* **47:** 176-180

Nakagawa T, Kurose T, Hino T, Tanaka K, Kawamukai M, Niwa Y, Toyooka K, Matsuoka K, Jinbo T, Kimura T (2007) Development of series of gateway binary vectors, pGWBs, for realizing efficient construction of fusion genes for plant transformation. *J Biosci Bioeng* **104:** 34-41

Nebenfuhr A, Gallagher LA, Dunahay TG, Frohlick JA, Mazurkiewicz AM, Meehl JB, Staehelin LA (1999) Stop-and-go movements of plant Golgi stacks are mediated by the acto-myosin system. *Plant Physiol* **121:** 1127-1141

Nelson BK, Cai X, Nebenfuehr A (2007) A multicolored set of in vivo organelle markers for co-localization studies in *Arabidopsis* and other plants. *Plant J* **51:** 1126-1136

Nishimura R, Hayashi M, Wu GJ, Kouchi H, Imaizumi-Anraku H, Murakami Y, Kawasaki S, Akao S, Ohmori M, Nagasawa M, Harada K, Kawaguchi M (2002a) HAR1 mediates systemic regulation of symbiotic organ development. *Nature* **420:** 426-429

Nishimura R, Ohmori M, Fujita H, Kawaguchi M (2002b) A *Lotus* basic leucine zipper protein with a RING-finger motif negatively regulates the developmental program of nodulation. *P Natl Acad Sci USA* **99:** 15206-15210

Niwa S, Kawaguchi M, Imaizumi-Anraku H, Chechetka SA, Ishizaka M, Ikuta A, Kouchi H (2001) Responses of a model legume *Lotus japonicus* to lipochitin oligosaccharide nodulation factors purified from *Mesorhizobium loti* JRL501. *Mol Plant-Microbe Interact* **14:** 848-856

Nontachalyapoom S, Scott PT, Men AE, Kinkema M, Schenk PM, Gresshoff PM (2007) Promoters of orthologous *Glycine max* and *Lotus japonicus* nodulation autoregulation genes interchangeably drive phloem-specific expression in transgenic plants. *Mol Plant-Microbe Interact* **20:** 769-780

Novak K (2010) Early action of pea symbiotic gene *NOD3* is confirmed by adventitious root phenotype. *Plant Sci* **179:** 472-478

Nutman PS (1952) Physiological studies on nodule formation: III. Experiments on the excision of root-tips and nodules. *Ann Bot* **16:** 79-101

Ogawa-Ohnishi M, Matsushita W, Matsubayashi Y (2013) Identification of three hydroxyproline O-arabinosyltransferases in *Arabidopsis thaliana*. *Nat Chem Biol* **9:** 726-730

Ogawa M, Shinohara H, Sakagami Y, Matsubayashi Y (2008) *Arabidopsis* CLV3 peptide directly binds CLV1 ectodomain. *Science* **319:** 294-294

Ohyama K, Shinohara H, Ogawa-Ohnishi M, Matsubayashi Y (2009) A glycopeptide regulating stem cell fate in *Arabidopsis thaliana*. *Nat Chem Biol* **5:** 578-580

Oka-Kira E, Kawaguchi M (2006) Long-distance signaling to control root nodule number. *Curr Opin Plant Biol* **9:** 496-502

Oka-Kira E, Tateno K, Miura K, Haga T, Hayashi M, Harada K, Sato S, Tabata S, Shikazono N, Tanaka A, Watanabe Y, Fukuhara I, Nagata T, Kawaguchi M (2005) *klavier* (*klv*), A novel hypernodulation mutant of *Lotus japonicus* affected in vascular tissue organization and floral induction. *Plant J* **44:** 505-515

Okamoto S, Ohnishi E, Sato S, Takahashi H, Nakazono M, Tabata S, Kawaguchi M (2009) Nod factor/nitrate-induced CLE genes that drive HAR1-mediated systemic regulation of nodulation. *Plant Cell Physiol* **50:** 67-77

Okamoto S, Shinohara H, Mori T, Matsubayashi Y, Kawaguchi M (2013a) Root-derived CLE glycopeptides control nodulation by direct binding to HAR1 receptor kinase. *Nat Commun* **4:** 2191

Okamoto S, Yoro E, Suzaki T, Kawaguchi M (2013b) Hairy root transformation in *Lotus japonicus*. *Bio-protocol* **3:** e795

Okazaki S, Kaneko T, Sato S, Saeki K (2013) Hijacking of leguminous nodulation signaling by the rhizobial type III secretion system. *P Natl Acad Sci USA* **110:** 17131-17136

Oldroyd GED (2013) Speak, friend, and enter: signalling systems that promote beneficial symbiotic associations in plants. *Nat Rev Microbiol* **11:** 252-263

Oldroyd GED, Engstrom EM, Long SR (2001) Ethylene inhibits the nod factor signal transduction pathway of *Medicago truncatula*. *Plant Cell* **13:** 1835-1849

Ooki Y, Banba M, Yano K, Maruya J, Sato S, Tabata S, Saeki K, Hayashi M, Kawaguchi M, Izui K, Hata S (2005) Characterization of the *Lotus japonicus* symbiotic mutant *lot1* that shows a reduced nodule number and distorted trichomes. *Plant Physiol* **137:** 1261-1271

Oshima Y, Mitsuda N, Nakata M, Nakagawa T, Nagaya S, Kato K, Ohme-Takagi M (2011) Novel vector systems to accelerate functional analysis of transcription factors using chimeric repressor gene-silencing technology (CRES-T). *Plant Biotechnol* **28:** 201-210

Osipova MA, Mortier V, Demchenko KN, Tsyganov VE, Tikhonovich IA, Lutova LA, Dolgikh EA, Goormachtig S (2012) WUSCHEL-RELATED HOMEOBOX5 gene expression and

interaction of CLE peptides with components of the systemic control add two pieces to the puzzle of autoregulation of nodulation. *Plant Physiol* **158:** 1329-1341

Ovchinnikova E, Journet EP, Chabaud M, Cosson V, Ratet P, Duc G, Fedorova E, Liu W, den Camp RO, Zhukov V, Tikhonovich I, Borisov A, Bisseling T, Limpens E (2011) IPD3 controls the formation of nitrogen-fixing symbiosomes in pea and *Medicago* Spp. *Mol Plant-Microbe Interact* **24:** 1333-1344

Ovtsyna AO, Dolgikh EA, Kilanova AS, Tsyganov VE, Borisov AY, Tikhonovich IA, Staehelin C (2005) Nod factors induce Nod factor cleaving enzymes in pea roots. Genetic and pharmacological approaches indicate different activation mechanisms. *Plant Physiol* **139:** 1051-1064

Peck MC, Fisher RF, Long SR (2006) Diverse flavonoids stimulate NodD1 binding to *nod* gene promoters in *Sinorhizobium meliloti*. *J Bacteriol* **188:** 5417-5427

Peiter E, Sun J, Heckmann AB, Venkateshwaran M, Riely BK, Otegui MS, Edwards A, Freshour G, Hahn MG, Cook DR, Sanders D, Oldroyd GED, Downie JA, Ane J-M (2007) The *Medicago truncatula* DMI1 protein modulates cytosolic calcium signaling. *Plant Physiol* **145:** 192-203

Penmetsa RV, Cook DR (1997) A legume ethylene-insensitive mutant hyperinfected by its rhizobial symbiont. *Science* **275:** 527-530

Penmetsa RV, Frugoli JA, Smith LS, Long SR, Cook DR (2003) Dual genetic pathways controlling nodule number in *Medicago truncatula*. *Plant Physiol* **131:** 998-1008

Perrine-Walker FM, Kouchi H, Ridge RW (2014) Endoplasmic reticulum-targeted GFP reveals ER remodeling in *Mesorhizobium*-treated *Lotus japonicus* root hairs during root hair curling and infection thread formation. *Protoplasma* **251:** 817-826

Perrine-Walker FM, Lartaud M, Kouchi H, Ridge RW (2014) Microtubule array formation during root hair infection thread initiation and elongation in the *Mesorhizobium-Lotus* symbiosis. *Protoplasma* **251:** 1099-1111

Plet J, Wasson A, Ariel F, Le Signor C, Baker D, Mathesius U, Crespi M, Frugier F (2011) MtCRE1-dependent cytokinin signaling integrates bacterial and plant cues to coordinate symbiotic nodule organogenesis in *Medicago truncatula*. *Plant J* **65:** 622-633

Popp C, Ott T (2011) Regulation of signal transduction and bacterial infection during root nodule symbiosis. *Curr Opin Plant Biol* **14:** 458-467

Postma JG, Jacobsen E, Feenstra WJ (1988) Three pea mutants with an altered nodulation studied by genetic analysis and grafting. *J Plant Physiol* **132:** 424-430

Radutoiu S, Madsen LH, Madsen EB, Felle HH, Umehara Y, Gronlund M, Sato S, Nakamura Y, Tabata S, Sandal N, Stougaard J (2003) Plant recognition of symbiotic bacteria requires two LysM receptor-like kinases. *Nature* **425:** 585-592

Ramu SK, Peng HM, Cook DR (2002) Nod factor induction of reactive oxygen species production is correlated with expression of the early nodulin gene *rip1* in *Medicago truncatula*. *Mol Plant-Microbe Interact* **15:** 522-528

Reid DE, Ferguson BJ, Gresshoff PM (2011a) Inoculation- and nitrate-induced CLE peptides of soybean control NARK-dependent nodule formation. *Mol Plant-Microbe Interact* **24:** 606-618

Reid DE, Ferguson BJ, Hayashi S, Lin YH, Gresshoff PM (2011b) Molecular mechanisms controlling legume autoregulation of nodulation. *Ann Bot* **108:** 789-795

Reid DE, Hayashi S, Lorenc M, Stiller J, Edwards D, Gresshoff PM, Ferguson BJ (2012) Identification of systemic responses in soybean nodulation by xylem sap feeding and complete transcriptome sequencing reveal a novel component of the autoregulation pathway. *Plant Biotechnol J* **10:** 680-689

Riely BK, Lougnon G, Ane J-M, Cook DR (2007) The symbiotic ion channel homolog DMI1 is localized in the nuclear membrane of *Medicago truncatula* roots. *Plant J* **49:** 208-216

Rightmyer AP, Long SR (2011) Pseudonodule formation by wild-type and symbiotic mutant *Medicago truncatula* in response to auxin transport inhibitors. *Mol Plant-Microbe Interact* **24:** 1372-1384

Rival P, de Billy F, Bono JJ, Gough C, Rosenberg C, Bensmihen S (2012) Epidermal and cortical roles of *NFP* and *DMI3* in coordinating early steps of nodulation in *Medicago truncatula*. *Development* **139:** 3383-3391

Robledo M, Jimenez-Zurdo JI, Velazquez E, Trujillo ME, Zurdo-Pineiro JL, Ramirez-Bahena MH, Ramos B, Diaz-Minguez JM, Dazzo F, Martinez-Molina E, Mateos PF (2008) *Rhizobium* cellulase CelC2 is essential for primary symbiotic infection of legume host roots. *P Natl Acad Sci USA* **105:** 7064-7069

Rodriguez-Llorente ID, Perez-Hormaeche J, El Mounadi K, Dary M, Caviedes MA, Cosson V, Kondorosi A, Ratet P, Palomares AJ (2004) From pollen tubes to infection threads: recruitment of *Medicago* floral pectic genes for symbiosis. *Plant J* **39:** 587-598

Russell JA, Moran NA (2005) Horizontal transfer of bacterial symbionts: Heritability and fitness effects in a novel aphid host. *Appl Environ Microbiol* **71:** 7987-7994

Saint-Jore-Dupas C, Nebenfuhr A, Boulaflous A, Follet-Gueye M-L, Plasson C, Hawes C, Driouich A, Faye L, Gomord V (2006) Plant N-glycan processing enzymes employ different targeting mechanisms for their spatial arrangement along the secretory pathway. *Plant Cell* **18:** 3182-3200

Saito K, Yoshikawa M, Yano K, Miwa H, Uchida H, Asamizu E, Sato S, Tabata S, Imaizumi-Anraku H, Umehara Y, Kouchi H, Murooka Y, Szczyglowski K, Downie JA, Parniske M, Hayashi M, Kawaguchi M (2007) NUCLEOPORIN85 is required for

calcium spiking, fungal and bacterial symbioses, and seed production in *Lotus japonicus*. *Plant Cell* **19:** 610-624

Sakaue-Sawano A, Ohtawa K, Hama H, Kawano M, Ogawa M, Miyawaki A (2008) Tracing the silhouette of individual cells in S/G_2/M phases with fluorescence. *Chem Biol* **15:** 1243-1248

Sandal N, Petersen TR, Murray J, Umehara Y, Karas B, Yano K, Kumagai H, Yoshikawa M, Saito K, Hayashi M, Murakami Y, Wang XW, Hakoyama T, Imaizumi-Anraku H, Sato S, Kato T, Chen WL, Hossain MS, Shibata S, Wang TL, Yokota K, Larsen K, Kanamori N, Madsen E, Radutoiu S, Madsen LH, Radu TG, Krusell L, Ooki Y, Banba M, Betti M, Rispail N, Skot L, Tuck E, Perry J, Yoshida S, Vickers K, Pike J, Mulder L, Charpentier M, Muller J, Ohtomo R, Kojima T, Ando S, Marquez AJ, Gresshoff PM, Harada K, Webb J, Hata S, Suganuma N, Kouchi H, Kawasaki S, Tabata S, Parniske M, Szczyglowski K, Kawaguchi M, Stougaard J (2006) Genetics of symbiosis in *Lotus japonicus*: Recombinant inbred lines, comparative genetic maps, and map position of 35 symbiotic loci. *Mol Plant-Microbe Interact* **19:** 80-91

Sasaki T, Suzaki T, Kawaguchi M (2013). Stable transformation in *Lotus japonicus*. *Bio-protocol* **3:** e796

Sasaki T, Suzaki T, Soyano T, Kojima M, Sakakibara H, Kawaguchi M (2014) Shoot-derived cytokinins systemically regulate root nodulation. *Nat Commun* **5:** 4983

Saur IML, Oakes M, Djordjevic MA, Imin N (2011) Crosstalk between the nodulation signaling pathway and the autoregulation of nodulation in *Medicago truncatula*. *New Phytol* **190:** 865-874

Schauser L, Roussis A, Stiller J, Stougaard J (1999) A plant regulator controlling development of symbiotic root nodules. *Nature* **402:** 191-195

Schnabel E, Journet EP, de Carvalho-Niebel F, Duc G, Frugoli J (2005) The *Medicago truncatula SUNN* gene encodes a CLV1-like leucine-rich repeat receptor kinase that regulates nodule number and root length. *Plant Mol Biol* **58:** 809-822

Schnabel EL, Kassaw TK, Smith LS, Marsh JF, Oldroyd GE, Long SR, Frugoli JA (2011) The *ROOT DETERMINED NODULATION1* gene regulates nodule number in roots of *Medicago truncatula* and defines a highly conserved, uncharacterized plant gene family. *Plant Physiol* **157:** 328-340

Searle IR, Men AE, Laniya TS, Buzas DM, Iturbe-Ormaetxe I, Carroll BJ, Gresshoff PM (2003) Long-distance signaling in nodulation directed by a CLAVATA1-like receptor kinase. *Science* **299:** 109-112

Seo HS, Li J, Lee S, Yu J, Kim K, Lee SH, Lee I, Paek N (2007) The hypernodulating *nts* mutation induces jasmonate synthetic pathway in soybean leaves. *Molecules and Cells* **24:** 185-193

Serbus LR, Casper-Lindley C, Landmann F, Sullivan W (2008) The genetics and cell biology of *Wolbachia*-host Interactions. *Annu Rev Genet* **42:** 683-707

Shimomura K, Nomura M, Tajima S, Kouchi H (2006) LjnsRING, a novel RING finger protein, is required for symbiotic interactions between *Mesorhizobium loti* and *Lotus japonicus*. *Plant Cell Physiol* **47:** 1572-1581

Shinohara H, Matsubayashi Y (2010) Arabinosylated glycopeptide hormones: new insights into CLAVATA3 structure. *Curr Opin Plant Biol* **13:** 515-519

Sieberer B, Emons AMC (2000) Cytoarchitecture and pattern of cytoplasmic streaming in root hairs of *Medicago truncatula* during development and deformation by nodulation factors. *Protoplasma* **214:** 118-127

Smit P, Limpens E, Geurts R, Fedorova E, Dolgikh E, Gough C, Bisseling T (2007) *Medicago* LYK3, an entry receptor in rhizobial nodulation factor signaling. *Plant Physiol* **145:** 183-191

Smit P, Raedts J, Portyanko V, Debelle F, Gough C, Bisseling T, Geurts R (2005) NSP1 of the GRAS protein family is essential for rhizobial Nod factor-induced transcription. *Science* **308:** 1789-1791

Soltis DE, Soltis PS, Morgan DR, Swensen SM, Mullin BC, Dowd JM, Martin PG (1995) Chloroplast gene sequence data suggest a single origin of the predisposition for symbiotic nitrogen fixation in angiosperms. *P Natl Acad Sci USA* **92:** 2647-2651

Soto MJ, Dominguez-Ferreras A, Perez-Mendoza D, Sanjuan J, Olivares J (2009) Mutualism versus pathogenesis: the give-and-take in plant-bacteria interactions. *Cell Microbiol* **11:** 381-388

Soyano T, Hirakawa H, Sato S, Hayashi M, Kawaguchi M (2014) NODULE INCEPTION creates a long-distance negative feedback loop involved in homeostatic regulation of nodule organ production. *P Natl Acad Sci USA* **111:** 14607-14612

Soyano T, Kouchi H, Hirota A, Hayashi M (2013) NODULE INCEPTION directly targets NF-Y subunit genes to regulate essential processes of root nodule development in *Lotus japonicus*. *PLoS Genet* **9:** e1003352

Sprent JI (2007) Evolving ideas of legume evolution and diversity: a taxonomic perspective on the occurrence of nodulation. *New Phytol* **174:** 11-25

Stacey G, McAlvin CB, Kim SY, Olivares J, Soto MJ (2006) Effects of endogenous salicylic acid on nodulation in the model legumes *Lotus japonicus* and *Medicago truncatula*. *Plant Physiol* **141:** 1473-1481

Stracke S, Kistner C, Yoshida S, Mulder L, Sato S, Kaneko T, Tabata S, Sandal N, Stougaard J, Szczyglowski K, Parniske M (2002) A plant receptor-like kinase required for both bacterial and fungal symbiosis. *Nature* **417:** 959-962

Suzaki T, Ito M, Yoro E, Sato S, Hirakawa H, Takeda N, Kawaguchi M (2014) Endoreduplication-mediated initiation of symbiotic organ development in *Lotus japonicus*. *Development* **141:** 2441-2445

Suzaki T, Yano K, Ito M, Umehara Y, Suganuma N, Kawaguchi M (2012) Positive and negative regulation of cortical cell division during root nodule development in *Lotus japonicus* is accompanied by auxin response. *Development* **139:** 3997-4006

Swensen SM (1996) The evolution of actinorhizal symbioses: Evidence for multiple origins of the symbiotic association. *Am J Bot* **83:** 1503-1512

Tabata R, Sumida K, Yoshii T, Ohyama K, Shinohara H, Matsubayashi Y (2014) Perception of root-derived peptides by shoot LRR-RKs mediates systemic N-demand signaling. *Science* **346:** 343-346

Takahara M, Magori S, Soyano T, Okamoto S, Yoshida C, Yano K, Sato S, Tabata S, Yamaguchi K, Shigenobu S, Takeda N, Suzaki T, Kawaguchi M (2013) TOO MUCH LOVE, a novel Kelch repeat-containing F-box protein, functions in the long-distance Regulation of the legume-rhizobium symbiosis. *Plant Cell Physiol* **54:** 433-447

Takeda N, Sato S, Asamizu E, Tabata S, Parniske M (2009) Apoplastic plant subtilases support arbuscular mycorrhiza development in *Lotus japonicus*. *Plant J* **58:** 766-777

Tamura K, Stecher G, Peterson D, Filipski A, Kumar S (2013) MEGA6: Molecular evolutionary genetics analysis version 6.0. *Mol Biol Evol* **30:** 2725-2729

Tansengco ML, Hayashi M, Kawaguchi M, Imaizumi-Anraku H, Murooka Y (2003) *crinkle*, a novel symbiotic mutant that affects the infection thread growth and alters the root hair, trichome, and seed development in *Lotus japonicus*. *Plant Physiol* **131:** 1054-1063

Tansengco ML, Imaizumi-Anraku H, Yoshikawa M, Takagi S, Kawaguchi M, Hayashi M, Murooka Y (2004) Pollen development and tube growth are affected in the symbiotic mutant of *Lotus japonicus*, *crinkle*. *Plant Cell Physiol* **45:** 511-520

Teillet A, Garcia J, de Billy F, Gherardi M, Huguet T, Barker DG, de Carvalho-Niebel F, Journet E-P (2008) *api*, a novel *Medicago truncatula* symbiotic mutant impaired in nodule primordium invasion. *Mol Plant-Microbe Interact* **21:** 535-546

Terakado J, Yoneyama T, Fujihara S (2006) Shoot-applied polyamines suppress nodule formation in soybean (*Glycine max*). *J Plant Physiol* **163:** 497-505

Tian CF, Garnerone AM, Mathieu-Demaziere C, Masson-Boivin C, Batut J (2012) Plant-activated bacterial receptor adenylate cyclases modulate epidermal infection in the *Sinorhizobium meliloti-Medicago* symbiosis. *P Natl Acad Sci USA* **109:** 6751-6756

Timmers ACJ, Auriac MC, Truchet G (1999) Refined analysis of early symbiotic steps of the *Rhizobium-Medicago* interaction in relationship with microtubular cytoskeleton rearrangements. *Development* **126:** 3617-3628

Tirichine L, Sandal N, Madsen LH, Radutoiu S, Albrektsen AS, Sato S, Asamizu E, Tabata S, Stougaard J (2007) A gain-of-function mutation in a cytokinin receptor triggers spontaneous root nodule organogenesis. *Science* **315:** 104-107

Tjepkema JD, Winship LJ (1980) Energy requirement for nitrogen fixation in actinorhizal and legume root nodules. *Science* **209:** 279-281

Tsyganov VE, Voroshilova VA, Priefer UB, Borisov AY, Tikhonovich IA (2002) Genetic dissection of the initiation of the infection process and nodule tissue development in the *Rhizobium*-pea (*Pisum sativum* L.) symbiosis. *Ann Bot* **89:** 357-366

Udvardi MK, Price GD, Gresshoff PM, Day DA (1988) A dicarboxylate transporter on the peribacteroid membrane of soybean nodules. *FEBS Lett* **231:** 36-40

Udvardi M, Poole PS (2013) Transport and metabolism in legume-rhizobia symbioses. *Annu Rev Plant Biol* **64:** 781-805

Van der Does D, Leon-Reyes A, Koornneef A, Van Verk MC, Rodenburg N, Pauwels L, Goossens A, Korbes AP, Memelink J, Ritsema T, Van Wees SCM, Pieterse CMJ (2013) Salicylic acid suppresses jasmonic acid signaling downstream of SCF^{COI1}-JAZ by targeting GCC promoter motifs via transcription factor ORA59. *Plant Cell* **25:** 744-761

van Brussel AAN, Bakhuizen R, Vanspronsen PC, Spaink HP, Tak T, Lugtenberg BJJ, Kijne JW (1992) Induction of pre-infection thread structures in the leguminous host plant by mitogenic lipo-oligosaccharides of *Rhizobium*. *Science* **257:** 70-72

Vasse J, Debilly F, Truchet G (1993) Abortion of infection during the *Rhizobium meliloti*-alfalfa symbiotic interaction is accompanied by a hypersensitive reaction. *Plant J* **4:** 555-566

Vasse JM, Truchet GL (1984) The *Rhizobium*-legume symbiosis: observation of root infection by bright-field microscopy after staining with methylene blue. *Planta* **161:** 487-489

Veereshlingam H, Haynes JG, Penmetsa RV, Cook DR, Sherrier DJ, Dickstein R (2004) *nip*, a symbiotic *Medicago truncatula* mutant that forms root nodules with aberrant infection threads and plant defense-like response. *Plant Physiol* **136:** 3692-3702

Vernie T, Moreau S, de Billy F, Plet J, Combier JP, Rogers C, Oldroyd G, Frugier F, Niebel A, Gamas P (2008) EFD is an ERF transcription factor involved in the control of nodule number and differentiation in *Medicago truncatula*. *Plant Cell* **20:** 2696-2713

Voinnet O, Rivas S, Mestre P, Baulcombe D (2003) An enhanced transient expression system in plants based on suppression of gene silencing by the p19 protein of tomato bushy stunt virus. *Plant J* **33:** 949-956

Wopereis J, Pajuelo E, Dazzo FB, Jiang QY, Gresshoff PM, de Bruijn FJ, Stougaard J, Szczyglowski K (2000) Short root mutant of *Lotus japonicus* with a dramatically altered symbiotic phenotype. *Plant J* **23:** 97-114

Xie F, Murray JD, Kim J, Heckmann AB, Edwards A, Oldroyd GED, Downie A (2012) Legume

pectate lyase required for root infection by rhizobia. *P Natl Acad Sci USA* **109:** 633-638

Yang WC, Deblank C, Meskiene I, Hirt H, Bakker J, Vankammen A, Franssen H, Bisseling T (1994) *Rhizobium* Nod factors reactivate the cell cycle during infection and nodule primordium formation, but the cycle is only completed in primordium formation. *Plant Cell* **6:** 1415-1426

Yano K, Shibata S, Chen WL, Sato S, Kaneko T, Jurkiewicz A, Sandal N, Banba M, Imaizumi-Anraku H, Kojima T, Ohtomo R, Szczyglowski K, Stougaard J, Tabata S, Hayashi M, Kouchi H, Umehara Y (2009) CERBERUS, a novel U-box protein containing WD-40 repeats, is required for formation of the infection thread and nodule development in the legume-*Rhizobium* symbiosis. *Plant J* **60:** 168-180

Yano K, Tansengco ML, Hio T, Higashi K, Murooka Y, Imaizumi-Anraku H, Kawaguchi M, Hayashi M (2006) New nodulation mutants responsible for infection thread development in *Lotus japonicus*. *Mol Plant-Microbe Interact* **19:** 801-810

Yano K, Yoshida S, Mueller J, Singh S, Banba M, Vickers K, Markmann K, White C, Schuller B, Sato S, Asamizu E, Tabata S, Murooka Y, Perry J, Wang TL, Kawaguchi M, Imaizumi-Anraku H, Hayashi M, Parniske M (2008) CYCLOPS, a mediator of symbiotic intracellular accommodation. *P Natl Acad Sci USA* **105:** 20540-20545

Yendrek CR, Lee Y-C, Morris V, Liang Y, Pislariu CI, Burkart G, Meckfessel MH, Salehin M, Kessler H, Wessler H, Lloyd M, Lutton H, Teillet A, Sherrier DJ, Journet E-P, Harris JM, Dickstein R (2010) A putative transporter is essential for integrating nutrient and hormone signaling with lateral root growth and nodule development in *Medicago truncatula*. *Plant J* **62:** 100-112

Yokota K, Fukai E, Madsen LH, Jurkiewicz A, Rueda P, Radutoiu S, Held M, Hossain MS, Szczyglowski K, Morieri G, Oldroyd GED, Downie JA, Nielsen MW, Rusek AM, Sato S, Tabata S, James EK, Oyaizu H, Sandal N, Stougaard J (2009) Rearrangement of actin cytoskeleton mediates invasion of *Lotus japonicus* roots by *Mesorhizobium loti*. *Plant Cell* **21:** 267-284

Yoon HJ, Hossain MS, Held M, Hou HW, Kehl M, Tromas A, Sato SS, Tabata S, Andersen SU, Stougaard J, Ross L, Szczyglowski K (2014) *Lotus japonicus SUNERGOS1* encodes a predicted subunit A of a DNA topoisomerase VI that is required for nodule differentiation and accommodation of rhizobial infection. *Plant J* **78:** 811-821

Yoro E, Suzaki T, Toyokura K, Miyazawa H, Fukaki H, Kawaguchi M (2014) A positive regulator of nodule organogenesis, NODULE INCEPTION, acts as a negative regulator of rhizobial infection in *Lotus japonicus*. *Plant Physiol* **165:** 747-758

Yoshida C, Funayama-Noguchi S, Kawaguchi M (2010) *plenty*, a novel hypernodulation mutant in *Lotus japonicus*. *Plant Cell Physiol* **51:** 1425-1435